UNIVERSITY OF AMSTERDAM

UvA-DARE (Digital Academic Repository)

Search for heavy resonances in final states with four leptons and missing transverse momentum or jets in pp collisions at √s = 13 TeV with the ATLAS detector

ATLAS Collaboration

DOI
10.1007/JHEP10(2024)130
Publication date
2024
Document Version
Final published version
Published in
Journal of High Energy Physics
License
CC BY

Link to publication

Citation for published version (APA):
ATLAS Collaboration (2024). Search for heavy resonances in final states with four leptons and missing transverse momentum or jets in *pp* collisions at √s = 13 TeV with the ATLAS detector. *Journal of High Energy Physics*, *2024*(10), Article 130. https://doi.org/10.1007/JHEP10(2024)130

General rights
It is not permitted to download or to forward/distribute the text or part of it without the consent of the author(s) and/or copyright holder(s), other than for strictly personal, individual use, unless the work is under an open content license (like Creative Commons).

Disclaimer/Complaints regulations
If you believe that digital publication of certain material infringes any of your rights or (privacy) interests, please let the Library know, stating your reasons. In case of a legitimate complaint, the Library will make the material inaccessible and/or remove it from the website. Please Ask the Library: https://uba.uva.nl/en/contact, or a letter to: Library of the University of Amsterdam, Secretariat, P.O. Box 19185, 1000 GD Amsterdam, The Netherlands. You will be contacted as soon as possible.
UvA-DARE is a service provided by the library of the University of Amsterdam (https://dare.uva.nl)

Download date:07 Oct 2026

Published for SISSA by Springer

Received: *January 11, 2024*
Revised: *August 22, 2024*
Accepted: *September 30, 2024*
Published: *October 17, 2024*

Search for heavy resonances in final states with four leptons and missing transverse momentum or jets in pp collisions at $\sqrt{s} = 13$ TeV with the ATLAS detector

The ATLAS collaboration

E-mail: atlas.publications@cern.ch

Abstract: A search for a new heavy boson produced via gluon-fusion in the four-lepton channel with missing transverse momentum or jets is performed. The search uses proton-proton collision data equivalent to an integrated luminosity of 139 fb^{-1} at a centre-of-mass energy of 13 TeV collected by the ATLAS detector between 2015 and 2018 at the Large Hadron Collider. This study explores the decays of heavy bosons: $R \to SH$ and $A \to ZH$, where R is a CP-even boson, A is a CP-odd boson, H is a CP-even boson, and S is considered to decay into invisible particles that are candidates for dark matter. In these processes, $S \to$ invisible and $H \to ZZ$. The Z boson associated with the heavy scalar boson H decays into all decay channels of the Z boson. The mass range under consideration is 390–1300 (320–1300) GeV for the R (A) boson and 220–1000 GeV for the H boson. No significant deviation from the Standard Model backgrounds is observed. The results are interpreted as upper limits at a 95% confidence level on the cross-section times the branching ratio of the heavy resonances.

Keywords: Hadron-Hadron Scattering , Particle and Resonance Production

ArXiv ePrint: 2401.04742

Open Access, Copyright CERN,
for the benefit of the ATLAS Collaboration.
Article funded by SCOAP^3.

https://doi.org/10.1007/JHEP10(2024)130

JHEP10(2024)130

Contents

1 Introduction **1**

2 The ATLAS detector **3**

3 Data and simulated event samples **4**

4 Object and event selection **5**
4.1 Object reconstruction 5
4.2 Event selection 8

5 Analysis strategy **8**

6 Signal and background modelling **10**
6.1 Signal model 10
6.2 Background model 11

7 Systematic uncertainties **13**
7.1 Experimental uncertainties 13
7.2 Theoretical uncertainties 14
7.3 Systematic uncertainties on background shapes 14

8 Statistical procedures **15**

9 Results **15**

10 Conclusion **23**

The ATLAS collaboration **31**

JHEP10(2024)130

1 Introduction

In 2012, the ATLAS and CMS collaborations independently discovered a new particle [1, 2] with properties that are consistent with the Higgs boson proposed by the Standard Model (SM) [3–6]. It is still debated whether the Higgs boson is a standalone particle or part of an extended Higgs sector suggested by, e.g., the two-Higgs-doublet model (2HDM) [7, 8]. The 2HDM predicts the existence of five Higgs bosons, including a CP-even particle similar to the SM Higgs boson (h), a heavier CP-even Higgs boson (H), a CP-odd particle (A), and charged Higgs bosons ($H^{\pm}$). Another extension of the SM is the 2HDM+S model [9, 10], which introduces a scalar boson (S) in addition to the 2HDM particles. The S boson is assumed to be a dark matter portal and a potential source of missing transverse momentum, achieved through its decay to a pair of dark matter candidates ($\chi\overline{\chi}$) [9].

This paper presents searches for bosonic resonances that decay to four charged leptons (4ℓ, where ℓ is either an electron or a muon), along with missing transverse momentum

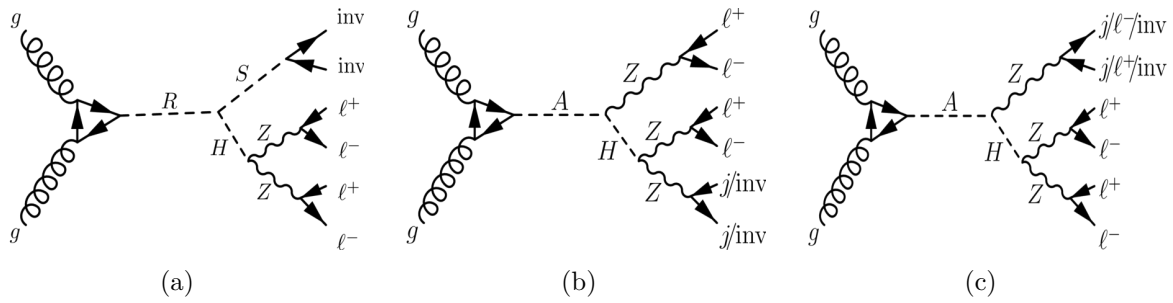

Figure 1. Feynman diagrams representing the production of heavy bosons via gluon-fusion at leading-order for the (a) $R \to SH \to 4\ell + E_{\mathrm{T}}^{\mathrm{miss}}$ signal, (b) $A \to Z(\to 2\ell)H(\to 2\ell + jj/\text{invisible})$ signal, and (c) $A \to Z(\to jj/\ell^+\ell^-/\text{invisible})H(\to 4\ell)$ signal, where ℓ could either be an electron or a muon, j represents a jet and inv denotes an invisible particle.

($E_{\mathrm{T}}^{\mathrm{miss}}$) or two jets ($jj$). The study focuses on the mass range of heavy bosons, where the invariant mass of the four leptons ($m_{4\ell}$) is above 200 GeV. This study uses proton-proton collision data at a centre-of-mass energy of 13 TeV and with an integrated luminosity of 139 fb^{-1} collected by the ATLAS detector in 2015–2018 at the Large Hadron Collider (LHC). Two different scenarios are considered for the signal model. First, the 2HDM+S model is extended to cover more general situations for various missing energy magnitudes by adding a heavy scalar R, where R decays to H and S bosons with $m_R > m_H + m_S$. The S boson decays into dark matter particles ($S \to$ invisible), and the H decays to 4ℓ through the decay of two Z bosons ($H \to ZZ \to 4\ell$). The phenomenology of the new $R \to SH$ topology can easily embed into the 2HDM+S model using an approach similar to that of ref. [9]. The masses of the R and H bosons are varied to control the missing transverse momentum, and the S mass is fixed to 160 GeV, see section 3. Second, a 2HDM-based baryogenesis scenario is considered, which generates matter and antimatter asymmetry. Searches for models consistent with baryogenesis were conducted at the LHC in several channels, such as $H \to hh$ [11, 12], $H \to WW/ZZ$ [13–18] and $A \to Zh$ [19, 20]. Searches in the $A \to ZH \to \ell^+\ell^- b\bar{b}/\ell^+\ell^-\tau^+\tau^-$ [21–24] and $A \to ZH \to \ell^+\ell^- t\bar{t}/\nu\bar{\nu}b\bar{b}$ [25] final states were also carried out at the LHC. In these searches, for a strong first-order phase transition to occur in the early universe, the hypothesis $m_A > m_H$ is preferred. Therefore, the $A \to ZH \to 4\ell + X$ channel is added to this study to explore regions with four leptons and jet activities. X could represent two leptons, two jets, or a pair of invisible particles, with the assumption that H decays into two Z bosons. In this signal, A is a CP-odd scalar which decays to a CP-even scalar H and a Z boson. Two decay scenarios are considered for the associated production of Z and H bosons: $A \to Z(\to \ell^+\ell^-/jj/\text{invisible})H(\to 4\ell)$ and $A \to Z(\to 2\ell)H(\to 2\ell + jj/\text{invisible})$, which are combined into one signal referred to as the $A \to ZH \to 4\ell + X$ signal. In this analysis, only the gluon-fusion production mode is considered for both the $R \to SH \to 4\ell + E_{\mathrm{T}}^{\mathrm{miss}}$ and $A \to ZH \to 4\ell + X$ signals, as illustrated by the Feynman diagrams of figure 1.

This paper is organised as follows. The ATLAS detector is described in section 2. Section 3 presents the data and Monte Carlo samples, followed by the object reconstruction in section 4. Section 5 describes the analysis strategy, and the signal and background modelling

JHEP10(2024)130

are discussed in section 6. Section 7 lists the experimental and theoretical systematic uncertainties. Section 8 explains the statistical model used in the analysis and the results are discussed in section 9. The conclusion is given in section 10.

2 The ATLAS detector

The ATLAS detector [26] at the LHC covers nearly the entire solid angle around the collision point.[1] It consists of an inner tracking detector surrounded by a thin superconducting solenoid, electromagnetic and hadron calorimeters, and a muon spectrometer incorporating three large superconducting air-core toroidal magnets.

The inner-detector system (ID) is immersed in a 2 T axial magnetic field and provides charged-particle tracking in the range $|\eta| < 2.5$. The high-granularity silicon pixel detector covers the vertex region and typically provides four measurements per track, the first hit normally being in the insertable B-layer (IBL) installed before Run 2 [27]. It is followed by the silicon microstrip tracker (SCT), which usually provides eight measurements per track. These silicon detectors are complemented by the transition radiation tracker (TRT), which enables radially extended track reconstruction up to $|\eta| = 2.0$. The TRT also provides electron identification information based on the fraction of hits (typically 30 in total) above a higher energy-deposit threshold corresponding to transition radiation.

The calorimeter system covers the pseudorapidity range $|\eta| < 4.9$. Within the region $|\eta| < 3.2$, electromagnetic calorimetry is provided by barrel and endcap high-granularity lead/liquid-argon (LAr) calorimeters, with an additional thin LAr presampler covering $|\eta| < 1.8$ to correct for energy loss in material upstream of the calorimeters. Hadron calorimetry is provided by the steel/scintillator-tile calorimeter, segmented into three barrel structures within $|\eta| < 1.7$, and two copper/LAr hadron endcap calorimeters. The solid angle coverage is completed with forward copper/LAr and tungsten/LAr calorimeter modules optimised for electromagnetic and hadronic energy measurements respectively.

The muon spectrometer (MS) comprises separate trigger and high-precision tracking chambers measuring the deflection of muons in a magnetic field generated by the superconducting air-core toroidal magnets. The field integral of the toroids ranges between 2.0 and 6.0 T m across most of the detector. Three layers of precision chambers, each consisting of layers of monitored drift tubes, cover the region $|\eta| < 2.7$, complemented by cathode-strip chambers in the forward region, where the background is highest. The muon trigger system covers the range $|\eta| < 2.4$ with resistive-plate chambers in the barrel, and thin-gap chambers in the endcap regions. Interesting events are selected by the first-level trigger system implemented in custom hardware, followed by selections made by algorithms implemented in software in the high-level trigger [28]. The first-level trigger accepts events from the 40 MHz bunch crossings at a rate below 100 kHz, which the high-level trigger further reduces in order to record events to disk at about 1 kHz. An extensive software suite [29] is used in

[1] ATLAS uses a right-handed coordinate system with its origin at the nominal interaction point (IP) in the centre of the detector and the z-axis along the beam pipe. The x-axis points from the IP to the centre of the LHC ring, and the y-axis points upwards. Polar coordinates (r, ϕ) are used in the transverse plane, ϕ being the azimuthal angle around the z-axis. The pseudorapidity is defined in terms of the polar angle θ as $\eta = -\ln\tan(\theta/2)$. Angular distance is measured in units of $\Delta R \equiv \sqrt{(\Delta\eta)^2 + (\Delta\phi)^2}$.

JHEP10(2024)130

data simulation, in the reconstruction and analysis of real and simulated data, in detector operations, and in the trigger and data acquisition systems of the experiment.

3 Data and simulated event samples

The data used in this analysis were produced through proton-proton (pp) collisions at a centre-of-mass energy of 13 TeV recorded by the ATLAS detector at the LHC from 2015 to 2018. Events are required to satisfy data-quality requirements, and after applying the event cleaning criteria, the total integrated luminosity of the entire data set is 139 fb^{-1} [30]. The data events in the four-lepton final state were recorded using a combination of single-lepton, dilepton, and trilepton triggers [31, 32]. The single-lepton triggers for isolated muons featured p_{T} thresholds ranging from 20 to 60 GeV and 50 GeV for muons without isolation requirement. In contrast, dilepton triggers had thresholds from 8 to 22 GeV, and trilepton triggers employed thresholds between 4 and 20 GeV. For electrons, the single-lepton triggers encompassed p_{T} thresholds ranging from 24 to 300 GeV, with dilepton triggers varying from 12 to 24 GeV and trilepton triggers featuring thresholds between 9 and 24 GeV. Additionally, when a dilepton trigger encountered an event with an electron and a muon, the p_{T} thresholds for electrons ranged from 7 to 26 GeV. For muons, the thresholds varied from 8 to 24 GeV. These p_{T} thresholds exhibited variations across the data-taking period from 2015 to 2018 due to rising luminosity [33, 34], but the overall trigger efficiency was about 98%.

Signal and background events were generated according to ATLAS detector configurations and utilised for signal optimisation, background parametrisation, and systematic uncertainty estimation. Each Monte Carlo (MC) generator produced events that underwent ATLAS detector simulation [35] within the GEANT4 framework [36]. The effect of multiple interactions in the same and neighbouring bunch crossings (pile-up) was modelled by overlaying the simulated hard-scattering event with inelastic pp events generated with PYTHIA 8.186 [37] at leading-order (LO) using the NNPDF2.3 LO set of parton distribution functions (PDFs) [38] and the A3 set of tuned parameters (tune) [39].

The $q\bar{q} \to ZZ$ background process was simulated with SHERPA 2.2.2 [40] using matrix elements at next-to-leading-order (NLO) accuracy in QCD for up to one additional parton and at LO accuracy for up to three additional parton emission. The virtual QCD corrections were provided by the OPENLOOPS library [41–43]. The $gg \to ZZ$ background process was generated by SHERPA 2.2.2, including off-shell effects and Higgs boson contributions, using LO-accurate matrix elements for up to one additional parton emission. The electroweak $q\bar{q} \to ZZ$ (EW) events, consisting of four leptons and two jets, were simulated using SHERPA 2.2.2. In addition, the VVV background events, including processes such as ZZZ, ZZW, and WWZ with at least four prompt charged leptons, were simulated using SHERPA 2.2.2. The matrix element calculations for these processes were matched and merged with the SHERPA parton shower based on Catani-Seymour dipole factorisation [44, 45] using the MEPS@NLO prescription [46–48]. The production of Z+jets was simulated with the SHERPA 2.2.1 generator using NLO matrix elements for up to two partons, and LO matrix elements for up to four partons calculated with the Comix [44] and OPENLOOPS libraries. All backgrounds simulated with SHERPA use NNPDF3.0 based on next-to-next-to-leading-order

JHEP10(2024)130

(NNLO) set of PDFs [49], along with the dedicated set of tuned parton shower parameters developed by the Sherpa authors.

Events containing charged leptons coming from the $t\bar{t}V$ background process ($V = Z$ or $W^{\pm}$) were modelled using the MadGraph5_aMC@NLO 2.3.3 [50] generator at NLO with the NNPDF3.0 NLO PDF. The events were interfaced to Pythia 8.210 using the A14 tune [51] and the NNPDF2.3 LO PDF set. The $t\bar{t}$ background was generated using Powheg-Box v2 [52, 52–54] at NLO with the NNPDF3.0 NLO PDF set. The events were interfaced to Pythia 8.230 to model the parton shower, hadronisation, and underlying event, with parameters set according to the A14 tune and using the NNPDF2.3 LO set of PDFs. The Powheg-Box v2 generator was used to simulate the WZ [55] production process at NLO accuracy in QCD. Events were interfaced to Pythia 8.230 for the modelling of the parton shower, hadronisation, and underlying event, with parameters set according to the AZNLO tune [56]. The CT10 PDF set [57] was used for the hard-scattering processes, whereas the CTEQ6L1 PDF set [58] was used for the parton shower. The decays of the bottom and charm hadrons for the top-quark processes were simulated using version 1.2 of the EvtGen program [59], except for using version 1.6 for $t\bar{t}$ production.

The $R \to SH \to 4\ell + E_{\mathrm{T}}^{\mathrm{miss}}$ signal was simulated using Pythia 8.244 with the A14 tune and NNPDF2.3 LO PDF set. The $A \to Z(\to jj/\ell^{+}\ell^{-}/\text{invisible})H(\to 4\ell)$ and $A \to Z(\to 2\ell)H(\to 2\ell + jj/\text{invisible})$ signals were generated by MadGraph5_aMC@NLO 2.7.2 at LO accuracy with the NNPDF2.3 LO PDF set, which is interfaced to Pythia 8.244 for parton showering and hadronisation with the A14 tune. The R mass is considered in the range of 390–1300 GeV, with the S mass fixed to 160 GeV, while the A mass is in the range of 320–1300 GeV. The H mass value for all signal processes is in the range of 220–1000 GeV. The assumption of the S mass is motivated by the phenomenology study presented in ref. [60]. However, the effect of this choice on the distribution of the missing transverse momentum was studied and it was found that the S mass only affects the distribution if its mass is above 200 GeV. Therefore, fixing the S mass reduces the free parameters and simplifies the analysis. Signals were generated using the narrow width approximation (NWA) [61] for both R and H in the $R \to SH \to 4\ell + E_{\mathrm{T}}^{\mathrm{miss}}$ signal, with the width of R and H set to 10 MeV. Similarly, for the $A \to ZH \to 4\ell + X$ signal, the narrow width approximation was employed with widths of 1 MeV for both A and H. Two mass points, $(m_A, m_H) = (320, 220)$ GeV and $(m_A, m_H) = (1190, 600)$ GeV, were also generated using the large width approximation (LWA) to evaluate the impact of non-negligible natural widths. Table 1 summarises the generators, shower model, matrix element accuracy, tune, and PDF sets used in signal and background simulation.

4 Object and event selection

4.1 Object reconstruction

The event selection relies on reconstructing and identifying electrons, muons, jets and missing transverse momentum. The electron energy measurement is improved using a dynamic, topological calorimeter-cell clustering-based method. This method is particularly effective in cases where an electron radiates a bremsstrahlung photon. More information about this

JHEP10(2024)130

Process	Generator and Parton shower	QCD accuracy	Tune and PDF
$R \to SH \to 4\ell + E_{\mathrm{T}}^{\mathrm{miss}}$	Pythia 8.244 [62]	LO	A14 and NNPDF2.3 LO [51, 63]
$A \to Z(\to jj/\ell^+\ell^-/\text{invisible})H(\to 4\ell)$	MadGraph5_aMC@NLO 2.7.2 + Pythia 8.244 [50, 62]	LO	A14 and NNPDF2.3 LO [51, 63]
$A \to Z(\to 2\ell)H(\to 2\ell + jj/\text{invisible})$	MadGraph5_aMC@NLO 2.7.2 + Pythia 8.244 [50, 62]	LO	A14 and NNPDF2.3 LO [51, 63]
$t\bar{t}V$ ($V = W/Z$)	MadGraph5_aMC@NLO 2.3.3 + Pythia 8.210 [50, 62]	NLO+LO	A14 and NNPDF3.0 NLO & NNPDF2.3 LO [49, 51, 63]
$q\bar{q} \to ZZ$	Sherpa 2.2.2 + MEPS@NLO [46–48]	NLO (0- and 1-jet), LO (2- and 3-jet)	Sherpa and NNPDF3.0 NNLO [49]
$gg \to ZZ$	Sherpa 2.2.2 + MEPS@NLO [46–48]	LO (0- and 1-jet)	Sherpa and NNPDF3.0 NNLO [49]
$q\bar{q} \to ZZ$ (EW)	Sherpa 2.2.2 + MEPS@NLO [46–48]	LO	Sherpa and NNPDF3.0 NNLO [49]
$ZZZ(4\ell 2\nu, 6\ell 0\nu)$	Sherpa 2.2.2 + MEPS@NLO [46–48]	NLO	Sherpa and NNPDF3.0 NNLO [49]
$WZZ(5\ell 1\nu)$	Sherpa 2.2.2 + MEPS@NLO [46–48]	NLO	Sherpa and NNPDF3.0 NNLO [49]
$WWZ(4\ell 2\nu)$	Sherpa 2.2.2 + MEPS@NLO [46–48]	NLO	Sherpa and NNPDF3.0 NNLO [49]
Z+jets	Sherpa 2.2.1 + MEPS@NLO [46–48]	NLO (0- and 2-jet), LO (3- and 4-jet)	Sherpa and NNPDF3.0 NNLO [49]
$t\bar{t}$	Powheg-Box v2 + Pythia 8.230 [52, 52–54, 62]	NLO+LO	A14 and (NNPDF3.0 NLO & NNPDF2.3 LO) [51, 59, 63]
$WZ \to 3\ell 1\nu$	Powheg-Box v2 + Pythia 8.230 [52, 52–54, 62]	NLO	AZNLO and (CT10NLO & CTEQ6L1) [56–58]

Table 1. Summary of the event generators used for the simulated signal and background samples, including the accuracy of the matrix element and parton distribution functions (PDFs). Additionally, the table lists the set of tuned parameters used.

technique can be found in ref. [64]. Electron candidates are identified as clusters of energy deposits in the calorimeter associated with ID tracks. The final track-cluster matching uses a Gaussian-sum filter (GSF) [65], accounting for bremsstrahlung energy losses. The electron transverse momentum (p_{T}) is calculated from the cluster energy and the track direction at the interaction point. The rejection of background noises, which consist of hadrons, non-prompt electrons mainly originating from photon conversions, and heavy flavour hadron decay, depends on the longitudinal and transverse shapes of the electromagnetic showers in the calorimeters, track-cluster matching, and properties of tracks in the ID. All this information, except for hits associated with the track, is used to create a likelihood discriminant. The selection criteria combine the likelihood with the number of track hits and define several working points (WP). Electrons with $p_{\mathrm{T}} > 4.5\,\mathrm{GeV}$ and pseudorapidity range $|\eta| < 2.47$ are selected. The analysis uses a "loose" WP, with an efficiency of at least 90% for electrons with $p_{\mathrm{T}} > 30\,\mathrm{GeV}$ [66].

Muon reconstruction is performed within $|\eta| < 2.7$ [67], covering the entire detector. In the ID coverage range, muon reconstruction primarily applies a global fit of fully reconstructed tracks in the ID and the MS, resulting in combined muons. However, in the central region ($|\eta| < 0.1$), where the MS coverage is limited, alternative methods are employed for muon identification. Muons in this region can be identified either by matching a fully reconstructed ID track to an MS track segment (segment-tagged muons) or by associating with a calorimetric energy deposit consistent with that of a minimum-ionising particle (calorimeter-tagged muons). In these cases, the muon momentum is determined by the ID track alone. In the forward MS region ($2.5 < |\eta| < 2.7$) outside the ID coverage, standalone muons are accepted if they have hits in all three MS layers. Additionally, if forward ID tracks are available, they are combined with standalone MS tracks to form silicon-associated forward muons. Calorimeter-tagged muons are required to have $p_{\mathrm{T}} > 15\,\mathrm{GeV}$, while all other muon candidates must have a minimum transverse momentum of 5 GeV. This analysis uses a "loose" muon identification WP that uses all muon types and has an efficiency of 98.5% [67].

Fake leptons from processes such as WZ and Z+jets are suppressed using impact-parameter and track- and calorimeter-based isolation requirements [66, 67]. The transverse impact-parameter significance is the impact parameter calculated with respect to the measured beamline position in the transverse plane divided by its uncertainty, $|d_0|/\sigma_{d_0}$. This significance

JHEP10(2024)130

is required to be less than 3 for muons and less than 5 for electrons. Leptons must be isolated using both track- and calorimeter-based information. The track-based discriminants take into account the scalar p_{T} sum of all tracks in a cone of width $\Delta R = 0.3$ for muons and 0.2 for electrons (excluding the lepton itself). The ratio of this sum to the lepton p_{T} is required to be less than 0.15. The pile-up contributions are suppressed by requiring the cone tracks to originate from the primary vertex. To retain efficiency at higher p_{T}, the size of the track-isolation cone is reduced to $10\,\mathrm{GeV}/p_{\mathrm{T}}$ for p_{T} above 33 GeV for muons and 50 GeV for electrons. A vertexing algorithm is used to fit the ID tracks of the 4ℓ candidates under the assumption that they emanate from a common vertex. The resulting fit quality, represented by the χ^2/ndof value, provides good discrimination between signal and background. For the 4μ channel, a cut of $\chi^2/\mathrm{ndof} < 9$ is applied, while a cut of $\chi^2/\mathrm{ndof} < 6$ is used for the other channels. This maintains a signal efficiency greater than 99% for all channels.

The reconstruction of jets applies a particle-flow algorithm [68], which combines measurements from the tracker and the calorimeter. The first step is to remove those calorimeter hits that are associated with reconstructed charged particles. Then, the remaining calorimeter energy and tracks matched to the hard interaction are used to create particle-flow objects for the jet reconstruction. The anti-k_t algorithm with a radius parameter of $R = 0.4$ is used to reconstruct particle-flow jets [69]. After the jets are reconstructed, pile-up is subtracted independently of the calibration [70]. Jets are required to have $p_{\mathrm{T}} > 30\,\mathrm{GeV}$ and $|\eta| < 2.5$. A multivariate jet-vertex-tagger algorithm (JVT) is employed to reject low-momentum jets originating from pile-up events. The JVT considers the reconstructed tracks' properties in the event and applies to jets with $p_{\mathrm{T}} < 60\,\mathrm{GeV}$ and $|\eta| < 2.4$ [71, 72].

Events containing b-hadrons (b-jets) are identified using a multivariate tagging algorithm (b-tagging) [73, 74]. This algorithm assesses the likelihood that a jet originates from b-quark hadronisation by analysing track impact parameters and reconstructed secondary vertices. In simulated $t\bar{t}$ events, the jet identification algorithm exhibits an average efficiency of 77% for identifying jets from b-quarks. Additionally, it achieves a rejection factor of approximately 30 for light-flavour quarks (u-, d-, and s-quarks), while the rejection factor for c-quarks and gluons is smaller, as reported in ref. [73].

After object reconstruction, an overlap removal procedure is applied to all selected objects to remove ambiguities resulting from objects being reconstructed by several algorithms. The electron with the highest p_{T} is kept when two electrons have overlapping energy deposits. If a reconstructed electron and muon share the same ID track, the electron is selected if the muon is calorimeter-tagged; otherwise, the muon is selected. Reconstructed jets which overlap with electrons (muons) in a cone of size $\Delta R = 0.2\,(0.1)$ are removed.

The magnitude of the missing transverse momentum is denoted by $E_{\mathrm{T}}^{\mathrm{miss}}$ and is calculated as the magnitude of the negative vectorial sum of the transverse momenta of calibrated leptons and jets. Also, a soft term is included in the calculation, which is constructed from all tracks originating from the primary vertex but not associated with any identified lepton or jet [75]. Selected events must have at least one vertex with two associated tracks with $p_{\mathrm{T}} > 500\,\mathrm{MeV}$, and the primary vertex is chosen to be the vertex with the largest $\sum p_{\mathrm{T}}^2$.

JHEP10(2024)130

4.2 Event selection

This analysis classifies events into three channels based on the flavours of the selected four leptons: 4μ, $4e$, and $2\mu 2e$. These channels are assigned based on the triggers activated in the event, which include single-lepton, dilepton, and trilepton triggers. The possible quadruplets in each channel of an event are created from two same flavour and opposite sign lepton pairs (SFOS). The p_{T} thresholds of the three leading leptons in the quadruplet follow this order: 20 GeV, 15 GeV, and 10 GeV. The leading and the sub-leading lepton pairs in the quadruplet are defined to have an invariant mass closest and second closest to the Z boson mass. The invariant mass of the leading and sub-leading lepton pairs are denoted m_{Z_1} and m_{Z_2}, respectively. In the selected quadruplet, m_{Z_1} must be within $50\,\mathrm{GeV} < m_{Z_1} < 106\,\mathrm{GeV}$, while m_{Z_2} must be within $50\,\mathrm{GeV} < m_{Z_2} < 115\,\mathrm{GeV}$. The selected quadruplets must have their lepton pairs separated from each other by $\Delta R > 0.1$. If any two SFOS leptons are detected with $m_{\ell\ell}$ below 5 GeV for 4μ and $4e$ quadruplets, the quadruplet is excluded to reduce the contamination from J/ψ mesons. In this analysis, the $Z + \Upsilon$ background contribution is negligible. If, at this point, several quadruplets of different channels are selected, only the quadruplet with the highest expected signal rate is retained, in the order: 4μ, $2e2\mu$, $4e$.

The resolution of the four lepton invariant mass system can be improved by recovering the radiative photon production in the Z boson decay (final-state-radiation (FSR)) and by applying constraints on the Z boson mass. In this analysis, the methodology presented in refs. [76–78] for the $h \to ZZ$ analysis was used to account for FSR photons in the reconstruction of Z bosons, and for applying constraints on the Z boson mass. The Z-mass constraint is applied to both Z candidates and improves the resolution of $m_{4\ell}$ by around 15%. This analysis employs the combined 4μ, $4e$, and $2\mu 2e$ channels, collectively called 4ℓ, to account for the limited statistics.

5 Analysis strategy

This analysis searches for heavy resonances that decay to four leptons and missing transverse momentum or jets, where the four-lepton invariant mass is above 200 GeV. The main source of background in this kinematic region involves the leptonic decay of two Z bosons. Among the various background processes, quark-antiquark annihilation ($q\bar{q} \to ZZ$) is the most significant, contributing 84.6% of the expected background, while gluon-initiated production ($gg \to ZZ$) accounts for approximately 11.7%. Other SM backgrounds, such as $q\bar{q} \to ZZ$ (EW), $t\bar{t}V$, Z+jets, $t\bar{t}$, WZ, and VVV, account for about 3.7% of the total background events. These numbers are estimated from simulation after the four-lepton quadruplet selection discussed in section 4.2. In the following, this study models the SM backgrounds using an analytical function, illustrated in section 6, where the normalisation is taken from the data.

A cut-based optimisation was used to increase the sensitivity of the $R \to SH \to 4\ell + E_{\mathrm{T}}^{\mathrm{miss}}$ and $A \to ZH \to 4\ell + X$ signals. This involves setting thresholds on various kinematic and topological variables, such as the number of jets (n_{jets}) and b-jets ($n_{b\text{-jets}}$), the transverse momentum of the four-lepton system ($p_{\mathrm{T}}^{4\ell}$), and the $E_{\mathrm{T}}^{\mathrm{miss}}$ significance ($E_{\mathrm{T}}^{\mathrm{miss}}/\sqrt{\sum E_{\mathrm{T}}}$). The term $\sum E_{\mathrm{T}}$ represents the scalar sum of the transverse energies of all reconstructed objects in the ATLAS detector. These variables exhibit kinematic differences between

JHEP10(2024)130

Signal region	$R \to SH \to 4\ell + E_{\mathrm{T}}^{\mathrm{miss}}$ and $A \to ZH \to 4\ell + X$			
SR1	$n_{b\text{-jets}} = 0$	$n_{\mathrm{jets}} = 0$	$p_{\mathrm{T}}^{4\ell} > 20\,\mathrm{GeV}$	$E_{\mathrm{T}}^{\mathrm{miss}}$ significance >2.0
SR2		$n_{\mathrm{jets}} \geq 1$	$p_{\mathrm{T}}^{4\ell} > 10\,\mathrm{GeV}$	$E_{\mathrm{T}}^{\mathrm{miss}}$ significance > 3.5
SR3			$p_{\mathrm{T}}^{4\ell} < 10\,\mathrm{GeV}$	$2.5 < E_{\mathrm{T}}^{\mathrm{miss}}$ significance < 3.5
	$A \to ZH \to 4\ell + X$			
SR4	$n_{b\text{-jets}} = 0$	$n_{\mathrm{jets}} \geq 2$	$\lvert m_{jj} - m_Z \rvert < 20\,\mathrm{GeV}$	
SR5			$\lvert m_{jj} - m_Z \rvert > 20\,\mathrm{GeV}$	
SR6		$n_{\mathrm{jets}} = 1$		
SR7	$n_{b\text{-jets}} \geq 1$			

Table 2. Summary of the requirements for the signal regions (SR) defined in the search for the $R \to SH \to 4\ell + E_{\mathrm{T}}^{\mathrm{miss}}$ and $A \to ZH \to 4\ell + X$ signals for $m_{4\ell} > 200\,\mathrm{GeV}$.

$R \to SH \to 4\ell + E_{\mathrm{T}}^{\mathrm{miss}}$ and $A \to ZH \to 4\ell + X$ signals and the background processes. The background composition varies depending on the n_{jets} and $n_{b\text{-jets}}$. For the $p_{\mathrm{T}}^{4\ell}$, most background processes peak around 20 GeV, with a tail stretch toward higher values. In contrast, the signal distribution peaks around 40 GeV. This difference in peak positions reflects the characteristic energy distribution of the signal compared to the background processes. Similarly, the $E_{\mathrm{T}}^{\mathrm{miss}}$ significance distribution also demonstrates distinguishable signal and background patterns. Background events peak at a $E_{\mathrm{T}}^{\mathrm{miss}}$ significance of around 1, indicating a relatively low significance of missing transverse energy. In contrast, the signal distribution peaks at a higher $E_{\mathrm{T}}^{\mathrm{miss}}$ significance of around 3, suggesting a stronger presence of genuine missing transverse energy associated with the signal process. Therefore, events with no b-jets are divided into two categories based on the n_{jets}: those with no jets ($n_{\mathrm{jets}} = 0$) and those with at least one jet ($n_{\mathrm{jets}} \geq 1$). A two-dimensional scan is applied twice to each group using $p_{\mathrm{T}}^{4\ell}$ and $E_{\mathrm{T}}^{\mathrm{miss}}$ significance to find the optimal cut between signal and background processes. The first scan determines the optimal threshold values for these variables corresponding to the highest value of the ratio of signal yields to the square root of background yields. After finding the optimal points, the events above these optimal thresholds are removed, and then a second scan is performed on the remaining events. This process results in specific requirements on the variables that define the signal regions (SR). Therefore, events in the SR are required to satisfy the following requirements:

- $n_{b\text{-jets}} = 0$ and $n_{\mathrm{jets}} = 0$ with $p_{\mathrm{T}}^{4\ell} > 20\,\mathrm{GeV}$ and $E_{\mathrm{T}}^{\mathrm{miss}}$ significance > 2.0 (SR1)
- $n_{b\text{-jets}} = 0$ and $n_{\mathrm{jets}} \geq 1$ with $p_{\mathrm{T}}^{4\ell} > 10\,\mathrm{GeV}$ and $E_{\mathrm{T}}^{\mathrm{miss}}$ significance > 3.5 (SR2)
- $n_{b\text{-jets}} = 0$ and $n_{\mathrm{jets}} \geq 1$ with $p_{\mathrm{T}}^{4\ell} < 10\,\mathrm{GeV}$ and $2.5 < E_{\mathrm{T}}^{\mathrm{miss}}$ significance < 3.5 (SR3)

The SRs mentioned above are used for both the $R \to SH \to 4\ell + E_{\mathrm{T}}^{\mathrm{miss}}$ and the $A \to ZH \to 4\ell + X$ models.

Jets in the $A \to ZH \to 4\ell + X$ signal can arise from initial state radiation and the decay of the Z boson. Therefore, it is crucial to accommodate scenarios with varying

JHEP10(2024)130

jet multiplicities and recover the b-jet events left from the abovementioned categorisation. Additionally, the invariant mass of the two leading jets (m_{jj}) shows a significant difference between the $A \to ZH \to 4\ell + X$ signal and backgrounds at $m_{jj} > 300\,\text{GeV}$. Given these differences, more categorisations were designed for the $A \to ZH \to 4\ell + X$ signal. This expanded categorisation comprises four additional SRs to capture distinct jet-related features:

- $n_{b\text{-jets}} = 0$, $n_{\text{jets}} \geq 2$, $|m_{jj} - m_Z| < 20\,\text{GeV}$ (SR4)
- $n_{b\text{-jets}} = 0$, $n_{\text{jets}} \geq 2$, $|m_{jj} - m_Z| > 20\,\text{GeV}$ (SR5)
- $n_{b\text{-jets}} = 0$, $n_{\text{jets}} = 1$ (SR6)
- $n_{b\text{-jets}} \geq 1$ (SR7)

These SRs are only considered if the events are not yet classified in SR1-3. SR6 is motivated by the need to capture signal events in which only one jet is detected. A single jet event occurs if the produced jet has very low momentum and falls outside the detector acceptance. SR7 is designed to include events with at least one b-jet, primarily due to the significant branching ratio of the Z boson into b quarks. Table 2 provides a summary of these seven SRs used in the analysis.

6 Signal and background modelling

Simulation is used to model and then parameterise the constructed $m_{4\ell}$ distribution for the SM backgrounds. Meanwhile, the signal shape is taken directly from the simulation, as illustrated below.

6.1 Signal model

Section 3 discussed the generation of signal mass points for $R \to SH \to 4\ell + E_{\text{T}}^{\text{miss}}$ and $A \to ZH \to 4\ell + X$ signals. Seventy-seven mass points were produced for the $R \to SH \to 4\ell + E_{\text{T}}^{\text{miss}}$ signal, while seventy-two were generated for the $A \to ZH \to 4\ell + X$ signal. To cover a broader mass range, a linear interpolation method described in ref. [79] is used to obtain signal shapes between the generated mass planes in either of the (m_R, m_H) or (m_A, m_H) masses. Interpolating the signal involves a two-step process due to its dependence on either (m_R, m_H) or (m_A, m_H) masses. In the first step, the H mass remains constant while interpolating the $(m_R - m_H)$ or $(m_A - m_H)$ mass parameters or interpolating the R or A mass. Subsequently, the interpolated signals obtained in the previous step serve as input for a second interpolation. In this stage, the R or A mass is fixed, while the H mass varies in steps of 10 GeV.

The interpolation was validated by comparing simulated and interpolated signal distributions at a few mass points, as shown in figure 2 for the $A \to ZH \to 4\ell + X$ $R \to SH \to 4\ell + E_{\text{T}}^{\text{miss}}$ signals. Some disagreement at the tails of the signals is observed and considered as potential systematic uncertainty. This systematic uncertainty was shown to have a negligible impact on the results and was omitted.

JHEP10(2024)130

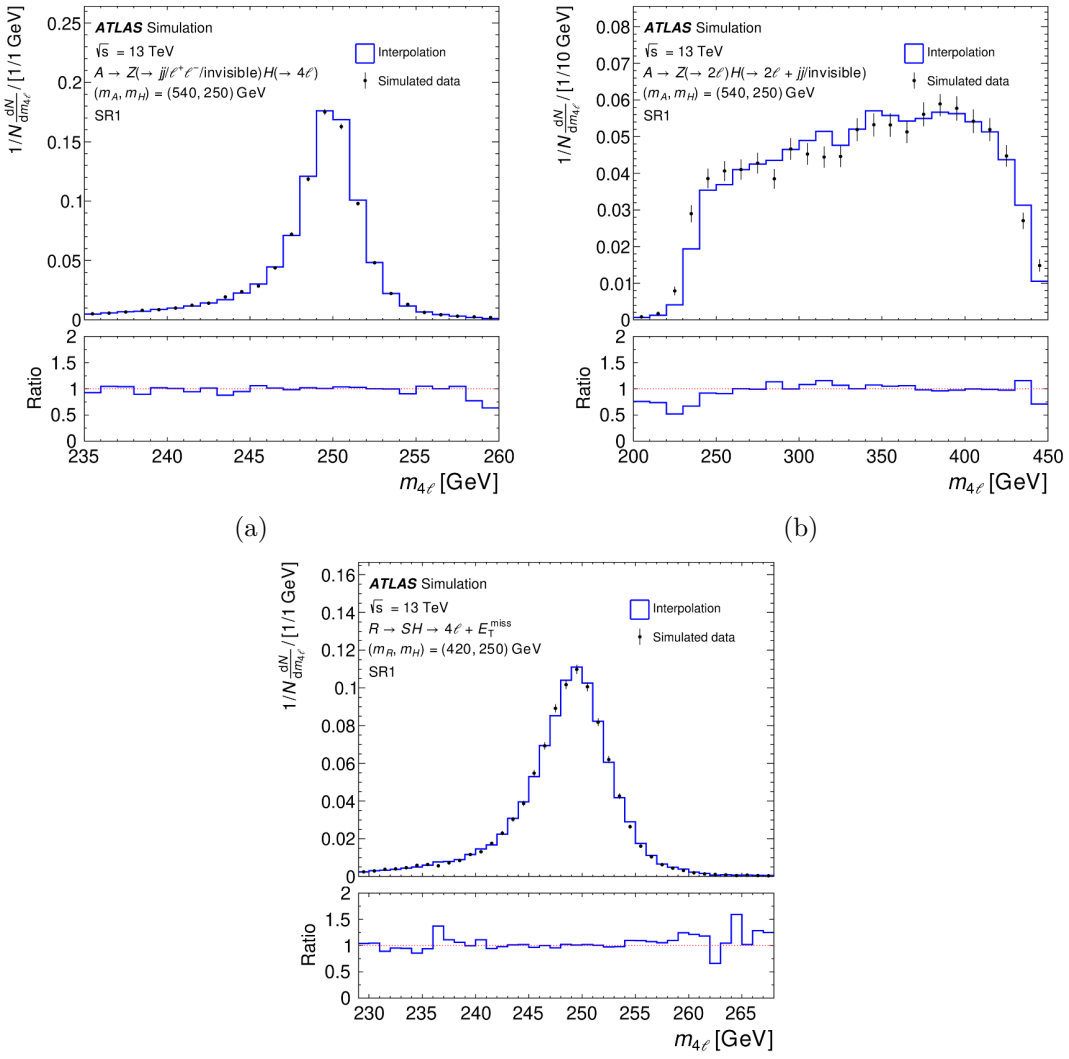

Figure 2. The $m_{4\ell}$ distributions of the interpolated (blue) and simulated (black-filled point) signals for the (a) $A \to Z(\to jj/\ell^+\ell^-/\text{invisible})H(\to 4\ell)$ and (b) $A \to Z(\to \ell^+\ell^-)H(\to 2\ell + jj/\text{invisible})$ signals with the $(m_A, m_H) = (540, 250)\,\text{GeV}$ mass point and the (c) $R \to SH \to 4\ell + E_{\text{T}}^{\text{miss}}$ signal with $(m_R, m_H) = (420, 250)\,\text{GeV}$ and $m_S = 160\,\text{GeV}$. The lower panels show the ratio between the interpolated and simulated histograms. The plots are only shown in SR1 for illustrative purposes.

6.2 Background model

The $m_{4\ell}$ shape of the backgrounds is obtained from simulation using a parameterised empirical function to decrease statistical uncertainties originating from the limited number of simulated events. Four background templates are used: $q\bar{q} \to ZZ$, $gg \to ZZ$, VVV, and other background processes. The other backgrounds contain processes such as $q\bar{q} \to ZZ$ (EW), $t\bar{t}V$, $t\bar{t}$, Z+jets and WZ. Each of the background templates is fitted with an analytical function for $m_{4\ell}$ between 200–1200 GeV, as follows:

$$f(m_{4\ell}) = H(m_0 - m_{4\ell})\, f_1(m_{4\ell})\, C_1 + H(m_{4\ell} - m_0)\, f_2(m_{4\ell})\, C_2, \tag{6.1}$$

JHEP10(2024)130

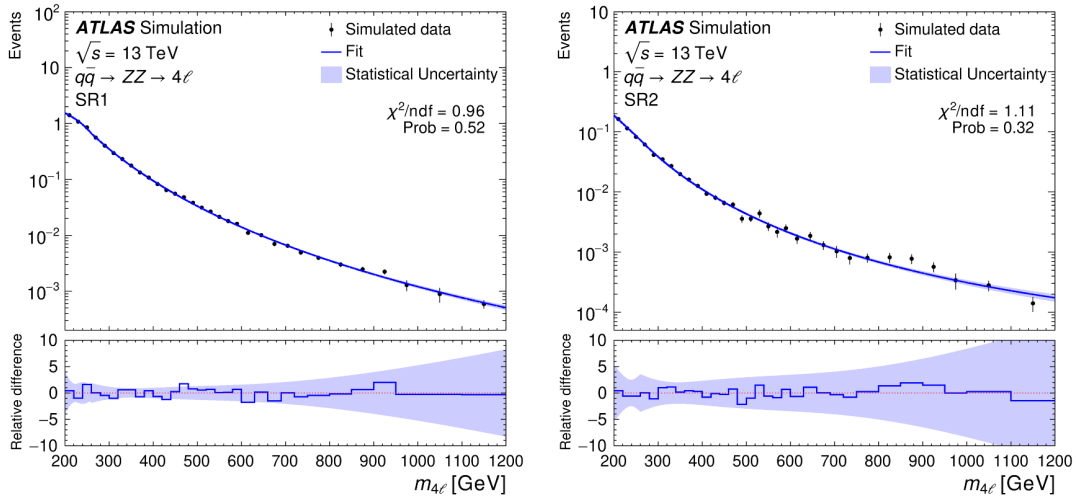

(a) (b)

Figure 3. The $m_{4\ell}$ distributions of the analytical function fit (blue) to the simulated $q\bar{q} \to ZZ$ background (black-filled point) in signal regions (a) SR1 and (b) SR2. The lower panels show the relative difference between the fitted function and simulated histograms. The overlaid light blue band indicates the statistical uncertainty of the fit function.

where:

$$f_1(m_{4\ell}) = \frac{a_1 \cdot m_{4\ell} + a_2 \cdot m_{4\ell}^2}{1 + \exp\left(\frac{m_{4\ell} - a_1}{a_3}\right)}, \tag{6.2}$$

$$f_2(m_{4\ell}) = \left(1 - \frac{m_{4\ell}}{n_C}\right)^{b_1} \cdot \left(\frac{m_{4\ell}}{n_C}\right)^{\left(b_2 + b_3 \cdot \ln\left(\frac{m_{4\ell}}{n_C}\right)\right)}, \tag{6.3}$$

$$C_1 = \frac{1}{f_1(m_0)}, \qquad C_2 = \frac{1}{f_2(m_0)}.$$

The functional form f_1 models the ZZ threshold around $2 \cdot m_Z$, and f_2 describes the high mass tail. The transition between the f_1 and f_2 functions is performed by the Heaviside step function $H(x)$ around m_0, where m_0 is fixed to 260 GeV, 240 GeV, 250 GeV and 230 GeV for the $q\bar{q} \to ZZ$, $gg \to ZZ$, VVV, and other backgrounds, respectively. The transition point is determined by the smoothness of the functional form. A constant $n_C = 13$ TeV scales $m_{4\ell}$ in the high mass region. C_1 and C_2 ensure the continuity of the function around the point m_0, where f_1 and f_2 are joined together. The parameters a_i and b_i are determined by fitting the $m_{4\ell}$ distribution in simulation for each specific SR. Overall, all regions achieved a good fit quality with the empirical function, assessed by the chi-squared values, which are approximately equal to unity for all signal regions. As an example, figure 3 demonstrates the fit of the analytical function given by Equation 6.1 to the dominant $q\bar{q} \to ZZ$ background process in SR1 and SR2. The integral error calculated from the fit function is considered a source of systematic uncertainty. It is treated as a nuisance parameter and propagated as a shape systematic uncertainty to the final fit.

JHEP10(2024)130

7 Systematic uncertainties

This section discusses the sources of systematic uncertainty considered in this analysis, including experimental and theoretical uncertainties for the signal and background processes. Statistical uncertainties arising from the MC event generation are also considered. Additionally, uncertainties introduced by the background parameterisation are considered and propagated to the final fit. The systematic uncertainties are evaluated using the invariant mass of the four lepton system as a discriminant. Each systematic uncertainty component is treated as a nuisance parameter and profiled in the final statistical analysis.

7.1 Experimental uncertainties

Experimental uncertainties, such as object reconstruction and identification, trigger efficiencies, energy scale and resolution, are calculated for signal and background processes. The systematic experimental uncertainties are evaluated by computing the ratio between the integral of the $m_{4\ell}$ distribution with the relevant nuisance parameter weight modified by one standard deviation and the integral of the $m_{4\ell}$ distribution using the nominal weight. Signal samples were divided into three categories depending on the size of the energy gap ($m_A - m_H$ or $m_R - m_H$) to simplify estimating the experimental systematic uncertainties for the signals. The gaps include samples with low ($< 500\,\text{GeV}$), medium ($> 500\,\text{GeV}$ and $< 700\,\text{GeV}$) and high ($> 1300\,\text{GeV}$) energy gaps. These ranges are for the $R \to SH \to 4\ell + E_{\text{T}}^{\text{miss}}$ process, and they are slightly different for the $A \to ZH \to 4\ell + X$ process. The systematic uncertainties are evaluated for three signal mass points from each energy gap for both signals. Each result is combined by calculating the mean of the three samples per energy gap. Only the effect on the absolute normalisation was found to be relevant for the signal. For the VVV and other backgrounds, the absolute normalisation and the shape variation were included in the fit. In contrast, only the shape variation for the $q\bar{q} \to ZZ$ and $gg \to ZZ$ was included as systematic uncertainty in the fit.

The lepton identification, isolation and reconstruction efficiency, energy/momentum scale, and resolution are derived from data using $J/\psi \to \ell\ell$ and $Z \to \ell\ell$ events. The uncertainties in the lepton efficiency are calculated following the method presented in refs. [66, 80] for muons and electrons. Generally, their effect on the signal yields is less than 1% for the $R \to SH \to 4\ell + E_{\text{T}}^{\text{miss}}$ signal, and up to 3.6% for the $A \to ZH \to 4\ell + X$ signal. These uncertainties are no more than 1.5% for the VVV background yields and at most 1.7% for the other background processes. The uncertainties in the jet energy scale and resolution come from sources such as uncertainties in the absolute and relative "in situ" calibration and the correction for pile-up [70]. In total, uncertainties due to the jet energy scale and energy resolution are estimated to a maximum of 4.3% for the $R \to SH \to 4\ell + E_{\text{T}}^{\text{miss}}$ signal, 4.7% for the $A \to ZH \to 4\ell + X$ signal, 7.0% for the VVV background and 10.4% for the other background processes. In addition, flavour tagging uncertainties are calculated by altering the uncertainty of the tagged jet flavour efficiency by $\pm 1\sigma$. The total estimated flavour tagging uncertainties are as high as 4.3% for the $R \to SH \to 4\ell + E_{\text{T}}^{\text{miss}}$ and $A \to ZH \to 4\ell + X$ signals, 8.9% for the VVV background and 8.5% for the other background processes. The uncertainty in the $E_{\text{T}}^{\text{miss}}$ is influenced by uncertainties in the energy scales of both leptons and jets [81]. Furthermore, there are contributions to the $E_{\text{T}}^{\text{miss}}$ uncertainty from the momentum

JHEP10(2024)130

scale and resolution of tracks that are not associated with any identified lepton or jet. The overall uncertainty in $E_{\mathrm{T}}^{\mathrm{miss}}$ due to scale and resolution for the $R \to SH \to 4\ell + E_{\mathrm{T}}^{\mathrm{miss}}$ signal and VVV background is less than 1%. For the $A \to ZH \to 4\ell + X$ signal, these uncertainties are up to 4.7% and 6.2% for the scale and resolution, respectively, while for the other background processes, it is at most 6.1% due to the momentum scale and 9.7% due to the resolution. These experimental systematic uncertainties have a negligible impact on the shape, so only normalisation uncertainties are considered.

The uncertainty in the combined 2015–2018 integrated luminosity is 1.7% [82], obtained using the LUCID-2 detector [83] for the primary luminosity measurements. In addition, a systematic uncertainty from re-scaling the simulated pile-up to the data is considered. It is estimated to be up to 2.5% for the $R \to SH \to 4\ell + E_{\mathrm{T}}^{\mathrm{miss}}$ signal, less than 1% for the $A \to ZH \to 4\ell + X$ signal, and about 3.0% for the VVV and other background processes.

In section 8, a common normalisation factor is introduced to scale the event yields for both $q\bar{q} \to ZZ$ and $gg \to ZZ$ backgrounds while keeping the VVV and other backgrounds fixed to their SM predictions. Subsequently, the relative acceptance difference is calculated between the $q\bar{q} \to ZZ$ and $gg \to ZZ$ backgrounds for each source of the experimental systematic uncertainties. These experimental systematic uncertainties are then propagated to the $gg \to ZZ$ background. Experimental systematic uncertainties, which affect the shape of the $m_{4\ell}$ distribution of the $q\bar{q} \to ZZ$ and $gg \to ZZ$ backgrounds, are considered in the analysis as shape systematic uncertainties.

7.2 Theoretical uncertainties

This analysis considers the uncertainties of the PDF, missing high-order QCD correction, initial- and final-state radiation (ISR/FSR), and parton showering (PS) and hadronisation. The theoretical scale uncertainties on the signal samples are assessed by varying the factorisation and renormalisation scales up and down from their nominal values by a factor of two in each SR. The largest effect of the scale uncertainties is taken as the systematic uncertainty. The PDF uncertainty is estimated using the SysCalc [84] package in conjunction with Madgraph5_aMC@NLO 2.9.5. The uncertainty is determined by considering how the envelope of variations among alternative PDFs differs from the internal PDF error sets (NNPDF2.3 PDF). The calculation follows the PDF4LHC recommendations provided in ref. [85]. Uncertainties related to the ISR/FSR, PS and hadronisation are evaluated by employing variations in tune eigenvectors in Pythia and comparing Herwig 7.1.3 [86] with Pythia 8.230 for the signal samples. The impact of the theoretical uncertainties on the signal acceptance is about 1%. The theoretical systematic uncertainties on the SM backgrounds are included as a shape systematic on the $m_{4\ell}$ distribution and summarised below.

7.3 Systematic uncertainties on background shapes

To account for any possible biases introduced by the analytical function discussed in section 6.2, uncertainties stemming from the background parameterisation are considered. These uncertainties are calculated by evaluating the error in the fit parameters while also taking into account the errors in the parameters resulting from the fit. The errors are estimated using the correlation values obtained from the fit.

JHEP10(2024)130

Incorporating PDF and QCD scale uncertainties into the analysis is motivated by their impact on the shape of the $m_{4\ell}$ distributions for the $q\bar{q} \to ZZ$ and $gg \to ZZ$ processes. The QCD scale uncertainty is estimated to be up to 10% for the $q\bar{q} \to ZZ$ and $gg \to ZZ$ backgrounds. The PDF uncertainty is less than 5% (1%) in the low mass region and about 25% (30%) in the high mass region for the $q\bar{q} \to ZZ$ ($gg \to ZZ$) background. A missing higher-order QCD correction uncertainty on the $m_{4\ell}$ shape is considered for the $q\bar{q} \to ZZ$ background, which is estimated to be less than 10%. The parton shower uncertainty is evaluated by varying parameters in the parton shower tunes, such as the CKKW and QSF settings, and by using different showering options.

8 Statistical procedures

The invariant mass of the four leptons is used as a discriminant to examine the null and alternative hypotheses using the profile likelihood ratio technique [87]. The null hypothesis corresponds to smoothed backgrounds that fall from the low mass range to the higher mass range of the $m_{4\ell}$ distribution. In contrast, the alternative hypothesis incorporates a signal structure around the H mass. The signal and background contributions in the $m_{4\ell}$ distribution are extracted via a binned maximum-likelihood fit of the signal-plus background hypotheses to extract any indication for new physics. The profile likelihood function is defined as the probability of observing n events. It is calculated as the product of the sum of weighted signal and background events, as shown below:

$$\mathcal{L}(m_{4\ell}^{n}|\sigma(gg \to A/R), \vec{\theta}) = \prod_{r=\text{SRs}}^{n_r} \prod_{i=\text{bin}}^{n_i} \text{Poisson}\left(n_{r,i} \mid s_{r,i} + \sum_{b} b_{r,i}(\vec{\theta})\right) \times \prod_{i} G_i(0|\vec{\theta}, 1), \quad (8.1)$$

where $\sigma(gg \to A/R)$ is the parameter of interest for the $A \to ZH \to 4\ell + X$ or $R \to SH \to 4\ell + E_{\text{T}}^{\text{miss}}$ signal. The expected signal and background yields in each $m_{4\ell}$ distribution bin are represented by s and b, respectively. The expected signal yield s is calculated by:

$$s = \sigma(gg \to A/R) \times \mathcal{B}(A/R \to ZH/SH) \times \mathcal{B}(H \to ZZ) \times AC \times \int L \, \mathrm{d}t, \quad (8.2)$$

where AC is the acceptance times efficiency, and $\int L \, \mathrm{d}t = 139\,\mathrm{fb}^{-1}$ is the integrated luminosity of the data. A collection of nuisance parameters is introduced to describe how systematic uncertainties influence the predicted number of signal and background events and the shape of the PDFs. These parameters are constrained to their nominal values within the calculated uncertainties using Gaussian constraints by $G(\vec{\theta})$, in which $\vec{\theta}$ is a vector containing the nuisance parameters. In the likelihood fit function, SRs are indicated in the product by the index "r". In each SR, the normalisation for the $q\bar{q} \to ZZ$ and $gg \to ZZ$ processes (ZZ background) are calculated by a likelihood fit to the data. The ZZ background normalisation is denoted by the μ_{norm}^{ZZ} parameter. The benefit of taking the ZZ background normalisation from the data is the reduction of the background dependence on the theoretical systematic uncertainties.

9 Results

Table 3 displays the yields in each of the seven SRs described in section 5. The observed and expected numbers of events in each SR were obtained using a simultaneous binned

JHEP10(2024)130

	SR1	SR2	SR3	SR4	SR5	SR6	SR7
$q\bar{q} \to ZZ$	132 ± 12	17 ± 6	42 ± 7	40 ± 7	156 ± 13	549 ± 70	86 ± 11
$gg \to ZZ$	32 ± 6	3.2 ± 3.1	8.3 ± 3.1	6.6 ± 2.8	22.1 ± 3.7	102 ± 70	9.4 ± 4.2
VVV	7.5 ± 0.4	4.77 ± 0.34	1.49 ± 0.19	0.19 ± 0.04	1.08 ± 0.11	1.59 ± 0.13	0.50 ± 0.07
Other backgrounds	5.5 ± 0.9	7.1 ± 1.1	3.6 ± 0.7	2.47 ± 0.30	17.5 ± 0.8	11.3 ± 0.8	37.6 ± 2.3
Total background	177 ± 13	32 ± 6	55 ± 7	49 ± 7	197 ± 14	664 ± 26	134 ± 12
Observed	177	32	55	49	197	664	135
μ^{ZZ}_{norm}	1.15 ± 0.15	1.3 ± 0.6	0.96 ± 0.22	0.90 ± 0.17	0.80 ± 0.08	1.02 ± 0.13	1.4 ± 0.3

Table 3. Observed and expected post-fit event yields for $m_{4\ell} > 200\,\text{GeV}$ with their uncertainties. The expected yields and their uncertainties are obtained from a simultaneous fit to data under the background-only hypothesis on all seven signal regions discussed in section 5. The μ^{ZZ}_{norm} is the normalisation factor for the $q\bar{q} \to ZZ$ and $gg \to ZZ$ backgrounds. The other backgrounds include $q\bar{q} \to ZZ$ (EW), $t\bar{t}V$, $t\bar{t}$, Z+jets and WZ processes. These backgrounds and the VVV background process were fixed to their SM prediction.

maximum-likelihood fit, assuming the background-only hypothesis. Signal+background binned maximum-likelihood fits were also performed on the $m_{4\ell}$ distribution to search for potential excesses beyond the expected SM backgrounds. This fit model is based on the statistical framework discussed in section 8. The m_R (m_A) range 390–1300 (320–1300) GeV and the m_H range 220–1000 GeV were scanned for the $R \to SH \to 4\ell + E_{\text{T}}^{\text{miss}}$ ($A \to ZH \to 4\ell + X$) search. The fit was performed in steps of 10 GeV, in which 4187 (m_R, m_H) and 4740 (m_A, m_H) mass points in NWA for each SR were tested for the $R \to SH \to 4\ell + E_{\text{T}}^{\text{miss}}$ and $A \to ZH \to 4\ell + X$ processes, respectively. The resulting test statistics were used to construct p-values and significance estimates, which were then used to evaluate the compatibility of the data with the background-only hypothesis and the presence of new physics in the data.

The four lepton invariant mass distributions for the $R \to SH \to 4\ell + E_{\text{T}}^{\text{miss}}$ search with the $(m_R, m_H) = (500, 300)\,\text{GeV}$ mass point in all three SRs are shown in figure 4. Figures 5 and 6 show the $m_{4\ell}$ distribution in the seven SRs defined for the $A \to ZH \to 4\ell + X$ search with the $(m_A, m_H) = (510, 380)\,\text{GeV}$ mass point. These plots are shown for a background-only fit to data, and signals are overlaid after being scaled to the observed upper limit on the cross-section. In the presented figures, statistical fluctuations are dominant, particularly in the high mass region of the $m_{4\ell}$. The binning was determined by considering the width and the stability of the upper limit on the cross-section of the $R \to SH \to 4\ell + E_{\text{T}}^{\text{miss}}$ and $A \to ZH \to 4\ell + X$ signals. The upper limit calculations were performed in bins with a fixed width of 5 GeV. However, for better visualisation, the plots are presented with variable binning.

No significant deviation from the SM backgrounds is observed in the data. Local excesses around two standard deviations for a few mass points are shown in figure 7(a) for the $R \to SH \to 4\ell + E_{\text{T}}^{\text{miss}}$ signal and in figure 7(b) for the $A \to ZH \to 4\ell + X$ signal. The most significant excess comes from the $A \to ZH \to 4\ell + X$ signal at the $(m_A, m_H) = (510, 380)\,\text{GeV}$ mass point with a local significance of 2.5 standard deviations. The impact of systematic uncertainties on the analysis is investigated based on their impact on the parameter of interest (best-fit cross-section) for the $R \to SH \to 4\ell + E_{\text{T}}^{\text{miss}}$ and $A \to ZH \to 4\ell + X$

JHEP10(2024)130

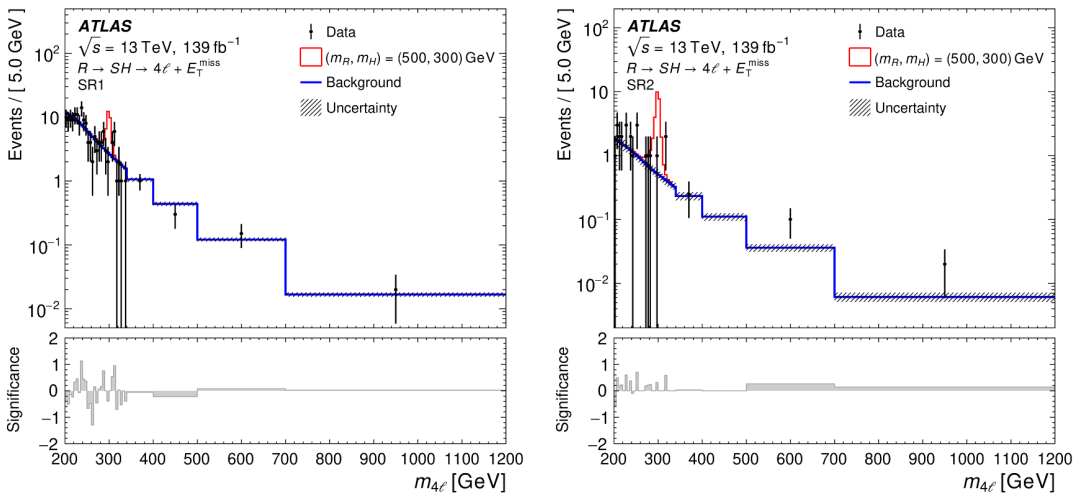

Figure 4. Observed and expected distributions of the invariant mass of the four-lepton system in the $R \to SH \to 4\ell + E_{\mathrm{T}}^{\mathrm{miss}}$ search for (a) SR1, (b) SR2 and (c) SR3 under a background-only fit to data. The total background (blue) includes the $q\bar{q} \to ZZ$, $gg \to ZZ$, $q\bar{q} \to ZZ$ (EW), VVV, $t\bar{t}V$, $t\bar{t}$, Z+jets and WZ processes. The overlaid distribution of the $(m_R, m_H) = (500, 300)$ GeV signal (red) is normalised to the observed upper limit on the cross-section (25.0 fb) discussed in section 9. The hatched lines show the systematic uncertainty of the background prediction, while the error bar on the data denote the statistical uncertainty. The lower panel displays the significance of each bin, which is determined by the residual of the data corresponding to the fitted background taking the statistical uncertainty of the data into account. The fit is performed in bins of 5 GeV width, while the plots are re-binned using variable binning for presentation purposes.

JHEP10(2024)130

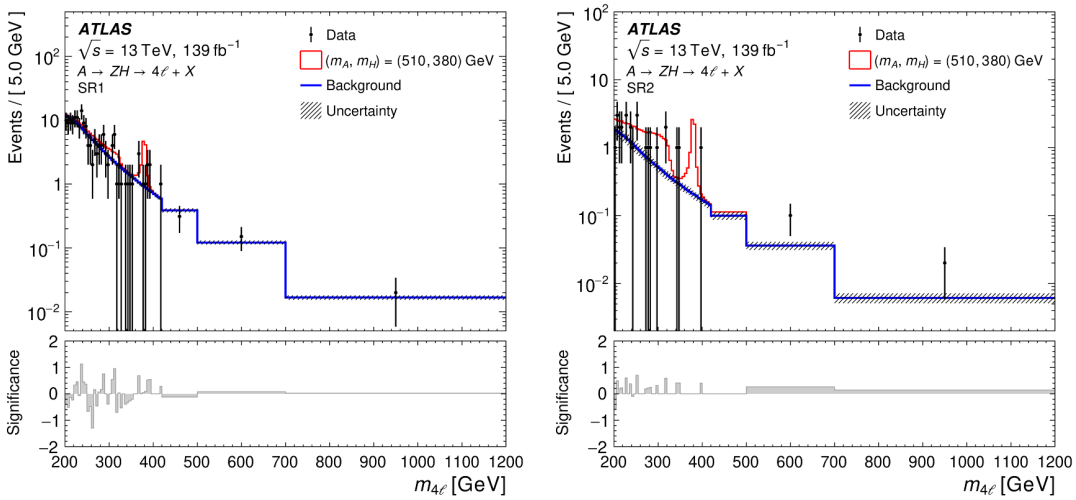

(a)

(b)

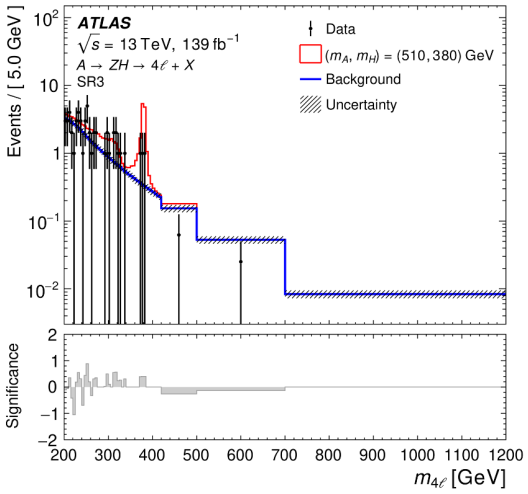

(c)

Figure 5. Observed and expected distributions of the invariant mass of the four-lepton system in the $A \to ZH \to 4\ell + X$ search for (a) SR1, (b) SR2 and (c) SR3 under a background-only fit to data. The total background (blue) includes the $q\bar{q} \to ZZ$, $gg \to ZZ$, $q\bar{q} \to ZZ$ (EW), VVV, $t\bar{t}V$, $t\bar{t}$, Z+jets and WZ processes. The overlaid distribution of the $(m_A, m_H) = (510, 380)$ GeV signal (red) is normalised to the observed upper limit on the cross-section (29.9 fb) discussed in section 9. The hatched lines show the systematic uncertainty of the background prediction, while the error bar on the data denote the statistical uncertainty. The lower panel displays the significance of each bin, which is determined by the residual of the data corresponding to the fitted background taking the statistical uncertainty of the data into account. The fit is performed in bins of 5 GeV width, while the plots are re-binned using variable binning for presentation purposes.

JHEP10(2024)130

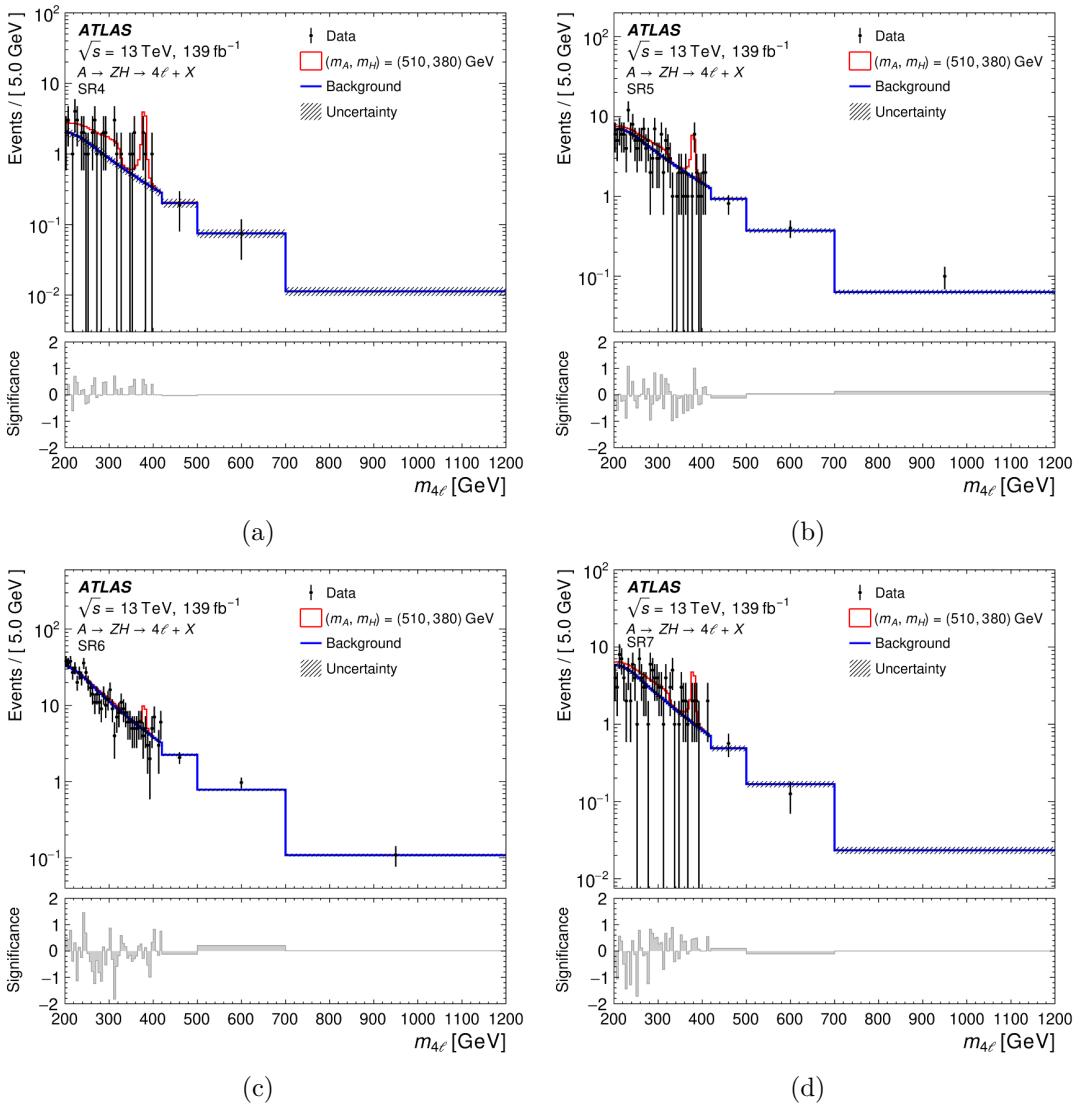

Figure 6. Observed and expected distributions of the invariant mass of the four-lepton system in the $A \to ZH \to 4\ell + X$ search for (a) SR4, (b) SR5, (c) SR6 and (d) SR7 under a background-only fit to data. The total background (blue) includes the $q\bar{q} \to ZZ$, $gg \to ZZ$, $q\bar{q} \to ZZ$ (EW), VVV, $t\bar{t}V$, $t\bar{t}$, Z+jets and WZ processes. The overlaid distribution of the $(m_A, m_H) = (510, 380)$ GeV signal (red) is normalised to the observed upper limit on the cross-section (29.9 fb) discussed in section 9. The hatched lines show the systematic uncertainty of the background prediction, while the error bar on the data denote the statistical uncertainty. The lower panel displays the significance of each bin, which is determined by the residual of the data corresponding to the fitted background taking the statistical uncertainty of the data into account. The fit is performed in bins of 5 GeV width, while the plots are re-binned using variable binning for presentation purposes.

JHEP10(2024)130

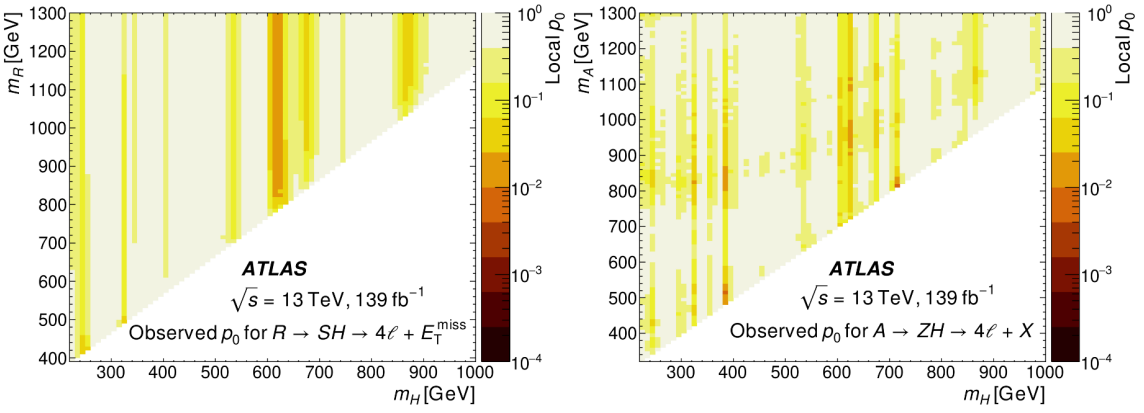

(a) (b)

Figure 7. Local p_0-values in the (m_H, m_R) plane for (a) the $R \to SH \to 4\ell + E_{\mathrm{T}}^{\mathrm{miss}}$ search with $m_S = 160\,\mathrm{GeV}$, and in the (m_H, m_A) plane for (b) the $A \to ZH \to 4\ell + X$ search.

signals. The uncertainties that have the most significant impact vary depending on the choice of the (m_R, m_H) or (m_A, m_H) mass points. Table 4 shows the first five leading sources of uncertainties in the best-fit σ value for three different mass points for each signal. The effect of the uncertainties is estimated using Asimov data produced with the signal cross-section set to the expected limits for the particular (m_R, m_H) or (m_A, m_H) mass points, assuming narrow width R or A and H bosons. In the $R \to SH \to 4\ell + E_{\mathrm{T}}^{\mathrm{miss}}$ search, systematic uncertainties related to jet characteristics, such as jet flavour composition, played a significant role and ranked first and second at mass points $(m_R, m_H) = (390, 220)\,\mathrm{GeV}$ and $(m_R, m_H) = (1300, 1000)\,\mathrm{GeV}$, respectively. It is noteworthy that the uncertainties associated with jet characteristics remained significant and played a pivotal role in the overall uncertainty assessment for both the $R \to SH \to 4\ell + E_{\mathrm{T}}^{\mathrm{miss}}$ and $A \to ZH \to 4\ell + X$ searches.

As no significant excess was observed in comparison to the background predictions, the results were translated into upper limits on the production cross-section of the $R \to SH \to 4\ell + E_{\mathrm{T}}^{\mathrm{miss}}$ and $A \to ZH \to 4\ell + X$ signals times the branching fractions. The branching fractions considered are $\mathcal{B}(R \to SH)$ and $\mathcal{B}(H \to ZZ)$ for the $R \to SH \to 4\ell + E_{\mathrm{T}}^{\mathrm{miss}}$ process. For the $A \to ZH \to 4\ell + X$ process, the branching fractions are $\mathcal{B}(A \to ZH)$ and $\mathcal{B}(H \to ZZ)$. The CL_s approach in the asymptotic approximation [87, 88] was used to calculate upper limits at 95% confidence level (CL) across the explored phase space. The upper limit, either on $\sigma(gg \to R) \times \mathcal{B}(R \to SH) \times \mathcal{B}(H \to ZZ)$ or on $\sigma(gg \to A) \times \mathcal{B}(A \to ZH) \times \mathcal{B}(H \to ZZ)$, for a specific mass hypothesis, is obtained by fixing the H mass parameter to a constant value and optimising the probability function for nuisance parameters. The observed and expected upper limits of NWA R and H bosons for the $R \to SH \to 4\ell + E_{\mathrm{T}}^{\mathrm{miss}}$ search are shown in figures 8(a) and 8(b) in the (m_H, m_R) plane where the z-axis displays the upper limits on $\sigma(gg \to R) \times \mathcal{B}(R \to SH) \times \mathcal{B}(H \to ZZ)$ in fb. The observed upper limits for the $R \to SH \to 4\ell + E_{\mathrm{T}}^{\mathrm{miss}}$ search range from 6.8 fb for $(m_R, m_H) = (1300, 980)\,\mathrm{GeV}$ to 119.2 fb for $(m_R, m_H) = (410, 240)\,\mathrm{GeV}$. In contrast, the expected upper limits vary from 7.7 fb to 70.3 fb for the same mass points. Similarly, figures 8(c) and 8(d) show the observed and expected upper limits for the $A \to ZH \to 4\ell + X$ search in the (m_H, m_A) plane, in which the z-axis

JHEP10(2024)130

$R \to SH \to 4\ell + E_{\mathrm{T}}^{\mathrm{miss}}$			$A \to ZH \to 4\ell + X$		
(m_R, m_H) [GeV]	Uncertainty source	$\Delta\sigma/\sigma$ [%]	(m_A, m_H) [GeV]	Uncertainty source	$\Delta\sigma/\sigma$ [%]
	Jet flavour composition	6.2		Other backgrounds parameterisation SR7	5.0
	Jet flavour response	4.8		$q\bar{q} \to ZZ$ parameterisation SR7	3.9
$(390, 220)$	Jet energy scale	4.2	$(320, 220)$	Jet flavour composition	3.9
	Pile-up reweighting	4.0		Luminosity	3.7
	CKKW parton showering ($gg \to ZZ$) SR2	3.8		$gg \to ZZ$ parameterisation SR6	3.6
	CKKW parton showering ($gg \to ZZ$) SR2	3.1		Luminosity	2.4
	QSF parton showering ($gg \to ZZ$) SR2	3.0		Jet flavour composition	2.4
$(500, 300)$	$q\bar{q} \to ZZ$ parameterisation SR2	2.0	$(510, 380)$	Jet energy scale	1.7
	Pile-up reweighting	1.9		Jet energy resolution	1.5
	VVV parameterisation SR2	1.9		Signal PDF	1.4
	$q\bar{q} \to ZZ$ parameterisation SR2	9.3		CKKW parton showering ($gg \to ZZ$) SR2	3.3
	Jet flavour composition	7.3		QSF parton showering ($gg \to ZZ$) SR2	3.3
$(1300, 1000)$	Jet flavour response	3.5	$(1300, 1000)$	Other backgrounds parameterisation SR2	2.6
	Pile-up reweighting	2.9		$q\bar{q} \to ZZ$ parameterisation SR5	2.1
	CKKW parton showering ($gg \to ZZ$) SR2	2.9		VVV parameterisation SR2	2.1

Table 4. The impact of the most important sources of uncertainty on the best-fit value of the signal cross-section for three mass points for each $R \to SH \to 4\ell + E_{\mathrm{T}}^{\mathrm{miss}}$ and $A \to ZH \to 4\ell + X$ signals after the fit. Sum in quadrature of the upward and downward effects ($\Delta\sigma$) is divided by the best fit value of the signal cross-section (σ) for each signal. Shape uncertainties are uncorrelated and hence affect each region separately.

represents the upper limits on $\sigma(gg \to A) \times \mathcal{B}(A \to ZH) \times \mathcal{B}(H \to ZZ)$. For the $A \to ZH \to 4\ell + X$ search, the observed upper limits range from 2.1 fb for $(m_A, m_H) = (1300, 760)$ GeV to 32.3 fb for $(m_A, m_H) = (430, 240)$ GeV, whereas the corresponding expected upper limits range from 2.9 fb to 18.8 fb. Pseudo-experiments were used to calculate upper limits for various mass points, but the results did not significantly deviate from the asymptotic upper limits.

The analysis focuses on studying heavy resonances with NWA A or R and H bosons produced via gluon-fusion for the $A \to ZH \to 4\ell + X$ and $R \to SH \to 4\ell + E_{\mathrm{T}}^{\mathrm{miss}}$ processes. However, the effect of the LWA in a similar scenario was also checked. For this purpose, two low and high mass points, $(m_A, m_H) = (320, 220)$ GeV and $(m_A, m_H) = (1190, 600)$ GeV, for the $A \to ZH \to 4\ell + X$ signal were generated using similar configurations as for the NWA signal. Upper limits were computed for signal assumptions in which the A and H bosons have a significant natural width relative to the true mass. They were found to increase as the natural width of the A and H bosons increases. For example, in the case of an $A \to ZH \to 4\ell + X$ signal that produces A and H bosons with natural widths of 15% and 5%, respectively, of their true mass, the upper limit worsened by a factor of 1.4 for the low mass point and 1.7 for the high mass point compared to the NWA upper limit. In the $(\Gamma_A/m_A, \Gamma_H/m_H) = (30\%, 10\%)$ case, the upper limit is worsened by a factor of 1.7 for the low mass point and by a factor of 1.9 for the high mass point when compared to the NWA scenario. Table 5 summarises width assumptions, mass points and upper limits for LWA and NWA signals.

JHEP10(2024)130

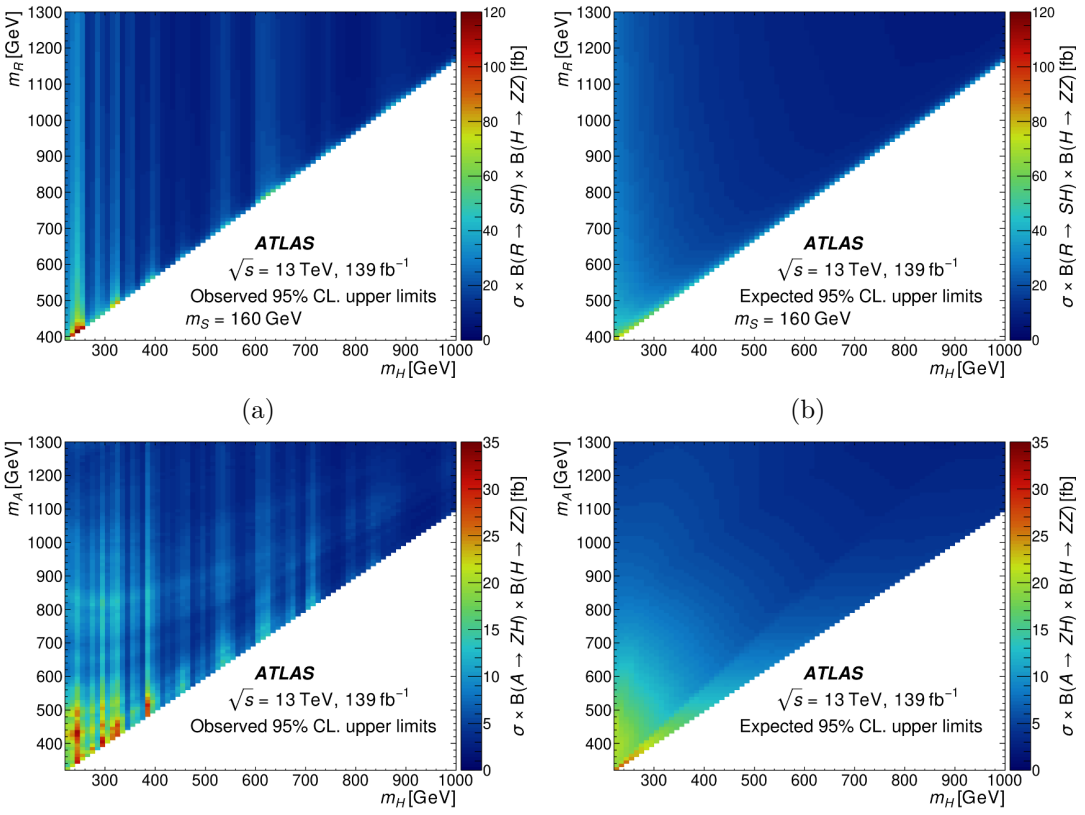

Figure 8. The observed (left) and expected (right) upper limits at 95% confidence level on (a)–(b) $\sigma(gg \to R) \times \mathcal{B}(R \to SH) \times \mathcal{B}(H \to ZZ)$ across the (m_H, m_R) plane with $m_S = 160\,\text{GeV}$ for the $R \to SH \to 4\ell + E_{\text{T}}^{\text{miss}}$ search, and on (c)–(d) $\sigma(gg \to A) \times \mathcal{B}(A \to ZH) \times \mathcal{B}(H \to ZZ)$ across the (m_H, m_A) plane for the $A \to ZH \to 4\ell + X$ search.

Width assumptions	Mass points [GeV]	Upper limits in the $\sigma(gg \to A)$ [fb]		Ratio w.r.t Narrow width
		Observed	Expected	
Narrow width	$(m_A, m_H) = (320, 220)$	19.6	25.1	1.0
	$(m_A, m_H) = (1190, 600)$	4.8	3.5	1.0
$(\Gamma_A/m_A, \Gamma_H/m_H) = (15\%, 5\%)$	$(m_A, m_H) = (320, 220)$	31.5	36.2	1.4
	$(m_A, m_H) = (1190, 600)$	8.3	6.0	1.7
$(\Gamma_A/m_A, \Gamma_H/m_H) = (30\%, 10\%)$	$(m_A, m_H) = (320, 220)$	38.9	42.5	1.7
	$(m_A, m_H) = (1190, 600)$	8.9	6.6	1.9

Table 5. Observed and expected upper limits at 95% confidence level (CL) on the $\sigma(gg \to A) \times \mathcal{B}(A \to ZH) \times \mathcal{B}(H \to ZZ)$ for different large width approximation signals for comparison with the narrow width approximation. The fraction in the rightmost column corresponds to the ratio between the expected upper limits with large- or narrow width signals. The Γ_A and Γ_H denote the widths of the A and H bosons, respectively.

JHEP10(2024)130

10 Conclusion

A search for new heavy resonances is performed in a final state with four leptons and missing transverse energy or jets. The search uses proton-proton collision data at a centre-of-mass energy of 13 TeV collected by the ATLAS detector from 2015 to 2018 at the Large Hadron Collider corresponding to a total integrated luminosity of 139 fb^{-1}. The search focuses on two signal processes: $R \to SH \to 4\ell + E_{\text{T}}^{\text{miss}}$ and $A \to ZH \to 4\ell + X$. For the $R \to SH \to 4\ell + E_{\text{T}}^{\text{miss}}$ search, the R boson decays to S and H bosons, where $S \to$ invisible and $H \to ZZ \to 4\ell$. In the $A \to ZH \to 4\ell + X$ search, the A boson decays to Z and H bosons, with two possible decay modes considered for the associated production of Z and H bosons: $A \to Z(\to jj/\ell^+\ell^-/\text{invisible})H(\to 4\ell)$ and $A \to Z(\to 2\ell)H(\to 2\ell + jj/\text{invisible})$. For both the $A \to ZH \to 4\ell + X$ and $R \to SH \to 4\ell + E_{\text{T}}^{\text{miss}}$ processes, the heavy boson H mass is between 220 GeV and 1000 GeV. The mass range considered for the hypothetical resonance is in the range of 320–1300 GeV for the A boson and 390–1300 GeV for the R boson, while the S boson mass is fixed at 160 GeV, without any significant impact on the results.

No significant deviation above the SM backgrounds is observed. The results are translated into upper limits on $\sigma(gg \to R) \times \mathcal{B}(R \to SH) \times \mathcal{B}(H \to ZZ)$ and $\sigma(gg \to A) \times \mathcal{B}(A \to ZH) \times \mathcal{B}(H \to ZZ)$ at 95% confidence level. For the $R \to SH \to 4\ell + E_{\text{T}}^{\text{miss}}$ search, the observed (expected) upper limits range from 6.8–119.2 (7.6–75.8) fb for $(m_R, m_H) = (390, 220)$ GeV to $(m_R, m_H) = (1300, 1000)$ GeV. For the $A \to ZH \to 4\ell + X$ search, the observed (expected) upper limits range from 2.1–32.3 (2.7–25.8) fb for $(m_A, m_H) = (320, 220)$ GeV to $(m_A, m_H) = (1300, 1000)$ GeV. This complements previous $A \to ZH$ searches in various channels (as discussed in section 1) and contributes to a more comprehensive understanding of the behaviour of A and H bosons. Furthermore, the $R \to SH \to 4\ell + E_{\text{T}}^{\text{miss}}$ search extends the gluon-fusion production of the $H \to ZZ \to 4\ell$ inclusive analysis, incorporating the possibility of missing transverse energy in the four-lepton final states and extending the phase-space of the search.

Acknowledgments

We thank CERN for the very successful operation of the LHC and its injectors, as well as the support staff at CERN and at our institutions worldwide without whom ATLAS could not be operated efficiently.

The crucial computing support from all WLCG partners is acknowledged gratefully, in particular from CERN, the ATLAS Tier-1 facilities at TRIUMF/SFU (Canada), NDGF (Denmark, Norway, Sweden), CC-IN2P3 (France), KIT/GridKA (Germany), INFN-CNAF (Italy), NL-T1 (Netherlands), PIC (Spain), RAL (U.K.) and BNL (U.S.A.), the Tier-2 facilities worldwide and large non-WLCG resource providers. Major contributors of computing resources are listed in ref. [89].

We gratefully acknowledge the support of ANPCyT, Argentina; YerPhI, Armenia; ARC, Australia; BMWFW and FWF, Austria; ANAS, Azerbaijan; CNPq and FAPESP, Brazil; NSERC, NRC and CFI, Canada; CERN; ANID, Chile; CAS, MOST and NSFC, China; Minciencias, Colombia; MEYS CR, Czech Republic; DNRF and DNSRC, Denmark; IN2P3-CNRS and CEA-DRF/IRFU, France; SRNSFG, Georgia; BMBF, HGF and MPG, Germany;

JHEP10(2024)130

GSRI, Greece; RGC and Hong Kong SAR, China; ISF and Benoziyo Center, Israel; INFN, Italy; MEXT and JSPS, Japan; CNRST, Morocco; NWO, Netherlands; RCN, Norway; MEiN, Poland; FCT, Portugal; MNE/IFA, Romania; MESTD, Serbia; MSSR, Slovakia; ARIS and MVZI, Slovenia; DSI/NRF, South Africa; MICINN, Spain; SRC and Wallenberg Foundation, Sweden; SERI, SNSF and Cantons of Bern and Geneva, Switzerland; NSTC, Taipei; TENMAK, Türkiye; STFC/UKRI, United Kingdom; DOE and NSF, United States of America.

Individual groups and members have received support from BCKDF, CANARIE, CRC and DRAC, Canada; CERN-CZ, PRIMUS 21/SCI/017 and UNCE SCI/013, Czech Republic; COST, ERC, ERDF, Horizon 2020, ICSC-NextGenerationEU and Marie Skłodowska-Curie Actions, European Union; Investissements d'Avenir Labex, Investissements d'Avenir Idex and ANR, France; DFG and AvH Foundation, Germany; Herakleitos, Thales and Aristeia programmes co-financed by EU-ESF and the Greek NSRF, Greece; BSF-NSF and MINERVA, Israel; Norwegian Financial Mechanism 2014-2021, Norway; NCN and NAWA, Poland; La Caixa Banking Foundation, CERCA Programme Generalitat de Catalunya and PROMETEO and GenT Programmes Generalitat Valenciana, Spain; Göran Gustafssons Stiftelse, Sweden; The Royal Society and Leverhulme Trust, United Kingdom.

In addition, individual members wish to acknowledge support from CERN: European Organization for Nuclear Research (CERN PJAS); Chile: Agencia Nacional de Investigación y Desarrollo (FONDECYT 1190886, FONDECYT 1210400, FONDECYT 1230812, FONDECYT 1230987); China: National Natural Science Foundation of China (NSFC — 12175119, NSFC 12275265, NSFC-12075060); Czech Republic: PRIMUS Research Programme (PRIMUS/21/SCI/017); EU: H2020 European Research Council (ERC — 101002463); European Union: European Research Council (ERC — 948254, ERC 101089007), Horizon 2020 Framework Programme (MUCCA — CHIST-ERA-19-XAI-00), European Union, Future Artificial Intelligence Research (FAIR-NextGenerationEU PE00000013), Italian Center for High Performance Computing, Big Data and Quantum Computing (ICSC, NextGenerationEU); France: Agence Nationale de la Recherche (ANR-20-CE31-0013, ANR-21-CE31-0013, ANR-21-CE31-0022, ANR-22-EDIR-0002), Investissements d'Avenir Labex (ANR-11-LABX-0012); Germany: Baden-Württemberg Stiftung (BW Stiftung-Postdoc Eliteprogramme), Deutsche Forschungsgemeinschaft (DFG — 469666862, DFG — CR 312/5-1); Italy: Istituto Nazionale di Fisica Nucleare (ICSC, NextGenerationEU), Ministero dell'Università e della Ricerca (PRIN — 20223N7F8K — PNRR M4.C2.1.1); Japan: Japan Society for the Promotion of Science (JSPS KAKENHI JP21H05085, JSPS KAKENHI JP22H01227, JSPS KAKENHI JP22H04944, JSPS KAKENHI JP22KK0227); Netherlands: Netherlands Organisation for Scientific Research (NWO Veni 2020 — VI.Veni.202.179); Norway: Research Council of Norway (RCN-314472); Poland: Polish National Agency for Academic Exchange (PPN/PPO/2020/1/00002/U/00001), Polish National Science Centre (NCN 2021/42/E/ST2/00350, NCN OPUS nr 2022/47/B/ST2/03059, NCN UMO-2019/34/E/ST2/00393, UMO-2020/37/B/ST2/01043, UMO-2021/40/C/ST2/00187, UMO-2022/47/O/ST2/00148); Slovenia: Slovenian Research Agency (ARIS grant J1-3010); Spain: BBVA Foundation (LEO22-1-603), Generalitat Valenciana (Artemisa, FEDER, IDIFEDER/2018/048), La Caixa Banking Foundation (LCF/BQ/PI20/11760025), Ministry of

JHEP10(2024)130

Science and Innovation (MCIN & NextGenEU PCI2022-135018-2, MICIN & FEDER PID2021-125273NB, RYC2019-028510-I, RYC2020-030254-I, RYC2021-031273-I, RYC2022-038164-I), PROMETEO and GenT Programmes Generalitat Valenciana (CIDEGENT/2019/023, CIDEGENT/2019/027); Sweden: Swedish Research Council (VR 2018-00482, VR 2022-03845, VR 2022-04683, VR grant 2021-03651), Knut and Alice Wallenberg Foundation (KAW 2017.0100, KAW 2018.0157, KAW 2018.0458, KAW 2019.0447); Switzerland: Swiss National Science Foundation (SNSF — PCEFP2_194658); United Kingdom: Leverhulme Trust (Leverhulme Trust RPG-2020-004); United States of America: U.S. Department of Energy (ECA DE-AC02-76SF00515), Neubauer Family Foundation.

Open Access. This article is distributed under the terms of the Creative Commons Attribution License (CC-BY4.0), which permits any use, distribution and reproduction in any medium, provided the original author(s) and source are credited.

JHEP10(2024)130

References

[1] ATLAS collaboration, *Observation of a new particle in the search for the Standard Model Higgs boson with the ATLAS detector at the LHC*, *Phys. Lett. B* **716** (2012) 1 [arXiv:1207.7214] [INSPIRE].

[2] CMS collaboration, *Observation of a new boson at a mass of 125 GeV with the CMS experiment at the LHC*, *Phys. Lett. B* **716** (2012) 30 [arXiv:1207.7235] [INSPIRE].

[3] ATLAS collaboration, *Measurements of the Higgs boson production and decay rates and coupling strengths using pp collision data at $\sqrt{s} = 7$ and 8 TeV in the ATLAS experiment*, *Eur. Phys. J. C* **76** (2016) 6 [arXiv:1507.04548] [INSPIRE].

[4] ATLAS collaboration, *Study of the spin and parity of the Higgs boson in diboson decays with the ATLAS detector*, *Eur. Phys. J. C* **75** (2015) 476 [*Erratum ibid.* **76** (2016) 152] [arXiv:1506.05669] [INSPIRE].

[5] CMS collaboration, *Precise determination of the mass of the Higgs boson and tests of compatibility of its couplings with the standard model predictions using proton collisions at 7 and 8 TeV*, *Eur. Phys. J. C* **75** (2015) 212 [arXiv:1412.8662] [INSPIRE].

[6] CMS collaboration, *Constraints on the spin-parity and anomalous HVV couplings of the Higgs boson in proton collisions at 7 and 8 TeV*, *Phys. Rev. D* **92** (2015) 012004 [arXiv:1411.3441] [INSPIRE].

[7] G.C. Branco et al., *Theory and phenomenology of two-Higgs-doublet models*, *Phys. Rept.* **516** (2012) 1 [arXiv:1106.0034] [INSPIRE].

[8] T.D. Lee, *A theory of spontaneous T violation*, *Phys. Rev. D* **8** (1973) 1226 [INSPIRE].

[9] S. von Buddenbrock et al., *Phenomenological signatures of additional scalar bosons at the LHC*, *Eur. Phys. J. C* **76** (2016) 580 [arXiv:1606.01674] [INSPIRE].

[10] M. Mühlleitner, M.O.P. Sampaio, R. Santos and J. Wittbrodt, *The N2HDM under theoretical and experimental scrutiny*, *JHEP* **03** (2017) 094 [arXiv:1612.01309] [INSPIRE].

[11] ATLAS collaboration, *Combination of searches for Higgs boson pairs in pp collisions at $\sqrt{s} = 13$ TeV with the ATLAS detector*, *Phys. Lett. B* **800** (2020) 135103 [arXiv:1906.02025] [INSPIRE].

[12] CMS collaboration, *Combination of searches for Higgs boson pair production in proton-proton collisions at* $\sqrt{s} = 13$ *TeV*, *Phys. Rev. Lett.* **122** (2019) 121803 [arXiv:1811.09689] [INSPIRE].

[13] ATLAS collaboration, *Searches for heavy ZZ and ZW resonances in the* $\ell\ell qq$ *and* $\nu\nu qq$ *final states in pp collisions at* $\sqrt{s} = 13$ *TeV with the ATLAS detector*, *JHEP* **03** (2018) 009 [arXiv:1708.09638] [INSPIRE].

[14] ATLAS collaboration, *Search for WW/WZ resonance production in* $\ell\nu qq$ *final states in pp collisions at* $\sqrt{s} = 13$ *TeV with the ATLAS detector*, *JHEP* **03** (2018) 042 [arXiv:1710.07235] [INSPIRE].

[15] ATLAS collaboration, *Search for heavy diboson resonances in semileptonic final states in pp collisions at* $\sqrt{s} = 13$ *TeV with the ATLAS detector*, *Eur. Phys. J. C* **80** (2020) 1165 [arXiv:2004.14636] [INSPIRE].

[16] ATLAS collaboration, *Search for diboson resonances in hadronic final states in* $139\,fb^{-1}$ *of pp collisions at* $\sqrt{s} = 13$ *TeV with the ATLAS detector*, *JHEP* **09** (2019) 091 [*Erratum ibid.* **06** (2020) 042] [arXiv:1906.08589] [INSPIRE].

[17] CMS collaboration, *Search for a heavy Higgs boson decaying to a pair of W bosons in proton-proton collisions at* $\sqrt{s} = 13$ *TeV*, *JHEP* **03** (2020) 034 [arXiv:1912.01594] [INSPIRE].

[18] CMS collaboration, *Search for a new scalar resonance decaying to a pair of Z bosons in proton-proton collisions at* $\sqrt{s} = 13$ *TeV*, *JHEP* **06** (2018) 127 [*Erratum ibid.* **03** (2019) 128] [arXiv:1804.01939] [INSPIRE].

[19] ATLAS collaboration, *Search for heavy resonances decaying into a W or Z boson and a Higgs boson in final states with leptons and b-jets in* $36\,fb^{-1}$ *of* $\sqrt{s} = 13$ *TeV pp collisions with the ATLAS detector*, *JHEP* **03** (2018) 174 [*Erratum ibid.* **11** (2018) 051] [arXiv:1712.06518] [INSPIRE].

[20] CMS collaboration, *Search for a heavy pseudoscalar Higgs boson decaying into a* 125 *GeV Higgs boson and a Z boson in final states with two tau and two light leptons at* $\sqrt{s} = 13$ *TeV*, *JHEP* **03** (2020) 065 [arXiv:1910.11634] [INSPIRE].

[21] CMS collaboration, *Search for neutral resonances decaying into a Z boson and a pair of b jets or* τ *leptons*, *Phys. Lett. B* **759** (2016) 369 [arXiv:1603.02991] [INSPIRE].

[22] CMS collaboration, *Search for new neutral Higgs bosons through the* $H \to ZA \to \ell^+\ell^- b\bar{b}$ *process in pp collisions at* $\sqrt{s} = 13$ *TeV*, *JHEP* **03** (2020) 055 [arXiv:1911.03781] [INSPIRE].

[23] ATLAS collaboration, *Search for a heavy Higgs boson decaying into a Z boson and another heavy Higgs boson in the* $\ell\ell bb$ *final state in pp collisions at* $\sqrt{s} = 13$ *TeV with the ATLAS detector*, *Phys. Lett. B* **783** (2018) 392 [arXiv:1804.01126] [INSPIRE].

[24] ATLAS collaboration, *Search for a heavy Higgs boson decaying into a Z boson and another heavy Higgs boson in the* $\ell\ell bb$ *and* $\ell\ell WW$ *final states in pp collisions at* $\sqrt{s} = 13$ *TeV with the ATLAS detector*, *Eur. Phys. J. C* **81** (2021) 396 [arXiv:2011.05639] [INSPIRE].

[25] ATLAS collaboration, *Search for a CP-odd Higgs boson decaying into a heavy CP-even Higgs boson and a Z boson in the* $\ell^+\ell^- t\bar{t}$ *and* $\nu\bar{\nu}b\bar{b}$ *final states using* $140\,fb^{-1}$ *of data collected with the ATLAS detector*, *JHEP* **02** (2024) 197 [arXiv:2311.04033] [INSPIRE].

[26] ATLAS collaboration, *The ATLAS experiment at the CERN Large Hadron Collider*, 2008 *JINST* **3** S08003 [INSPIRE].

[27] ATLAS IBL collaboration, *Production and integration of the ATLAS Insertable B-Layer*, 2018 *JINST* **13** T05008 [arXiv:1803.00844] [INSPIRE].

JHEP10(2024)130

[28] ATLAS collaboration, *Performance of the ATLAS trigger system in 2015*, *Eur. Phys. J. C* **77** (2017) 317 [arXiv:1611.09661] [INSPIRE].

[29] ATLAS collaboration, *The ATLAS collaboration software and firmware*, ATL-SOFT-PUB-2021-001, CERN, Geneva, Switzerland (2021).

[30] ATLAS collaboration, *ATLAS data quality operations and performance for 2015–2018 data-taking*, 2020 *JINST* **15** P04003 [arXiv:1911.04632] [INSPIRE].

[31] ATLAS collaboration, *Performance of electron and photon triggers in ATLAS during LHC run 2*, *Eur. Phys. J. C* **80** (2020) 47 [arXiv:1909.00761] [INSPIRE].

[32] ATLAS collaboration, *Performance of the ATLAS muon triggers in run 2*, 2020 *JINST* **15** P09015 [arXiv:2004.13447] [INSPIRE].

[33] ATLAS collaboration, *2015 start-up trigger menu and initial performance assessment of the ATLAS trigger using run-2 data*, ATL-DAQ-PUB-2016-001, CERN, Geneva, Switzerland (2016).

[34] ATLAS collaboration, *Trigger menu in 2016*, ATL-DAQ-PUB-2017-001, CERN, Geneva, Switzerland (2017).

[35] ATLAS collaboration, *The ATLAS simulation infrastructure*, *Eur. Phys. J. C* **70** (2010) 823 [arXiv:1005.4568] [INSPIRE].

[36] GEANT4 collaboration, *GEANT4 — a simulation toolkit*, *Nucl. Instrum. Meth. A* **506** (2003) 250 [INSPIRE].

[37] T. Sjöstrand, S. Mrenna and P.Z. Skands, *A brief introduction to PYTHIA 8.1*, *Comput. Phys. Commun.* **178** (2008) 852 [arXiv:0710.3820] [INSPIRE].

[38] R.D. Ball et al., *Parton distributions with LHC data*, *Nucl. Phys. B* **867** (2013) 244 [arXiv:1207.1303] [INSPIRE].

[39] ATLAS collaboration, *The Pythia 8 A3 tune description of ATLAS minimum bias and inelastic measurements incorporating the Donnachie-Landshoff diffractive model*, ATL-PHYS-PUB-2016-017, CERN, Geneva, Switzerland (2016).

[40] SHERPA collaboration, *Event generation with Sherpa 2.2*, *SciPost Phys.* **7** (2019) 034 [arXiv:1905.09127] [INSPIRE].

[41] F. Buccioni et al., *OpenLoops 2*, *Eur. Phys. J. C* **79** (2019) 866 [arXiv:1907.13071] [INSPIRE].

[42] F. Cascioli, P. Maierhöfer and S. Pozzorini, *Scattering amplitudes with OpenLoops*, *Phys. Rev. Lett.* **108** (2012) 111601 [arXiv:1111.5206] [INSPIRE].

[43] A. Denner, S. Dittmaier and L. Hofer, *Collier: a fortran-based Complex One-Loop LIbrary in Extended Regularizations*, *Comput. Phys. Commun.* **212** (2017) 220 [arXiv:1604.06792] [INSPIRE].

[44] T. Gleisberg and S. Höche, *Comix, a new matrix element generator*, *JHEP* **12** (2008) 039 [arXiv:0808.3674] [INSPIRE].

[45] S. Schumann and F. Krauss, *A parton shower algorithm based on Catani-Seymour dipole factorisation*, *JHEP* **03** (2008) 038 [arXiv:0709.1027] [INSPIRE].

[46] S. Höche, F. Krauss, M. Schönherr and F. Siegert, *A critical appraisal of NLO+PS matching methods*, *JHEP* **09** (2012) 049 [arXiv:1111.1220] [INSPIRE].

[47] S. Höche, F. Krauss, M. Schönherr and F. Siegert, *QCD matrix elements + parton showers: the NLO case*, *JHEP* **04** (2013) 027 [arXiv:1207.5030] [INSPIRE].

JHEP10(2024)130

[48] S. Höche, F. Krauss, S. Schumann and F. Siegert, *QCD matrix elements and truncated showers*, *JHEP* **05** (2009) 053 [arXiv:0903.1219] [INSPIRE].

[49] NNPDF collaboration, *Parton distributions for the LHC run II*, *JHEP* **04** (2015) 040 [arXiv:1410.8849] [INSPIRE].

[50] J. Alwall et al., *MadGraph 5: going beyond*, *JHEP* **06** (2011) 128 [arXiv:1106.0522] [INSPIRE].

[51] ATLAS collaboration, *ATLAS Pythia 8 tunes to 7 TeV data*, ATL-PHYS-PUB-2014-021, CERN, Geneva, Switzerland (2014).

[52] S. Alioli, P. Nason, C. Oleari and E. Re, *A general framework for implementing NLO calculations in shower Monte Carlo programs: the POWHEG BOX*, *JHEP* **06** (2010) 043 [arXiv:1002.2581] [INSPIRE].

[53] P. Nason, *A new method for combining NLO QCD with shower Monte Carlo algorithms*, *JHEP* **11** (2004) 040 [hep-ph/0409146] [INSPIRE].

[54] S. Frixione, P. Nason and C. Oleari, *Matching NLO QCD computations with parton shower simulations: the POWHEG method*, *JHEP* **11** (2007) 070 [arXiv:0709.2092] [INSPIRE].

[55] P. Nason and G. Zanderighi, W^+W^-, WZ *and* ZZ *production in the POWHEG-BOX-V2*, *Eur. Phys. J. C* **74** (2014) 2702 [arXiv:1311.1365] [INSPIRE].

[56] ATLAS collaboration, *Measurement of the* Z/γ^* *boson transverse momentum distribution in* pp *collisions at* $\sqrt{s} = 7$ *TeV with the ATLAS detector*, *JHEP* **09** (2014) 145 [arXiv:1406.3660] [INSPIRE].

[57] H.-L. Lai et al., *New parton distributions for collider physics*, *Phys. Rev. D* **82** (2010) 074024 [arXiv:1007.2241] [INSPIRE].

[58] J. Pumplin et al., *New generation of parton distributions with uncertainties from global QCD analysis*, *JHEP* **07** (2002) 012 [hep-ph/0201195] [INSPIRE].

[59] D.J. Lange, *The EvtGen particle decay simulation package*, *Nucl. Instrum. Meth. A* **462** (2001) 152 [INSPIRE].

[60] S. von Buddenbrock et al., *Multi-lepton signatures of additional scalar bosons beyond the standard model at the LHC*, *J. Phys. G* **45** (2018) 115003 [arXiv:1711.07874] [INSPIRE].

[61] D. Berdine, N. Kauer and D. Rainwater, *Breakdown of the narrow width approximation for new physics*, *Phys. Rev. Lett.* **99** (2007) 111601 [hep-ph/0703058] [INSPIRE].

[62] T. Sjöstrand et al., *An introduction to PYTHIA 8.2*, *Comput. Phys. Commun.* **191** (2015) 159 [arXiv:1410.3012] [INSPIRE].

[63] R.D. Ball et al., *Impact of heavy quark masses on parton distributions and LHC phenomenology*, *Nucl. Phys. B* **849** (2011) 296 [arXiv:1101.1300] [INSPIRE].

[64] ATLAS collaboration, *Electron and photon performance measurements with the ATLAS detector using the 2015–2017 LHC proton-proton collision data*, 2019 *JINST* **14** P12006 [arXiv:1908.00005] [INSPIRE].

[65] ATLAS collaboration, *Improved electron reconstruction in ATLAS using the Gaussian sum filter-based model for bremsstrahlung*, ATLAS-CONF-2012-047, CERN, Geneva, Switzerland (2012).

[66] ATLAS collaboration, *Electron reconstruction and identification in the ATLAS experiment using the 2015 and 2016 LHC proton-proton collision data at* $\sqrt{s} = 13$ *TeV*, *Eur. Phys. J. C* **79** (2019) 639 [arXiv:1902.04655] [INSPIRE].

JHEP10(2024)130

[67] ATLAS collaboration, *Muon reconstruction and identification efficiency in ATLAS using the full run 2 pp collision data set at* $\sqrt{s} = 13$ *TeV*, *Eur. Phys. J. C* **81** (2021) 578 [arXiv:2012.00578] [INSPIRE].

[68] ATLAS collaboration, *Jet reconstruction and performance using particle flow with the ATLAS detector*, *Eur. Phys. J. C* **77** (2017) 466 [arXiv:1703.10485] [INSPIRE].

[69] M. Cacciari, G.P. Salam and G. Soyez, *The anti-k_t jet clustering algorithm*, *JHEP* **04** (2008) 063 [arXiv:0802.1189] [INSPIRE].

[70] ATLAS collaboration, *Jet energy scale and resolution measured in proton-proton collisions at* $\sqrt{s} = 13$ *TeV with the ATLAS detector*, *Eur. Phys. J. C* **81** (2021) 689 [arXiv:2007.02645] [INSPIRE].

[71] ATLAS collaboration, *Performance of pile-up mitigation techniques for jets in pp collisions at* $\sqrt{s} = 8$ *TeV using the ATLAS detector*, *Eur. Phys. J. C* **76** (2016) 581 [arXiv:1510.03823] [INSPIRE].

[72] ATLAS collaboration, *Tagging and suppression of pileup jets with the ATLAS detector*, ATLAS-CONF-2014-018, CERN, Geneva, Switzerland (2014).

[73] ATLAS collaboration, *ATLAS b-jet identification performance and efficiency measurement with* $t\bar{t}$ *events in pp collisions at* $\sqrt{s} = 13$ *TeV*, *Eur. Phys. J. C* **79** (2019) 970 [arXiv:1907.05120] [INSPIRE].

[74] ATLAS collaboration, *Optimisation and performance studies of the ATLAS b-tagging algorithms for the 2017–18 LHC run*, ATL-PHYS-PUB-2017-013, CERN, Geneva, Switzerland (2017).

[75] ATLAS collaboration, E_T^{miss} *performance in the ATLAS detector using 2015–2016 LHC p-p collisions*, ATLAS-CONF-2018-023, CERN, Geneva, Switzerland (2018).

[76] ATLAS collaboration, *Search for an additional, heavy Higgs boson in the* $H \to ZZ$ *decay channel at* $\sqrt{s} = 8$ *TeV in pp collision data with the ATLAS detector*, *Eur. Phys. J. C* **76** (2016) 45 [arXiv:1507.05930] [INSPIRE].

[77] ATLAS collaboration, *Search for heavy ZZ resonances in the* $\ell^+\ell^-\ell^+\ell^-$ *and* $\ell^+\ell^-\nu\bar{\nu}$ *final states using proton-proton collisions at* $\sqrt{s} = 13$ *TeV with the ATLAS detector*, *Eur. Phys. J. C* **78** (2018) 293 [arXiv:1712.06386] [INSPIRE].

[78] ATLAS collaboration, *Search for heavy resonances decaying into a pair of Z bosons in the* $\ell^+\ell^-\ell'^+\ell'^-$ *and* $\ell^+\ell^-\nu\bar{\nu}$ *final states using 139 fb*$^{-1}$ *of proton-proton collisions at* $\sqrt{s} = 13$ *TeV with the ATLAS detector*, *Eur. Phys. J. C* **81** (2021) 332 [arXiv:2009.14791] [INSPIRE].

[79] A.L. Read, *Linear interpolation of histograms*, *Nucl. Instrum. Meth. A* **425** (1999) 357 [INSPIRE].

[80] ATLAS collaboration, *Muon reconstruction performance of the ATLAS detector in proton-proton collision data at* $\sqrt{s} = 13$ *TeV*, *Eur. Phys. J. C* **76** (2016) 292 [arXiv:1603.05598] [INSPIRE].

[81] ATLAS collaboration, *Performance of the missing transverse momentum triggers for the ATLAS detector during run-2 data taking*, *JHEP* **08** (2020) 080 [arXiv:2005.09554] [INSPIRE].

[82] ATLAS collaboration, *Luminosity determination in pp collisions at* $\sqrt{s} = 13$ *TeV using the ATLAS detector at the LHC*, ATLAS-CONF-2019-021, CERN, Geneva, Switzerland (2019).

[83] G. Avoni et al., *The new LUCID-2 detector for luminosity measurement and monitoring in ATLAS*, 2018 *JINST* **13** P07017 [INSPIRE].

[84] A. Kalogeropoulos and J. Alwall, *The SysCalc code: a tool to derive theoretical systematic uncertainties*, arXiv:1801.08401 [INSPIRE].

JHEP10(2024)130

[85] J. Butterworth et al., *PDF4LHC recommendations for LHC run II*, *J. Phys. G* **43** (2016) 023001 [arXiv:1510.03865] [INSPIRE].

[86] J. Bellm et al., *Herwig 7.0/Herwig++ 3.0 release note*, *Eur. Phys. J. C* **76** (2016) 196 [arXiv:1512.01178] [INSPIRE].

[87] G. Cowan, K. Cranmer, E. Gross and O. Vitells, *Asymptotic formulae for likelihood-based tests of new physics*, *Eur. Phys. J. C* **71** (2011) 1554 [*Erratum ibid.* **73** (2013) 2501] [arXiv:1007.1727] [INSPIRE].

[88] A.L. Read, *Presentation of search results: the CL_s technique*, *J. Phys. G* **28** (2002) 2693 [INSPIRE].

[89] ATLAS collaboration, *ATLAS computing acknowledgements*, ATL-SOFT-PUB-2023-001, CERN, Geneva, Switzerland (2023).

JHEP10(2024)130

The ATLAS collaboration

G. Aad[102], E. Aakvaag[16], B. Abbott[120], K. Abeling[55], N.J. Abicht[49], S.H. Abidi[29], A. Aboulhorma[35e], H. Abramowicz[151], H. Abreu[150], Y. Abulaiti[117], B.S. Acharya[69a,69b,m], C. Adam Bourdarios[4], L. Adamczyk[86a], S.V. Addepalli[26], M.J. Addison[101], J. Adelman[115], A. Adiguzel[21c], T. Adye[134], A.A. Affolder[136], Y. Afik[39], M.N. Agaras[13], J. Agarwala[73a,73b], A. Aggarwal[100], C. Agheorghiesei[27c], A. Ahmad[36], F. Ahmadov[38,aa], W.S. Ahmed[104], S. Ahuja[95], X. Ai[62e], G. Aielli[76a,76b], A. Aikot[163], M. Ait Tamlihat[35e], B. Aitbenchikh[35a], I. Aizenberg[169], M. Akbiyik[100], T.P.A. Åkesson[98], A.V. Akimov[37], D. Akiyama[168], N.N. Akolkar[24], S. Aktas[21a], K. Al Khoury[41], G.L. Alberghi[23b], J. Albert[165], P. Albicocco[53], G.L. Albouy[60], S. Alderweireldt[52], Z.L. Alegria[121], M. Aleksa[36], I.N. Aleksandrov[38], C. Alexa[27b], T. Alexopoulos[10], F. Alfonsi[23b], M. Algren[56], M. Alhroob[141], B. Ali[132], H.M.J. Ali[91], S. Ali[148], S.W. Alibocus[92], M. Aliev[33c], G. Alimonti[71a], W. Alkakhi[55], C. Allaire[66], B.M.M. Allbrooke[146], J.F. Allen[52], C.A. Allendes Flores[137f], P.P. Allport[20], A. Aloisio[72a,72b], F. Alonso[90], C. Alpigiani[138], M. Alvarez Estevez[99], A. Alvarez Fernandez[100], M. Alves Cardoso[56], M.G. Alviggi[72a,72b], M. Aly[101], Y. Amaral Coutinho[83b], A. Ambler[104], C. Amelung[36], M. Amerl[101], C.G. Ames[109], D. Amidei[106], S.P. Amor Dos Santos[130a], K.R. Amos[163], V. Ananiev[125], C. Anastopoulos[139], T. Andeen[11], J.K. Anders[36], S.Y. Andrean[47a,47b], A. Andreazza[71a,71b], S. Angelidakis[9], A. Angerami[41,ad], A.V. Anisenkov[37], A. Annovi[74a], C. Antel[56], M.T. Anthony[139], E. Antipov[145], M. Antonelli[53], F. Anulli[75a], M. Aoki[84], T. Aoki[153], J.A. Aparisi Pozo[163], M.A. Aparo[146], L. Aperio Bella[48], C. Appelt[18], A. Apyan[26], S.J. Arbiol Val[87], C. Arcangeletti[53], A.T.H. Arce[51], E. Arena[92], J-F. Arguin[108], S. Argyropoulos[54], J.-H. Arling[48], O. Arnaez[4], H. Arnold[114], G. Artoni[75a,75b], H. Asada[111], K. Asai[118], S. Asai[153], N.A. Asbah[36], K. Assamagan[29], R. Astalos[28a], S. Atashi[159], R.J. Atkin[33a], M. Atkinson[162], H. Atmani[35f], P.A. Atmasiddha[128], K. Augsten[132], S. Auricchio[72a,72b], A.D. Auriol[20], V.A. Austrup[101], G. Avolio[36], K. Axiotis[56], G. Azuelos[108,ah], D. Babal[28b], H. Bachacou[135], K. Bachas[152,q], A. Bachiu[34], F. Backman[47a,47b], A. Badea[39], T.M. Baer[106], P. Bagnaia[75a,75b], M. Bahmani[18], D. Bahner[54], K. Bai[123], A.J. Bailey[163], V.R. Bailey[162], J.T. Baines[134], L. Baines[94], O.K. Baker[172], E. Bakos[15], D. Bakshi Gupta[8], V. Balakrishnan[120], R. Balasubramanian[114], E.M. Baldin[37], P. Balek[86a], E. Ballabene[23b,23a], F. Balli[135], L.M. Baltes[63a], W.K. Balunas[32], J. Balz[100], E. Banas[87], M. Bandieramonte[129], A. Bandyopadhyay[24], S. Bansal[24], L. Barak[151], M. Barakat[48], E.L. Barberio[105], D. Barberis[57b,57a], M. Barbero[102], M.Z. Barel[114], K.N. Barends[33a], T. Barillari[110], M-S. Barisits[36], T. Barklow[143], P. Baron[122], D.A. Baron Moreno[101], A. Baroncelli[62a], G. Barone[29], A.J. Barr[126], J.D. Barr[96], F. Barreiro[99], J. Barreiro Guimarães da Costa[14a], U. Barron[151], M.G. Barros Teixeira[130a], S. Barsov[37], F. Bartels[63a], R. Bartoldus[143], A.E. Barton[91], P. Bartos[28a], A. Basan[100], M. Baselga[49], A. Bassalat[66,b], M.J. Basso[156a], C.R. Basson[101], R.L. Bates[59], S. Batlamous[35e], B. Batool[141], M. Battaglia[136], D. Battulga[18], M. Bauce[75a,75b], M. Bauer[36], P. Bauer[24], L.T. Bazzano Hurrell[30], J.B. Beacham[51], T. Beau[127], J.Y. Beaucamp[90], P.H. Beauchemin[158], P. Bechtle[24], H.P. Beck[19,p], K. Becker[167], A.J. Beddall[82], V.A. Bednyakov[38], C.P. Bee[145], L.J. Beemster[15], T.A. Beermann[36], M. Begalli[83d], M. Begel[29], A. Behera[145], J.K. Behr[48],

JHEP10(2024)130

J.F. Beirer[36], F. Beisiegel[24], M. Belfkir[116b], G. Bella[151], L. Bellagamba[23b], A. Bellerive[34], P. Bellos[20], K. Beloborodov[37], D. Benchekroun[35a], F. Bendebba[35a], Y. Benhammou[151], K.C. Benkendorfer[61], L. Beresford[48], M. Beretta[53], E. Bergeaas Kuutmann[161], N. Berger[4], B. Bergmann[132], J. Beringer[17a], G. Bernardi[5], C. Bernius[143], F.U. Bernlochner[24], F. Bernon[36,102], A. Berrocal Guardia[13], T. Berry[95], P. Berta[133], A. Berthold[50], S. Bethke[110], A. Betti[75a,75b], A.J. Bevan[94], N.K. Bhalla[54], M. Bhamjee[33c], S. Bhatta[145], D.S. Bhattacharya[166], P. Bhattarai[143], K.D. Bhide[54], V.S. Bhopatkar[121], R.M. Bianchi[129], G. Bianco[23b,23a], O. Biebel[109], R. Bielski[123], M. Biglietti[77a], C.S. Billingsley[44], M. Bindi[55], A. Bingul[21b], C. Bini[75a,75b], A. Biondini[92], C.J. Birch-sykes[101], G.A. Bird[32], M. Birman[169], M. Biros[133], S. Biryukov[146], T. Bisanz[49], E. Bisceglie[43b,43a], J.P. Biswal[134], D. Biswas[141], K. Bjørke[125], I. Bloch[48], A. Blue[59], U. Blumenschein[94], J. Blumenthal[100], V.S. Bobrovnikov[37], M. Boehler[54], B. Boehm[166], D. Bogavac[36], A.G. Bogdanchikov[37], C. Bohm[47a], V. Boisvert[95], P. Bokan[36], T. Bold[86a], M. Bomben[5], M. Bona[94], M. Boonekamp[135], C.D. Booth[95], A.G. Borbély[59], I.S. Bordulev[37], H.M. Borecka-Bielska[108], G. Borissov[91], D. Bortoletto[126], D. Boscherini[23b], M. Bosman[13], J.D. Bossio Sola[36], K. Bouaouda[35a], N. Bouchhar[163], J. Boudreau[129], E.V. Bouhova-Thacker[91], D. Boumediene[40], R. Bouquet[57b,57a], A. Boveia[119], J. Boyd[36], D. Boye[29], I.R. Boyko[38], J. Bracinik[20], N. Brahimi[4], G. Brandt[171], O. Brandt[32], F. Braren[48], B. Brau[103], J.E. Brau[123], R. Brener[169], L. Brenner[114], R. Brenner[161], S. Bressler[169], D. Britton[59], D. Britzger[110], I. Brock[24], G. Brooijmans[41], E. Brost[29], L.M. Brown[165], L.E. Bruce[61], T.L. Bruckler[126], P.A. Bruckman de Renstrom[87], B. Brüers[48], A. Bruni[23b], G. Bruni[23b], M. Bruschi[23b], N. Bruscino[75a,75b], T. Buanes[16], Q. Buat[138], D. Buchin[110], A.G. Buckley[59], O. Bulekov[37], B.A. Bullard[143], S. Burdin[92], C.D. Burgard[49], A.M. Burger[36], B. Burghgrave[8], O. Burlayenko[54], J.T.P. Burr[32], C.D. Burton[11], J.C. Burzynski[142], E.L. Busch[41], V. Büscher[100], P.J. Bussey[59], J.M. Butler[25], C.M. Buttar[59], J.M. Butterworth[96], W. Buttinger[134], C.J. Buxo Vazquez[107], A.R. Buzykaev[37], S. Cabrera Urbán[163], L. Cadamuro[66], D. Caforio[58], H. Cai[129], Y. Cai[14a,14e], Y. Cai[14c], V.M.M. Cairo[36], O. Cakir[3a], N. Calace[36], P. Calafiura[17a], G. Calderini[127], P. Calfayan[68], G. Callea[59], L.P. Caloba[83b], D. Calvet[40], S. Calvet[40], M. Calvetti[74a,74b], R. Camacho Toro[127], S. Camarda[36], D. Camarero Munoz[26], P. Camarri[76a,76b], M.T. Camerlingo[72a,72b], D. Cameron[36], C. Camincher[165], M. Campanelli[96], A. Camplani[42], V. Canale[72a,72b], A.C. Canbay[3a], J. Cantero[163], Y. Cao[162], F. Capocasa[26], M. Capua[43b,43a], A. Carbone[71a,71b], R. Cardarelli[76a], J.C.J. Cardenas[8], F. Cardillo[163], G. Carducci[43b,43a], T. Carli[36], G. Carlino[72a], J.I. Carlotto[13], B.T. Carlson[129,r], E.M. Carlson[165,156a], L. Carminati[71a,71b], A. Carnelli[135], M. Carnesale[75a,75b], S. Caron[113], E. Carquin[137f], S. Carrá[71a], G. Carratta[23b,23a], A.M. Carroll[123], T.M. Carter[52], M.P. Casado[13,i], M. Caspar[48], F.L. Castillo[4], L. Castillo Garcia[13], V. Castillo Gimenez[163], N.F. Castro[130a,130e], A. Catinaccio[36], J.R. Catmore[125], T. Cavaliere[4], V. Cavaliere[29], N. Cavalli[23b,23a], Y.C. Cekmecelioglu[48], E. Celebi[21a], F. Celli[126], M.S. Centonze[70a,70b], V. Cepaitis[56], K. Cerny[122], A.S. Cerqueira[83a], A. Cerri[146], L. Cerrito[76a,76b], F. Cerutti[17a], B. Cervato[141], A. Cervelli[23b], G. Cesarini[53], S.A. Cetin[82], D. Chakraborty[115], J. Chan[17a], W.Y. Chan[153], J.D. Chapman[32], E. Chapon[135], B. Chargeishvili[149b],

JHEP10(2024)130

D.G. Charlton[20], M. Chatterjee[19], C. Chauhan[133], Y. Che[14c], S. Chekanov[6], S.V. Chekulaev[156a], G.A. Chelkov[38,a], A. Chen[106], B. Chen[151], B. Chen[165], H. Chen[14c], H. Chen[29], J. Chen[62c], J. Chen[142], M. Chen[126], S. Chen[153], S.J. Chen[14c], X. Chen[62c,135], X. Chen[14b,ag], Y. Chen[62a], C.L. Cheng[170], H.C. Cheng[64a], S. Cheong[143], A. Cheplakov[38], E. Cheremushkina[48], E. Cherepanova[114], R. Cherkaoui El Moursli[35e], E. Cheu[7], K. Cheung[65], L. Chevalier[135], V. Chiarella[53], G. Chiarelli[74a], N. Chiedde[102], G. Chiodini[70a], A.S. Chisholm[20], A. Chitan[27b], M. Chitishvili[163], M.V. Chizhov[38,s], K. Choi[11], Y. Chou[138], E.Y.S. Chow[113], K.L. Chu[169], M.C. Chu[64a], X. Chu[14a,14e], J. Chudoba[131], J.J. Chwastowski[87], D. Cieri[110], K.M. Ciesla[86a], V. Cindro[93], A. Ciocio[17a], F. Cirotto[72a,72b], Z.H. Citron[169,k], M. Citterio[71a], D.A. Ciubotaru[27b], A. Clark[56], P.J. Clark[52], C. Clarry[155], J.M. Clavijo Columbie[48], S.E. Clawson[48], C. Clement[47a,47b], J. Clercx[48], Y. Coadou[102], M. Cobal[69a,69c], A. Coccaro[57b], R.F. Coelho Barrue[130a], R. Coelho Lopes De Sa[103], S. Coelli[71a], B. Cole[41], J. Collot[60], P. Conde Muiño[130a,130g], M.P. Connell[33c], S.H. Connell[33c], E.I. Conroy[126], F. Conventi[72a,ai], H.G. Cooke[20], A.M. Cooper-Sarkar[126], A. Cordeiro Oudot Choi[127], L.D. Corpe[40], M. Corradi[75a,75b], F. Corriveau[104,y], A. Cortes-Gonzalez[18], M.J. Costa[163], F. Costanza[4], D. Costanzo[139], B.M. Cote[119], G. Cowan[95], K. Cranmer[170], D. Cremonini[23b,23a], S. Crépé-Renaudin[60], F. Crescioli[127], M. Cristinziani[141], M. Cristoforetti[78a,78b], V. Croft[114], J.E. Crosby[121], G. Crosetti[43b,43a], A. Cueto[99], T. Cuhadar Donszelmann[159], H. Cui[14a,14e], Z. Cui[7], W.R. Cunningham[59], F. Curcio[43b,43a], P. Czodrowski[36], M.M. Czurylo[63b], M.J. Da Cunha Sargedas De Sousa[57b,57a], J.V. Da Fonseca Pinto[83b], C. Da Via[101], W. Dabrowski[86a], T. Dado[49], S. Dahbi[148], T. Dai[106], D. Dal Santo[19], C. Dallapiccola[103], M. Dam[42], G. D'amen[29], V. D'Amico[109], J. Damp[100], J.R. Dandoy[34], M. Danninger[142], V. Dao[36], G. Darbo[57b], S. Darmora[6], S.J. Das[29,aj], S. D'Auria[71a,71b], A. D'avanzo[130a], C. David[33a], T. Davidek[133], B. Davis-Purcell[34], I. Dawson[94], H.A. Day-hall[132], K. De[8], R. De Asmundis[72a], N. De Biase[48], S. De Castro[23b,23a], N. De Groot[113], P. de Jong[114], H. De la Torre[115], A. De Maria[14c], A. De Salvo[75a], U. De Sanctis[76a,76b], F. De Santis[70a,70b], A. De Santo[146], J.B. De Vivie De Regie[60], D.V. Dedovich[38], J. Degens[114], A.M. Deiana[44], F. Del Corso[23b,23a], J. Del Peso[99], F. Del Rio[63a], L. Delagrange[127], F. Deliot[135], C.M. Delitzsch[49], M. Della Pietra[72a,72b], D. Della Volpe[56], A. Dell'Acqua[36], L. Dell'Asta[71a,71b], M. Delmastro[4], P.A. Delsart[60], S. Demers[172], M. Demichev[38], S.P. Denisov[37], L. D'Eramo[40], D. Derendarz[87], F. Derue[127], P. Dervan[92], K. Desch[24], C. Deutsch[24], F.A. Di Bello[57b,57a], A. Di Ciaccio[76a,76b], L. Di Ciaccio[4], A. Di Domenico[75a,75b], C. Di Donato[72a,72b], A. Di Girolamo[36], G. Di Gregorio[36], A. Di Luca[78a,78b], B. Di Micco[77a,77b], R. Di Nardo[77a,77b], M. Diamantopoulou[34], F.A. Dias[114], T. Dias Do Vale[142], M.A. Diaz[137a,137b], F.G. Diaz Capriles[24], M. Didenko[163], E.B. Diehl[106], S. Díez Cornell[48], C. Diez Pardos[141], C. Dimitriadi[161,24], A. Dimitrievska[17a], J. Dingfelder[24], I-M. Dinu[27b], S.J. Dittmeier[63b], F. Dittus[36], F. Djama[102], T. Djobava[149b], C. Doglioni[101,98], A. Dohnalova[28a], J. Dolejsi[133], Z. Dolezal[133], K.M. Dona[39], M. Donadelli[83c], B. Dong[107], J. Donini[40], A. D'Onofrio[72a,72b], M. D'Onofrio[92], J. Dopke[134], A. Doria[72a], N. Dos Santos Fernandes[130a], P. Dougan[101], M.T. Dova[90], A.T. Doyle[59], M.A. Draguet[126],

JHEP10(2024)130

E. Dreyer[169], I. Drivas-koulouris[10], M. Drnevich[117], M. Drozdova[56], D. Du[62a], T.A. du Pree[114], F. Dubinin[37], M. Dubovsky[28a], E. Duchovni[169], G. Duckeck[109], O.A. Ducu[27b], D. Duda[52], A. Dudarev[36], E.R. Duden[26], M. D'uffizi[101], L. Duflot[66], M. Dührssen[36], A.E. Dumitriu[27b], M. Dunford[63a], S. Dungs[49], K. Dunne[47a,47b], A. Duperrin[102], H. Duran Yildiz[3a], M. Düren[58], A. Durglishvili[149b], B.L. Dwyer[115], G.I. Dyckes[17a], M. Dyndal[86a], B.S. Dziedzic[87], Z.O. Earnshaw[146], G.H. Eberwein[126], B. Eckerova[28a], S. Eggebrecht[55], E. Egidio Purcino De Souza[127], L.F. Ehrke[56], G. Eigen[16], K. Einsweiler[17a], T. Ekelof[161], P.A. Ekman[98], S. El Farkh[35b], Y. El Ghazali[35b], H. El Jarrari[36], A. El Moussaouy[108], V. Ellajosyula[161], M. Ellert[161], F. Ellinghaus[171], N. Ellis[36], J. Elmsheuser[29], M. Elsing[36], D. Emeliyanov[134], Y. Enari[153], I. Ene[17a], S. Epari[13], P.A. Erland[87], M. Errenst[171], M. Escalier[66], C. Escobar[163], E. Etzion[151], G. Evans[130a], H. Evans[68], L.S. Evans[95], A. Ezhilov[37], S. Ezzarqtouni[35a], F. Fabbri[23b,23a], L. Fabbri[23b,23a], G. Facini[96], V. Fadeyev[136], R.M. Fakhrutdinov[37], D. Fakoudis[100], S. Falciano[75a], L.F. Falda Ulhoa Coelho[36], P.J. Falke[24], J. Faltova[133], C. Fan[162], Y. Fan[14a], Y. Fang[14a,14e], M. Fanti[71a,71b], M. Faraj[69a,69b], Z. Farazpay[97], A. Farbin[8], A. Farilla[77a], T. Farooque[107], S.M. Farrington[52], F. Fassi[35e], D. Fassouliotis[9], M. Faucci Giannelli[76a,76b], W.J. Fawcett[32], L. Fayard[66], P. Federic[133], P. Federicova[131], O.L. Fedin[37,a], M. Feickert[170], L. Feligioni[102], D.E. Fellers[123], C. Feng[62b], M. Feng[14b], Z. Feng[114], M.J. Fenton[159], L. Ferencz[48], R.A.M. Ferguson[91], S.I. Fernandez Luengo[137f], P. Fernandez Martinez[13], M.J.V. Fernoux[102], J. Ferrando[91], A. Ferrari[161], P. Ferrari[114,113], R. Ferrari[73a], D. Ferrere[56], C. Ferretti[106], F. Fiedler[100], P. Fiedler[132], A. Filipčič[93], E.K. Filmer[1], F. Filthaut[113], M.C.N. Fiolhais[130a,130c,c], L. Fiorini[163], W.C. Fisher[107], T. Fitschen[101], P.M. Fitzhugh[135], I. Fleck[141], P. Fleischmann[106], T. Flick[171], M. Flores[33d,ae], L.R. Flores Castillo[64a], L. Flores Sanz De Acedo[36], F.M. Follega[78a,78b], N. Fomin[16], J.H. Foo[155], A. Formica[135], A.C. Forti[101], E. Fortin[36], A.W. Fortman[17a], M.G. Foti[17a], L. Fountas[9,j], D. Fournier[66], H. Fox[91], P. Francavilla[74a,74b], S. Francescato[61], S. Franchellucci[56], M. Franchini[23b,23a], S. Franchino[63a], D. Francis[36], L. Franco[113], V. Franco Lima[36], L. Franconi[48], M. Franklin[61], G. Frattari[26], W.S. Freund[83b], Y.Y. Frid[151], J. Friend[59], N. Fritzsche[50], A. Froch[54], D. Froidevaux[36], J.A. Frost[126], Y. Fu[62a], S. Fuenzalida Garrido[137f], M. Fujimoto[102], K.Y. Fung[64a], E. Furtado De Simas Filho[83b], M. Furukawa[153], J. Fuster[163], A. Gabrielli[23b,23a], A. Gabrielli[155], P. Gadow[36], G. Gagliardi[57b,57a], L.G. Gagnon[17a], S. Galantzan[151], E.J. Gallas[126], B.J. Gallop[134], K.K. Gan[119], S. Ganguly[153], Y. Gao[52], F.M. Garay Walls[137a,137b], B. Garcia[29], C. García[163], A. Garcia Alonso[114], A.G. Garcia Caffaro[172], J.E. García Navarro[163], M. Garcia-Sciveres[17a], G.L. Gardner[128], R.W. Gardner[39], N. Garelli[158], D. Garg[80], R.B. Garg[143,n], J.M. Gargan[52], C.A. Garner[155], C.M. Garvey[33a], P. Gaspar[83b], V.K. Gassmann[158], G. Gaudio[73a], V. Gautam[13], P. Gauzzi[75a,75b], I.L. Gavrilenko[37], A. Gavrilyuk[37], C. Gay[164], G. Gaycken[48], E.N. Gazis[10], A.A. Geanta[27b], C.M. Gee[136], A. Gekow[119], C. Gemme[57b], M.H. Genest[60], A.D. Gentry[112], S. George[95], W.F. George[20], T. Geralis[46], P. Gessinger-Befurt[36], M.E. Geyik[171], M. Ghani[167], M. Ghneimat[141], K. Ghorbanian[94], A. Ghosal[141], A. Ghosh[159], A. Ghosh[7], B. Giacobbe[23b], S. Giagu[75a,75b], T. Giani[114], P. Giannetti[74a], A. Giannini[62a], S.M. Gibson[95], M. Gignac[136], D.T. Gil[86b],

JHEP10(2024)130

A.K. Gilbert[86a], B.J. Gilbert[41], D. Gillberg[34], G. Gilles[114], L. Ginabat[127], D.M. Gingrich[2,ah], M.P. Giordani[69a,69c], P.F. Giraud[135], G. Giugliarelli[69a,69c], D. Giugni[71a], F. Giuli[36], I. Gkialas[9,j], L.K. Gladilin[37], C. Glasman[99], G.R. Gledhill[123], G. Glemža[48], M. Glisic[123], I. Gnesi[43b,f], Y. Go[29], M. Goblirsch-Kolb[36], B. Gocke[49], D. Godin[108], B. Gokturk[21a], S. Goldfarb[105], T. Golling[56], M.G.D. Gololo[33g], D. Golubkov[37], J.P. Gombas[107], A. Gomes[130a,130b], G. Gomes Da Silva[141], A.J. Gomez Delegido[163], R. Gonçalo[130a,130c], L. Gonella[20], A. Gongadze[149c], F. Gonnella[20], J.L. Gonski[143], R.Y. González Andana[52], S. González de la Hoz[163], R. Gonzalez Lopez[92], C. Gonzalez Renteria[17a], M.V. Gonzalez Rodrigues[48], R. Gonzalez Suarez[161], S. Gonzalez-Sevilla[56], G.R. Gonzalvo Rodriguez[163], L. Goossens[36], B. Gorini[36], E. Gorini[70a,70b], A. Gorišek[93], T.C. Gosart[128], A.T. Goshaw[51], M.I. Gostkin[38], S. Goswami[121], C.A. Gottardo[36], S.A. Gotz[109], M. Gouighri[35b], V. Goumarre[48], A.G. Goussiou[138], N. Govender[33c], I. Grabowska-Bold[86a], K. Graham[34], E. Gramstad[125], S. Grancagnolo[70a,70b], C.M. Grant[1,135], P.M. Gravila[27f], F.G. Gravili[70a,70b], H.M. Gray[17a], M. Greco[70a,70b], C. Grefe[24], I.M. Gregor[48], P. Grenier[143], S.G. Grewe[110], A.A. Grillo[136], K. Grimm[31], S. Grinstein[13,u], J.-F. Grivaz[66], E. Gross[169], J. Grosse-Knetter[55], J.C. Grundy[126], L. Guan[106], C. Gubbels[164], J.G.R. Guerrero Rojas[163], G. Guerrieri[69a,69c], F. Guescini[110], R. Gugel[100], J.A.M. Guhit[106], A. Guida[18], E. Guilloton[167], S. Guindon[36], F. Guo[14a,14e], J. Guo[62c], L. Guo[48], Y. Guo[106], R. Gupta[48], R. Gupta[129], S. Gurbuz[24], S.S. Gurdasani[54], G. Gustavino[36], M. Guth[56], P. Gutierrez[120], L.F. Gutierrez Zagazeta[128], M. Gutsche[50], C. Gutschow[96], C. Gwenlan[126], C.B. Gwilliam[92], E.S. Haaland[125], A. Haas[117], M. Habedank[48], C. Haber[17a], H.K. Hadavand[8], A. Hadef[50], S. Hadzic[110], A.I. Hagan[91], J.J. Hahn[141], E.H. Haines[96], M. Haleem[166], J. Haley[121], J.J. Hall[139], G.D. Hallewell[102], L. Halser[19], K. Hamano[165], M. Hamer[24], G.N. Hamity[52], E.J. Hampshire[95], J. Han[62b], K. Han[62a], L. Han[14c], L. Han[62a], S. Han[17a], Y.F. Han[155], K. Hanagaki[84], M. Hance[136], D.A. Hangal[41], H. Hanif[142], M.D. Hank[128], J.B. Hansen[42], P.H. Hansen[42], K. Hara[157], D. Harada[56], T. Harenberg[171], S. Harkusha[37], M.L. Harris[103], Y.T. Harris[126], J. Harrison[13], N.M. Harrison[119], P.F. Harrison[167], N.M. Hartman[110], N.M. Hartmann[109], Y. Hasegawa[140], R. Hauser[107], C.M. Hawkes[20], R.J. Hawkings[36], Y. Hayashi[153], S. Hayashida[111], D. Hayden[107], C. Hayes[106], R.L. Hayes[114], C.P. Hays[126], J.M. Hays[94], H.S. Hayward[92], F. He[62a], M. He[14a,14e], Y. He[154], Y. He[48], Y. He[96], N.B. Heatley[94], V. Hedberg[98], A.L. Heggelund[125], N.D. Hehir[94,*], C. Heidegger[54], K.K. Heidegger[54], W.D. Heidorn[81], J. Heilman[34], S. Heim[48], T. Heim[17a], J.G. Heinlein[128], J.J. Heinrich[123], L. Heinrich[110,af], J. Hejbal[131], A. Held[170], S. Hellesund[16], C.M. Helling[164], S. Hellman[47a,47b], R.C.W. Henderson[91], L. Henkelmann[32], A.M. Henriques Correia[36], H. Herde[98], Y. Hernández Jiménez[145], L.M. Herrmann[24], T. Herrmann[50], G. Herten[54], R. Hertenberger[109], L. Hervas[36], M.E. Hesping[100], N.P. Hessey[156a], E. Hill[155], S.J. Hillier[20], J.R. Hinds[107], F. Hinterkeuser[24], M. Hirose[124], S. Hirose[157], D. Hirschbuehl[171], T.G. Hitchings[101], B. Hiti[93], J. Hobbs[145], R. Hobincu[27e], N. Hod[169], M.C. Hodgkinson[139], B.H. Hodkinson[126], A. Hoecker[36], D.D. Hofer[106], J. Hofer[48], T. Holm[24], M. Holzbock[110], L.B.A.H. Hommels[32], B.P. Honan[101], J. Hong[62c], T.M. Hong[129], B.H. Hooberman[162], W.H. Hopkins[6],

JHEP10(2024)130

Y. Horii[111], S. Hou[148], A.S. Howard[93], J. Howarth[59], J. Hoya[6], M. Hrabovsky[122], A. Hrynevich[48], T. Hryn'ova[4], P.J. Hsu[65], S.-C. Hsu[138], Q. Hu[62a], S. Huang[64b], X. Huang[14c], X. Huang[14a,14e], Y. Huang[139], Y. Huang[14a], Z. Huang[101], Z. Hubacek[132], M. Huebner[24], F. Huegging[24], T.B. Huffman[126], C.A. Hugli[48], M. Huhtinen[36], S.K. Huiberts[16], R. Hulsken[104], N. Huseynov[12], J. Huston[107], J. Huth[61], R. Hyneman[143], G. Iacobucci[56], G. Iakovidis[29], I. Ibragimov[141], L. Iconomidou-Fayard[66], J.P. Iddon[36], P. Iengo[72a,72b], R. Iguchi[153], T. Iizawa[126], Y. Ikegami[84], N. Ilic[155], H. Imam[35a], M. Ince Lezki[56], T. Ingebretsen Carlson[47a,47b], G. Introzzi[73a,73b], M. Iodice[77a], V. Ippolito[75a,75b], R.K. Irwin[92], M. Ishino[153], W. Islam[170], C. Issever[18,48], S. Istin[21a,al], H. Ito[168], R. Iuppa[78a,78b], A. Ivina[169], J.M. Izen[45], V. Izzo[72a], P. Jacka[131,132], P. Jackson[1], B.P. Jaeger[142], C.S. Jagfeld[109], G. Jain[156a], P. Jain[54], K. Jakobs[54], T. Jakoubek[169], J. Jamieson[59], K.W. Janas[86a], M. Javurkova[103], L. Jeanty[123], J. Jejelava[149a,ab], P. Jenni[54,g], C.E. Jessiman[34], C. Jia[62b], J. Jia[145], X. Jia[61], X. Jia[14a,14e], Z. Jia[14c], S. Jiggins[48], J. Jimenez Pena[13], S. Jin[14c], A. Jinaru[27b], O. Jinnouchi[154], P. Johansson[139], K.A. Johns[7], J.W. Johnson[136], D.M. Jones[32], E. Jones[48], P. Jones[32], R.W.L. Jones[91], T.J. Jones[92], H.L. Joos[55,36], R. Joshi[119], J. Jovicevic[15], X. Ju[17a], J.J. Junggeburth[103], T. Junkermann[63a], A. Juste Rozas[13,u], M.K. Juzek[87], S. Kabana[137e], A. Kaczmarska[87], M. Kado[110], H. Kagan[119], M. Kagan[143], A. Kahn[41], A. Kahn[128], C. Kahra[100], T. Kaji[153], E. Kajomovitz[150], N. Kakati[169], I. Kalaitzidou[54], C.W. Kalderon[29], N.J. Kang[136], D. Kar[33g], K. Karava[126], M.J. Kareem[156b], E. Karentzos[54], I. Karkanias[152], O. Karkout[114], S.N. Karpov[38], Z.M. Karpova[38], V. Kartvelishvili[91], A.N. Karyukhin[37], E. Kasimi[152], J. Katzy[48], S. Kaur[34], K. Kawade[140], M.P. Kawale[120], C. Kawamoto[88], T. Kawamoto[62a], E.F. Kay[36], F.I. Kaya[158], S. Kazakos[107], V.F. Kazanin[37], Y. Ke[145], J.M. Keaveney[33a], R. Keeler[165], G.V. Kehris[61], J.S. Keller[34], A.S. Kelly[96], J.J. Kempster[146], P.D. Kennedy[100], O. Kepka[131], B.P. Kerridge[134], S. Kersten[171], B.P. Kerševan[93], S. Keshri[66], L. Keszeghova[28a], S. Ketabchi Haghighat[155], R.A. Khan[129], A. Khanov[121], A.G. Kharlamov[37], T. Kharlamova[37], E.E. Khoda[138], M. Kholodenko[37], T.J. Khoo[18], G. Khoriauli[166], J. Khubua[149b,*], Y.A.R. Khwaira[66], B. Kibirige[33g], A. Kilgallon[123], D.W. Kim[47a,47b], Y.K. Kim[39], N. Kimura[96], M.K. Kingston[55], A. Kirchhoff[55], C. Kirfel[24], F. Kirfel[24], J. Kirk[134], A.E. Kiryunin[110], C. Kitsaki[10], O. Kivernyk[24], M. Klassen[63a], C. Klein[34], L. Klein[166], M.H. Klein[44], S.B. Klein[56], U. Klein[92], P. Klimek[36], A. Klimentov[29], T. Klioutchnikova[36], P. Kluit[114], S. Kluth[110], E. Kneringer[79], T.M. Knight[155], A. Knue[49], R. Kobayashi[88], D. Kobylianskii[169], S.F. Koch[126], M. Kocian[143], P. Kodyš[133], D.M. Koeck[123], P.T. Koenig[24], T. Koffas[34], O. Kolay[50], I. Koletsou[4], T. Komarek[122], K. Köneke[54], A.X.Y. Kong[1], T. Kono[118], N. Konstantinidis[96], P. Kontaxakis[56], B. Konya[98], R. Kopeliansky[68], S. Koperny[86a], K. Korcyl[87], K. Kordas[152,e], A. Korn[96], S. Korn[55], I. Korolkov[13], N. Korotkova[37], B. Kortman[114], O. Kortner[110], S. Kortner[110], W.H. Kostecka[115], V.V. Kostyukhin[141], A. Kotsokechagia[135], A. Kotwal[51], A. Koulouris[36], A. Kourkoumeli-Charalampidi[73a,73b], C. Kourkoumelis[9], E. Kourlitis[110,af], O. Kovanda[123], R. Kowalewski[165], W. Kozanecki[135], A.S. Kozhin[37], V.A. Kramarenko[37], G. Kramberger[93], P. Kramer[100], M.W. Krasny[127], A. Krasznahorkay[36], J.W. Kraus[171], J.A. Kremer[48], T. Kresse[50], J. Kretzschmar[92],

JHEP10(2024)130

K. Kreul[18], P. Krieger[155], S. Krishnamurthy[103], M. Krivos[133], K. Krizka[20], K. Kroeninger[49], H. Kroha[110], J. Kroll[131], J. Kroll[128], K.S. Krowpman[107], U. Kruchonak[38], H. Krüger[24], N. Krumnack[81], M.C. Kruse[51], O. Kuchinskaia[37], S. Kuday[3a], S. Kuehn[36], R. Kuesters[54], T. Kuhl[48], V. Kukhtin[38], Y. Kulchitsky[37,a], S. Kuleshov[137d,137b], M. Kumar[33g], N. Kumari[48], P. Kumari[156b], A. Kupco[131], T. Kupfer[49], A. Kupich[37], O. Kuprash[54], H. Kurashige[85], L.L. Kurchaninov[156a], O. Kurdysh[66], Y.A. Kurochkin[37], A. Kurova[37], M. Kuze[154], A.K. Kvam[103], J. Kvita[122], T. Kwan[104], N.G. Kyriacou[106], L.A.O. Laatu[102], C. Lacasta[163], F. Lacava[75a,75b], H. Lacker[18], D. Lacour[127], N.N. Lad[96], E. Ladygin[38], B. Laforge[127], T. Lagouri[27b], F.Z. Lahbabi[35a], S. Lai[55], I.K. Lakomiec[86a], N. Lalloue[60], J.E. Lambert[165], S. Lammers[68], W. Lampl[7], C. Lampoudis[152,e], G. Lamprinoudis[100], A.N. Lancaster[115], E. Lançon[29], U. Landgraf[54], M.P.J. Landon[94], V.S. Lang[54], O.K.B. Langrekken[125], A.J. Lankford[159], F. Lanni[36], K. Lantzsch[24], A. Lanza[73a], A. Lapertosa[57b,57a], J.F. Laporte[135], T. Lari[71a], F. Lasagni Manghi[23b], M. Lassnig[36], V. Latonova[131], A. Laudrain[100], A. Laurier[150], S.D. Lawlor[139], Z. Lawrence[101], R. Lazaridou[167], M. Lazzaroni[71a,71b], B. Le[101], E.M. Le Boulicaut[51], B. Leban[93], A. Lebedev[81], M. LeBlanc[101], F. Ledroit-Guillon[60], A.C.A. Lee[96], S.C. Lee[148], S. Lee[47a,47b], T.F. Lee[92], L.L. Leeuw[33c], H.P. Lefebvre[95], M. Lefebvre[165], C. Leggett[17a], G. Lehmann Miotto[36], M. Leigh[56], W.A. Leight[103], W. Leinonen[113], A. Leisos[152,t], M.A.L. Leite[83c], C.E. Leitgeb[18], R. Leitner[133], K.J.C. Leney[44], T. Lenz[24], S. Leone[74a], C. Leonidopoulos[52], A. Leopold[144], C. Leroy[108], R. Les[107], C.G. Lester[32], M. Levchenko[37], J. Levêque[4], L.J. Levinson[169], G. Levrini[23b,23a], M.P. Lewicki[87], D.J. Lewis[4], A. Li[5], B. Li[62b], C. Li[62a], C-Q. Li[110], H. Li[62a], H. Li[62b], H. Li[14c], H. Li[14b], H. Li[62b], J. Li[62c], K. Li[138], L. Li[62c], M. Li[14a,14e], Q.Y. Li[62a], S. Li[14a,14e], S. Li[62d,62c,d], T. Li[5], X. Li[104], Z. Li[126], Z. Li[104], Z. Li[14a,14e], S. Liang[14a,14e], Z. Liang[14a], M. Liberatore[135], B. Liberti[76a], K. Lie[64c], J. Lieber Marin[83b], H. Lien[68], K. Lin[107], R.E. Lindley[7], J.H. Lindon[2], E. Lipeles[128], A. Lipniacka[16], A. Lister[164], J.D. Little[4], B. Liu[14a], B.X. Liu[142], D. Liu[62d,62c], J.B. Liu[62a], J.K.K. Liu[32], K. Liu[62d,62c], M. Liu[62a], M.Y. Liu[62a], P. Liu[14a], Q. Liu[62d,138,62c], X. Liu[62a], X. Liu[62b], Y. Liu[14d,14e], Y.L. Liu[62b], Y.W. Liu[62a], J. Llorente Merino[142], S.L. Lloyd[94], E.M. Lobodzinska[48], P. Loch[7], T. Lohse[18], K. Lohwasser[139], E. Loiacono[48], M. Lokajicek[131,*], J.D. Lomas[20], J.D. Long[162], I. Longarini[159], L. Longo[70a,70b], R. Longo[162], I. Lopez Paz[67], A. Lopez Solis[48], N. Lorenzo Martinez[4], A.M. Lory[109], G. Löschcke Centeno[146], O. Loseva[37], X. Lou[47a,47b], X. Lou[14a,14e], A. Lounis[66], P.A. Love[91], G. Lu[14a,14e], M. Lu[80], S. Lu[128], Y.J. Lu[65], H.J. Lubatti[138], C. Luci[75a,75b], F.L. Lucio Alves[14c], F. Luehring[68], I. Luise[145], O. Lukianchuk[66], O. Lundberg[144], B. Lund-Jensen[144,*], N.A. Luongo[6], M.S. Lutz[36], A.B. Lux[25], D. Lynn[29], R. Lysak[131], E. Lytken[98], V. Lyubushkin[38], T. Lyubushkina[38], M.M. Lyukova[145], H. Ma[29], K. Ma[62a], L.L. Ma[62b], W. Ma[62a], Y. Ma[121], D.M. Mac Donell[165], G. Maccarrone[53], J.C. MacDonald[100], P.C. Machado De Abreu Farias[83b], R. Madar[40], W.F. Mader[50], T. Madula[96], J. Maeda[85], T. Maeno[29], H. Maguire[139], V. Maiboroda[135], A. Maio[130a,130b,130d], K. Maj[86a], O. Majersky[48], S. Majewski[123], N. Makovec[66], V. Maksimovic[15], B. Malaescu[127], Pa. Malecki[87], V.P. Maleev[37], F. Malek[60,o], M. Mali[93], D. Malito[95], U. Mallik[80,*],

JHEP10(2024)130

S. Maltezos[10], S. Malyukov[38], J. Mamuzic[13], G. Mancini[53], M.N. Mancini[26], G. Manco[73a,73b], J.P. Mandalia[94], I. Mandić[93], L. Manhaes de Andrade Filho[83a], I.M. Maniatis[169], J. Manjarres Ramos[102,ac], D.C. Mankad[169], A. Mann[109], S. Manzoni[36], L. Mao[62c], X. Mapekula[33c], A. Marantis[152,t], G. Marchiori[5], M. Marcisovsky[131], C. Marcon[71a], M. Marinescu[20], S. Marium[48], M. Marjanovic[120], E.J. Marshall[91], Z. Marshall[17a], S. Marti-Garcia[163], T.A. Martin[167], V.J. Martin[52], B. Martin dit Latour[16], L. Martinelli[75a,75b], M. Martinez[13,u], P. Martinez Agullo[163], V.I. Martinez Outschoorn[103], P. Martinez Suarez[13], S. Martin-Haugh[134], V.S. Martoiu[27b], A.C. Martyniuk[96], A. Marzin[36], D. Mascione[78a,78b], L. Masetti[100], T. Mashimo[153], J. Masik[101], A.L. Maslennikov[37], P. Massarotti[72a,72b], P. Mastrandrea[74a,74b], A. Mastroberardino[43b,43a], T. Masubuchi[153], T. Mathisen[161], J. Matousek[133], N. Matsuzawa[153], J. Maurer[27b], B. Maček[93], D.A. Maximov[37], R. Mazini[148], I. Maznas[115], M. Mazza[107], S.M. Mazza[136], E. Mazzeo[71a,71b], C. Mc Ginn[29], J.P. Mc Gowan[104], S.P. Mc Kee[106], C.C. McCracken[164], E.F. McDonald[105], A.E. McDougall[114], J.A. Mcfayden[146], R.P. McGovern[128], G. Mchedlidze[149b], R.P. Mckenzie[33g], T.C. Mclachlan[48], D.J. Mclaughlin[96], S.J. McMahon[134], C.M. Mcpartland[92], R.A. McPherson[165,y], S. Mehlhase[109], A. Mehta[92], D. Melini[163], B.R. Mellado Garcia[33g], A.H. Melo[55], F. Meloni[48], A.M. Mendes Jacques Da Costa[101], H.Y. Meng[155], L. Meng[91], S. Menke[110], M. Mentink[36], E. Meoni[43b,43a], G. Mercado[115], C. Merlassino[69a,69c], L. Merola[72a,72b], C. Meroni[71a,71b], J. Metcalfe[6], A.S. Mete[6], C. Meyer[68], J-P. Meyer[135], R.P. Middleton[134], L. Mijović[52], G. Mikenberg[169], M. Mikestikova[131], M. Mikuž[93], H. Mildner[100], A. Milic[36], D.W. Miller[39], E.H. Miller[143], L.S. Miller[34], A. Milov[169], D.A. Milstead[47a,47b], T. Min[14c], A.A. Minaenko[37], I.A. Minashvili[149b], L. Mince[59], A.I. Mincer[117], B. Mindur[86a], M. Mineev[38], Y. Mino[88], L.M. Mir[13], M. Miralles Lopez[59], M. Mironova[17a], A. Mishima[153], M.C. Missio[113], A. Mitra[167], V.A. Mitsou[163], Y. Mitsumori[111], O. Miu[155], P.S. Miyagawa[94], T. Mkrtchyan[63a], M. Mlinarevic[96], T. Mlinarevic[96], M. Mlynarikova[36], S. Mobius[19], P. Mogg[109], M.H. Mohamed Farook[112], A.F. Mohammed[14a,14e], S. Mohapatra[41], G. Mokgatitswane[33g], L. Moleri[169], B. Mondal[141], S. Mondal[132], K. Mönig[48], E. Monnier[102], L. Monsonis Romero[163], J. Montejo Berlingen[13], M. Montella[119], F. Montereali[77a,77b], F. Monticelli[90], S. Monzani[69a,69c], N. Morange[66], A.L. Moreira De Carvalho[130a], M. Moreno Llácer[163], C. Moreno Martinez[56], P. Morettini[57b], S. Morgenstern[36], M. Morii[61], M. Morinaga[153], F. Morodei[75a,75b], L. Morvaj[36], P. Moschovakos[36], B. Moser[36], M. Mosidze[149b], T. Moskalets[54], P. Moskvitina[113], J. Moss[31,l], A. Moussa[35d], E.J.W. Moyse[103], O. Mtintsilana[33g], S. Muanza[102], J. Mueller[129], D. Muenstermann[91], R. Müller[19], G.A. Mullier[161], A.J. Mullin[32], J.J. Mullin[128], D.P. Mungo[155], D. Munoz Perez[163], F.J. Munoz Sanchez[101], M. Murin[101], W.J. Murray[167,134], M. Muškinja[93], C. Mwewa[29], A.G. Myagkov[37,a], A.J. Myers[8], G. Myers[106], M. Myska[132], B.P. Nachman[17a], O. Nackenhorst[49], K. Nagai[126], K. Nagano[84], J.L. Nagle[29,aj], E. Nagy[102], A.M. Nairz[36], Y. Nakahama[84], K. Nakamura[84], K. Nakkalil[5], H. Nanjo[124], R. Narayan[44], E.A. Narayanan[112], I. Naryshkin[37], M. Naseri[34], S. Nasri[116b], C. Nass[24], G. Navarro[22a], J. Navarro-Gonzalez[163], R. Nayak[151], A. Nayaz[18], P.Y. Nechaeva[37], F. Nechansky[48], L. Nedic[126], T.J. Neep[20], A. Negri[73a,73b], M. Negrini[23b], C. Nellist[114], C. Nelson[104],

JHEP10(2024)130

K. Nelson[106], S. Nemecek[131], M. Nessi[36,h], M.S. Neubauer[162], F. Neuhaus[100], J. Neundorf[48], R. Newhouse[164], P.R. Newman[20], C.W. Ng[129], Y.W.Y. Ng[48], B. Ngair[116a], H.D.N. Nguyen[108], R.B. Nickerson[126], R. Nicolaidou[135], J. Nielsen[136], M. Niemeyer[55], J. Niermann[55], N. Nikiforou[36], V. Nikolaenko[37,a], I. Nikolic-Audit[127], K. Nikolopoulos[20], P. Nilsson[29], I. Ninca[48], H.R. Nindhito[56], G. Ninio[151], A. Nisati[75a], N. Nishu[2], R. Nisius[110], J-E. Nitschke[50], E.K. Nkadimeng[33g], T. Nobe[153], D.L. Noel[32], T. Nommensen[147], M.B. Norfolk[139], R.R.B. Norisam[96], B.J. Norman[34], M. Noury[35a], J. Novak[93], T. Novak[48], L. Novotny[132], R. Novotny[112], L. Nozka[122], K. Ntekas[159], N.M.J. Nunes De Moura Junior[83b], J. Ocariz[127], A. Ochi[85], I. Ochoa[130a], S. Oerdek[48,v], J.T. Offermann[39], A. Ogrodnik[133], A. Oh[101], C.C. Ohm[144], H. Oide[84], R. Oishi[153], M.L. Ojeda[48], Y. Okumura[153], L.F. Oleiro Seabra[130a], S.A. Olivares Pino[137d], D. Oliveira Damazio[29], D. Oliveira Goncalves[83a], J.L. Oliver[159], Ö.O. Öncel[54], A.P. O'Neill[19], A. Onofre[130a,130e], P.U.E. Onyisi[11], M.J. Oreglia[39], G.E. Orellana[90], D. Orestano[77a,77b], N. Orlando[13], R.S. Orr[155], V. O'Shea[59], L.M. Osojnak[128], R. Ospanov[62a], G. Otero y Garzon[30], H. Otono[89], P.S. Ott[63a], G.J. Ottino[17a], M. Ouchrif[35d], F. Ould-Saada[125], M. Owen[59], R.E. Owen[134], K.Y. Oyulmaz[21a], V.E. Ozcan[21a], F. Ozturk[87], N. Ozturk[8], S. Ozturk[82], H.A. Pacey[126], A. Pacheco Pages[13], C. Padilla Aranda[13], G. Padovano[75a,75b], S. Pagan Griso[17a], G. Palacino[68], A. Palazzo[70a,70b], J. Pampel[24], J. Pan[172], T. Pan[64a], D.K. Panchal[11], C.E. Pandini[114], J.G. Panduro Vazquez[95], H.D. Pandya[1], H. Pang[14b], P. Pani[48], G. Panizzo[69a,69c], L. Panwar[127], L. Paolozzi[56], S. Parajuli[162], A. Paramonov[6], C. Paraskevopoulos[53], D. Paredes Hernandez[64b], A. Pareti[73a,73b], K.R. Park[41], T.H. Park[155], M.A. Parker[32], F. Parodi[57b,57a], E.W. Parrish[115], V.A. Parrish[52], J.A. Parsons[41], U. Parzefall[54], B. Pascual Dias[108], L. Pascual Dominguez[151], E. Pasqualucci[75a], S. Passaggio[57b], F. Pastore[95], P. Patel[87], U.M. Patel[51], J.R. Pater[101], T. Pauly[36], C.I. Pazos[158], J. Pearkes[143], M. Pedersen[125], R. Pedro[130a], S.V. Peleganchuk[37], O. Penc[36], E.A. Pender[52], G.D. Penn[172], K.E. Penski[109], M. Penzin[37], B.S. Peralva[83d], A.P. Pereira Peixoto[60], L. Pereira Sanchez[143], D.V. Perepelitsa[29,aj], E. Perez Codina[156a], M. Perganti[10], H. Pernegger[36], O. Perrin[40], K. Peters[48], R.F.Y. Peters[101], B.A. Petersen[36], T.C. Petersen[42], E. Petit[102], V. Petousis[132], C. Petridou[152,e], T. Petru[133], A. Petrukhin[141], M. Pettee[17a], N.E. Pettersson[36], A. Petukhov[37], K. Petukhova[133], R. Pezoa[137f], L. Pezzotti[36], G. Pezzullo[172], T.M. Pham[170], T. Pham[105], P.W. Phillips[134], G. Piacquadio[145], E. Pianori[17a], F. Piazza[123], R. Piegaia[30], D. Pietreanu[27b], A.D. Pilkington[101], M. Pinamonti[69a,69c], J.L. Pinfold[2], B.C. Pinheiro Pereira[130a], A.E. Pinto Pinoargote[100,135], L. Pintucci[69a,69c], K.M. Piper[146], A. Pirttikoski[56], D.A. Pizzi[34], L. Pizzimento[64b], A. Pizzini[114], M.-A. Pleier[29], V. Plesanovs[54], V. Pleskot[133], E. Plotnikova[38], G. Poddar[94], R. Poettgen[98], L. Poggioli[127], I. Pokharel[55], S. Polacek[133], G. Polesello[73a], A. Poley[142,156a], A. Polini[23b], C.S. Pollard[167], Z.B. Pollock[119], E. Pompa Pacchi[75a,75b], D. Ponomarenko[113], L. Pontecorvo[36], S. Popa[27a], G.A. Popeneciu[27d], A. Poreba[36], D.M. Portillo Quintero[156a], S. Pospisil[132], M.A. Postill[139], P. Postolache[27c], K. Potamianos[167], P.A. Potepa[86a], I.N. Potrap[38], C.J. Potter[32], H. Potti[1], T. Poulsen[48], J. Poveda[163], M.E. Pozo Astigarraga[36], A. Prades Ibanez[163], J. Pretel[54], D. Price[101],

JHEP10(2024)130

M. Primavera[70a], M.A. Principe Martin[99], R. Privara[122], T. Procter[59], M.L. Proffitt[138], N. Proklova[128], K. Prokofiev[64c], G. Proto[110], J. Proudfoot[6], M. Przybycien[86a], W.W. Przygoda[86b], A. Psallidas[46], J.E. Puddefoot[139], D. Pudzha[37], D. Pyatiizbyantseva[37], J. Qian[106], D. Qichen[101], Y. Qin[101], T. Qiu[52], A. Quadt[55], M. Queitsch-Maitland[101], G. Quetant[56], R.P. Quinn[164], G. Rabanal Bolanos[61], D. Rafanoharana[54], F. Ragusa[71a,71b], J.L. Rainbolt[39], J.A. Raine[56], S. Rajagopalan[29], E. Ramakoti[37], I.A. Ramirez-Berend[34], K. Ran[48,14e], N.P. Rapheeha[33g], H. Rasheed[27b], V. Raskina[127], D.F. Rassloff[63a], A. Rastogi[17a], S. Rave[100], B. Ravina[55], I. Ravinovich[169], M. Raymond[36], A.L. Read[125], N.P. Readioff[139], D.M. Rebuzzi[73a,73b], G. Redlinger[29], A.S. Reed[110], K. Reeves[26], J.A. Reidelsturz[171], D. Reikher[151], A. Rej[49], C. Rembser[36], M. Renda[27b], M.B. Rendel[110], F. Renner[48], A.G. Rennie[159], A.L. Rescia[48], S. Resconi[71a], M. Ressegotti[57b,57a], S. Rettie[36], J.G. Reyes Rivera[107], E. Reynolds[17a], O.L. Rezanova[37], P. Reznicek[133], H. Riani[35d], N. Ribaric[91], E. Ricci[78a,78b], R. Richter[110], S. Richter[47a,47b], E. Richter-Was[86b], M. Ridel[127], S. Ridouani[35d], P. Rieck[117], P. Riedler[36], E.M. Riefel[47a,47b], J.O. Rieger[114], M. Rijssenbeek[145], M. Rimoldi[36], L. Rinaldi[23b,23a], T.T. Rinn[29], M.P. Rinnagel[109], G. Ripellino[161], I. Riu[13], J.C. Rivera Vergara[165], F. Rizatdinova[121], E. Rizvi[94], B.R. Roberts[17a], S.H. Robertson[104,y], D. Robinson[32], C.M. Robles Gajardo[137f], M. Robles Manzano[100], A. Robson[59], A. Rocchi[76a,76b], C. Roda[74a,74b], S. Rodriguez Bosca[36], Y. Rodriguez Garcia[22a], A. Rodriguez Rodriguez[54], A.M. Rodríguez Vera[156b], S. Roe[36], J.T. Roemer[159], A.R. Roepe-Gier[136], J. Roggel[171], O. Røhne[125], R.A. Rojas[103], C.P.A. Roland[127], J. Roloff[29], A. Romaniouk[37], E. Romano[73a,73b], M. Romano[23b], A.C. Romero Hernandez[162], N. Rompotis[92], L. Roos[127], S. Rosati[75a], B.J. Rosser[39], E. Rossi[126], E. Rossi[72a,72b], L.P. Rossi[61], L. Rossini[54], R. Rosten[119], M. Rotaru[27b], B. Rottler[54], C. Rougier[102], D. Rousseau[66], D. Rousso[32], A. Roy[162], S. Roy-Garand[155], A. Rozanov[102], Z.M.A. Rozario[59], Y. Rozen[150], A. Rubio Jimenez[163], A.J. Ruby[92], V.H. Ruelas Rivera[18], T.A. Ruggeri[1], A. Ruggiero[126], A. Ruiz-Martinez[163], A. Rummler[36], Z. Rurikova[54], N.A. Rusakovich[38], H.L. Russell[165], G. Russo[75a,75b], J.P. Rutherfoord[7], S. Rutherford Colmenares[32], K. Rybacki[91], M. Rybar[133], E.B. Rye[125], A. Ryzhov[44], J.A. Sabater Iglesias[56], P. Sabatini[163], H.F-W. Sadrozinski[136], F. Safai Tehrani[75a], B. Safarzadeh Samani[134], M. Safdari[143], S. Saha[165], M. Sahinsoy[110], A. Saibel[163], M. Saimpert[135], M. Saito[153], T. Saito[153], D. Salamani[36], A. Salnikov[143], J. Salt[163], A. Salvador Salas[151], D. Salvatore[43b,43a], F. Salvatore[146], A. Salzburger[36], D. Sammel[54], D. Sampsonidis[152,e], D. Sampsonidou[123], J. Sánchez[163], V. Sanchez Sebastian[163], H. Sandaker[125], C.O. Sander[48], J.A. Sandesara[103], M. Sandhoff[171], C. Sandoval[22b], D.P.C. Sankey[134], T. Sano[88], A. Sansoni[53], L. Santi[75a,75b], C. Santoni[40], H. Santos[130a,130b], A. Santra[169], K.A. Saoucha[160], J.G. Saraiva[130a,130d], J. Sardain[7], O. Sasaki[84], K. Sato[157], C. Sauer[63b], F. Sauerburger[54], E. Sauvan[4], P. Savard[155,ah], R. Sawada[153], C. Sawyer[134], L. Sawyer[97], I. Sayago Galvan[163], C. Sbarra[23b], A. Sbrizzi[23b,23a], T. Scanlon[96], J. Schaarschmidt[138], U. Schäfer[100], A.C. Schaffer[66,44], D. Schaile[109], R.D. Schamberger[145], C. Scharf[18], M.M. Schefer[19], V.A. Schegelsky[37], D. Scheirich[133], F. Schenck[18], M. Schernau[159], C. Scheulen[55], C. Schiavi[57b,57a], M. Schioppa[43b,43a], B. Schlag[143,n], K.E. Schleicher[54], S. Schlenker[36], J. Schmeing[171], M.A. Schmidt[171], K. Schmieden[100], C. Schmitt[100],

JHEP10(2024)130

N. Schmitt[100], S. Schmitt[48], L. Schoeffel[135], A. Schoening[63b], P.G. Scholer[34], E. Schopf[126], M. Schott[100], J. Schovancova[36], S. Schramm[56], T. Schroer[56], H-C. Schultz-Coulon[63a], M. Schumacher[54], B.A. Schumm[136], Ph. Schune[135], A.J. Schuy[138], H.R. Schwartz[136], A. Schwartzman[143], T.A. Schwarz[106], Ph. Schwemling[135], R. Schwienhorst[107], A. Sciandra[136], G. Sciolla[26], F. Scuri[74a], C.D. Sebastiani[92], K. Sedlaczek[115], P. Seema[18], S.C. Seidel[112], A. Seiden[136], B.D. Seidlitz[41], C. Seitz[48], J.M. Seixas[83b], G. Sekhniaidze[72a], L. Selem[60], N. Semprini-Cesari[23b,23a], D. Sengupta[56], V. Senthilkumar[163], L. Serin[66], L. Serkin[69a,69b], M. Sessa[76a,76b], H. Severini[120], F. Sforza[57b,57a], A. Sfyrla[56], Q. Sha[14a], E. Shabalina[55], R. Shaheen[144], J.D. Shahinian[128], D. Shaked Renous[169], L.Y. Shan[14a], M. Shapiro[17a], A. Sharma[36], A.S. Sharma[164], P. Sharma[80], P.B. Shatalov[37], K. Shaw[146], S.M. Shaw[101], A. Shcherbakova[37], Q. Shen[62c,5], D.J. Sheppard[142], P. Sherwood[96], L. Shi[96], X. Shi[14a], C.O. Shimmin[172], J.D. Shinner[95], I.P.J. Shipsey[126], S. Shirabe[89], M. Shiyakova[38,w], J. Shlomi[169], M.J. Shochet[39], J. Shojaii[105], D.R. Shope[125], B. Shrestha[120], S. Shrestha[119,ak], E.M. Shrif[33g], M.J. Shroff[165], P. Sicho[131], A.M. Sickles[162], E. Sideras Haddad[33g], A. Sidoti[23b], F. Siegert[50], Dj. Sijacki[15], F. Sili[90], J.M. Silva[52], M.V. Silva Oliveira[29], S.B. Silverstein[47a], S. Simion[66], R. Simoniello[36], E.L. Simpson[59], H. Simpson[146], L.R. Simpson[106], N.D. Simpson[98], S. Simsek[82], S. Sindhu[55], P. Sinervo[155], S. Singh[155], S. Sinha[48], S. Sinha[101], M. Sioli[23b,23a], I. Siral[36], E. Sitnikova[48], J. Sjölin[47a,47b], A. Skaf[55], E. Skorda[20], P. Skubic[120], M. Slawinska[87], V. Smakhtin[169], B.H. Smart[134], S.Yu. Smirnov[37], Y. Smirnov[37], L.N. Smirnova[37,a], O. Smirnova[98], A.C. Smith[41], E.A. Smith[39], H.A. Smith[126], J.L. Smith[92], R. Smith[143], M. Smizanska[91], K. Smolek[132], A.A. Snesarev[37], S.R. Snider[155], H.L. Snoek[114], S. Snyder[29], R. Sobie[165,y], A. Soffer[151], C.A. Solans Sanchez[36], E.Yu. Soldatov[37], U. Soldevila[163], A.A. Solodkov[37], S. Solomon[26], A. Soloshenko[38], K. Solovieva[54], O.V. Solovyanov[40], V. Solovyev[37], P. Sommer[36], A. Sonay[13], W.Y. Song[156b], A. Sopczak[132], A.L. Sopio[96], F. Sopkova[28b], J.D. Sorenson[112], I.R. Sotarriva Alvarez[154], V. Sothilingam[63a], O.J. Soto Sandoval[137c,137b], S. Sottocornola[68], R. Soualah[160], Z. Soumaimi[35e], D. South[48], N. Soybelman[169], S. Spagnolo[70a,70b], M. Spalla[110], D. Sperlich[54], G. Spigo[36], S. Spinali[91], D.P. Spiteri[59], M. Spousta[133], E.J. Staats[34], R. Stamen[63a], A. Stampekis[20], M. Standke[24], E. Stanecka[87], M.V. Stange[50], B. Stanislaus[17a], M.M. Stanitzki[48], B. Stapf[48], E.A. Starchenko[37], G.H. Stark[136], J. Stark[102,ac], P. Staroba[131], P. Starovoitov[63a], S. Stärz[104], R. Staszewski[87], G. Stavropoulos[46], J. Steentoft[161], P. Steinberg[29], B. Stelzer[142,156a], H.J. Stelzer[129], O. Stelzer-Chilton[156a], H. Stenzel[58], T.J. Stevenson[146], G.A. Stewart[36], J.R. Stewart[121], M.C. Stockton[36], G. Stoicea[27b], M. Stolarski[130a], S. Stonjek[110], A. Straessner[50], J. Strandberg[144], S. Strandberg[47a,47b], M. Stratmann[171], M. Strauss[120], T. Strebler[102], P. Strizenec[28b], R. Ströhmer[166], D.M. Strom[123], R. Stroynowski[44], A. Strubig[47a,47b], S.A. Stucci[29], B. Stugu[16], J. Stupak[120], N.A. Styles[48], D. Su[143], S. Su[62a], W. Su[62d], X. Su[62a], K. Sugizaki[153], V.V. Sulin[37], M.J. Sullivan[92], D.M.S. Sultan[126], L. Sultanaliyeva[37], S. Sultansoy[3b], T. Sumida[88], S. Sun[106], S. Sun[170], O. Sunneborn Gudnadottir[161], N. Sur[102], M.R. Sutton[146], H. Suzuki[157], M. Svatos[131], M. Swiatlowski[156a], T. Swirski[166], I. Sykora[28a], M. Sykora[133], T. Sykora[133], D. Ta[100], K. Tackmann[48,v], A. Taffard[159],

JHEP10(2024)130

R. Tafirout[156a], J.S. Tafoya Vargas[66], Y. Takubo[84], M. Talby[102], A.A. Talyshev[37], K.C. Tam[64b], N.M. Tamir[151], A. Tanaka[153], J. Tanaka[153], R. Tanaka[66], M. Tanasini[57b,57a], Z. Tao[164], S. Tapia Araya[137f], S. Tapprogge[100], A. Tarek Abouelfadl Mohamed[107], S. Tarem[150], K. Tariq[14a], G. Tarna[102,27b], G.F. Tartarelli[71a], P. Tas[133], M. Tasevsky[131], E. Tassi[43b,43a], A.C. Tate[162], G. Tateno[153], Y. Tayalati[35e,x], G.N. Taylor[105], W. Taylor[156b], A.S. Tee[170], R. Teixeira De Lima[143], P. Teixeira-Dias[95], J.J. Teoh[155], K. Terashi[153], J. Terron[99], S. Terzo[13], M. Testa[53], R.J. Teuscher[155,y], A. Thaler[79], O. Theiner[56], N. Themistokleous[52], T. Theveneaux-Pelzer[102], O. Thielmann[171], D.W. Thomas[95], J.P. Thomas[20], E.A. Thompson[17a], P.D. Thompson[20], E. Thomson[128], Y. Tian[55], V. Tikhomirov[37,a], Yu.A. Tikhonov[37], S. Timoshenko[37], D. Timoshyn[133], E.X.L. Ting[1], P. Tipton[172], S.H. Tlou[33g], A. Tnourji[40], K. Todome[154], S. Todorova-Nova[133], S. Todt[50], M. Togawa[84], J. Tojo[89], S. Tokár[28a], K. Tokushuku[84], O. Toldaiev[68], R. Tombs[32], M. Tomoto[84,111], L. Tompkins[143,n], K.W. Topolnicki[86b], E. Torrence[123], H. Torres[102,ac], E. Torró Pastor[163], M. Toscani[30], C. Tosciri[39], M. Tost[11], D.R. Tovey[139], A. Traeet[16], I.S. Trandafir[27b], T. Trefzger[166], A. Tricoli[29], I.M. Trigger[156a], S. Trincaz-Duvoid[127], D.A. Trischuk[26], B. Trocmé[60], L. Truong[33c], M. Trzebinski[87], A. Trzupek[87], F. Tsai[145], M. Tsai[106], A. Tsiamis[152,e], P.V. Tsiareshka[37], S. Tsigaridas[156a], A. Tsirigotis[152,t], V. Tsiskaridze[155], E.G. Tskhadadze[149a], M. Tsopoulou[152], Y. Tsujikawa[88], I.I. Tsukerman[37], V. Tsulaia[17a], S. Tsuno[84], K. Tsuri[118], D. Tsybychev[145], Y. Tu[64b], A. Tudorache[27b], V. Tudorache[27b], A.N. Tuna[61], S. Turchikhin[57b,57a], I. Turk Cakir[3a], R. Turra[71a], T. Turtuvshin[38,z], P.M. Tuts[41], S. Tzamarias[152,e], P. Tzanis[10], E. Tzovara[100], F. Ukegawa[157], P.A. Ulloa Poblete[137c,137b], E.N. Umaka[29], G. Unal[36], M. Unal[11], A. Undrus[29], G. Unel[159], J. Urban[28b], P. Urquijo[105], P. Urrejola[137a], G. Usai[8], R. Ushioda[154], M. Usman[108], Z. Uysal[82], V. Vacek[132], B. Vachon[104], K.O.H. Vadla[125], T. Vafeiadis[36], A. Vaitkus[96], C. Valderanis[109], E. Valdes Santurio[47a,47b], M. Valente[156a], S. Valentinetti[23b,23a], A. Valero[163], E. Valiente Moreno[163], A. Vallier[102,ac], J.A. Valls Ferrer[163], D.R. Van Arneman[114], T.R. Van Daalen[138], A. Van Der Graaf[49], P. Van Gemmeren[6], M. Van Rijnbach[125], S. Van Stroud[96], I. Van Vulpen[114], M. Vanadia[76a,76b], W. Vandelli[36], E.R. Vandewall[121], D. Vannicola[151], L. Vannoli[57b,57a], R. Vari[75a], E.W. Varnes[7], C. Varni[17b], T. Varol[148], D. Varouchas[66], L. Varriale[163], K.E. Varvell[147], M.E. Vasile[27b], L. Vaslin[84], G.A. Vasquez[165], A. Vasyukov[38], R. Vavricka[100], F. Vazeille[40], T. Vazquez Schroeder[36], J. Veatch[31], V. Vecchio[101], M.J. Veen[103], I. Veliscek[126], L.M. Veloce[155], F. Veloso[130a,130c], S. Veneziano[75a], A. Ventura[70a,70b], S. Ventura Gonzalez[135], A. Verbytskyi[110], M. Verducci[74a,74b], C. Vergis[24], M. Verissimo De Araujo[83b], W. Verkerke[114], J.C. Vermeulen[114], C. Vernieri[143], M. Vessella[103], M.C. Vetterli[142,ah], A. Vgenopoulos[152,e], N. Viaux Maira[137f], T. Vickey[139], O.E. Vickey Boeriu[139], G.H.A. Viehhauser[126], L. Vigani[63b], M. Villa[23b,23a], M. Villaplana Perez[163], E.M. Villhauer[52], E. Vilucchi[53], M.G. Vincter[34], G.S. Virdee[20], A. Vishwakarma[52], A. Visibile[114], C. Vittori[36], I. Vivarelli[23b,23a], E. Voevodina[110], F. Vogel[109], J.C. Voigt[50], P. Vokac[132], Yu. Volkotrub[86a], J. Von Ahnen[48], E. Von Toerne[24], B. Vormwald[36], V. Vorobel[133], K. Vorobev[37], M. Vos[163], K. Voss[141], M. Vozak[114], L. Vozdecky[120], N. Vranjes[15], M. Vranjes Milosavljevic[15], M. Vreeswijk[114],

JHEP10(2024)130

N.K. Vu[62d,62c], R. Vuillermet[36], O. Vujinovic[100], I. Vukotic[39], S. Wada[157], C. Wagner[103], J.M. Wagner[17a], W. Wagner[171], S. Wahdan[171], H. Wahlberg[90], M. Wakida[111], J. Walder[134], R. Walker[109], W. Walkowiak[141], A. Wall[128], E.J. Wallin[98], T. Wamorkar[6], A.Z. Wang[136], C. Wang[100], C. Wang[11], H. Wang[17a], J. Wang[64c], R.-J. Wang[100], R. Wang[61], R. Wang[6], S.M. Wang[148], S. Wang[62b], T. Wang[62a], W.T. Wang[80], W. Wang[14a], X. Wang[14c], X. Wang[162], X. Wang[62c], Y. Wang[62d], Y. Wang[14c], Z. Wang[106], Z. Wang[62d,51,62c], Z. Wang[106], A. Warburton[104], R.J. Ward[20], N. Warrack[59], S. Waterhouse[95], A.T. Watson[20], H. Watson[59], M.F. Watson[20], E. Watton[59,134], G. Watts[138], B.M. Waugh[96], C. Weber[29], H.A. Weber[18], M.S. Weber[19], S.M. Weber[63a], C. Wei[62a], Y. Wei[126], A.R. Weidberg[126], E.J. Weik[117], J. Weingarten[49], M. Weirich[100], C. Weiser[54], C.J. Wells[48], T. Wenaus[29], B. Wendland[49], T. Wengler[36], N.S. Wenke[110], N. Wermes[24], M. Wessels[63a], A.M. Wharton[91], A.S. White[61], A. White[8], M.J. White[1], D. Whiteson[159], L. Wickremasinghe[124], W. Wiedenmann[170], M. Wielers[134], C. Wiglesworth[42], D.J. Wilbern[120], H.G. Wilkens[36], D.M. Williams[41], H.H. Williams[128], S. Williams[32], S. Willocq[103], B.J. Wilson[101], P.J. Windischhofer[39], F.I. Winkel[30], F. Winklmeier[123], B.T. Winter[54], J.K. Winter[101], M. Wittgen[143], M. Wobisch[97], Z. Wolffs[114], J. Wollrath[159], M.W. Wolter[87], H. Wolters[130a,130c], E.L. Woodward[41], S.D. Worm[48], B.K. Wosiek[87], K.W. Woźniak[87], S. Wozniewski[55], K. Wraight[59], C. Wu[20], M. Wu[14d], M. Wu[113], S.L. Wu[170], X. Wu[56], Y. Wu[62a], Z. Wu[135], J. Wuerzinger[110,af], T.R. Wyatt[101], B.M. Wynne[52], S. Xella[42], L. Xia[14c], M. Xia[14b], J. Xiang[64c], M. Xie[62a], X. Xie[62a], S. Xin[14a,14e], A. Xiong[123], J. Xiong[17a], D. Xu[14a], H. Xu[62a], L. Xu[62a], R. Xu[128], T. Xu[106], Y. Xu[14b], Z. Xu[52], Z. Xu[14c], B. Yabsley[147], S. Yacoob[33a], Y. Yamaguchi[154], E. Yamashita[153], H. Yamauchi[157], T. Yamazaki[17a], Y. Yamazaki[85], J. Yan[62c], S. Yan[59], Z. Yan[103], H.J. Yang[62c,62d], H.T. Yang[62a], S. Yang[62a], T. Yang[64c], X. Yang[36], X. Yang[14a], Y. Yang[44], Y. Yang[62a], Z. Yang[62a], W-M. Yao[17a], H. Ye[14c], H. Ye[55], J. Ye[14a], S. Ye[29], X. Ye[62a], Y. Yeh[96], I. Yeletskikh[38], B. Yeo[17b], M.R. Yexley[96], P. Yin[41], K. Yorita[168], S. Younas[27b], C.J.S. Young[36], C. Young[143], C. Yu[14a,14e], Y. Yu[62a], M. Yuan[106], R. Yuan[62b], L. Yue[96], M. Zaazoua[62a], B. Zabinski[87], E. Zaid[52], Z.K. Zak[87], T. Zakareishvili[163], N. Zakharchuk[34], S. Zambito[56], J.A. Zamora Saa[137d,137b], J. Zang[153], D. Zanzi[54], O. Zaplatilek[132], C. Zeitnitz[171], H. Zeng[14a], J.C. Zeng[162], D.T. Zenger Jr[26], O. Zenin[37], T. Ženiš[28a], S. Zenz[94], S. Zerradi[35a], D. Zerwas[66], M. Zhai[14a,14e], D.F. Zhang[139], J. Zhang[62b], J. Zhang[6], K. Zhang[14a,14e], L. Zhang[14c], P. Zhang[14a,14e], R. Zhang[170], S. Zhang[106], S. Zhang[44], T. Zhang[153], X. Zhang[62c], X. Zhang[62b], Y. Zhang[62c,5], Y. Zhang[96], Y. Zhang[14c], Z. Zhang[17a], Z. Zhang[66], H. Zhao[138], T. Zhao[62b], Y. Zhao[136], Z. Zhao[62a], A. Zhemchugov[38], J. Zheng[14c], K. Zheng[162], X. Zheng[62a], Z. Zheng[143], D. Zhong[162], B. Zhou[106], H. Zhou[7], N. Zhou[62c], Y. Zhou[14c], Y. Zhou[7], C.G. Zhu[62b], J. Zhu[106], Y. Zhu[62c], Y. Zhu[62a], X. Zhuang[14a], K. Zhukov[37], N.I. Zimine[38], J. Zinsser[63b], M. Ziolkowski[141], L. Živković[15], A. Zoccoli[23b,23a], K. Zoch[61], T.G. Zorbas[139], O. Zormpa[46], W. Zou[41], L. Zwalinski[36]

[1] *Department of Physics, University of Adelaide, Adelaide; Australia*
[2] *Department of Physics, University of Alberta, Edmonton AB; Canada*

JHEP10(2024)130

[3] [(a)] Department of Physics, Ankara University, Ankara;[(b)] Division of Physics, TOBB University of Economics and Technology, Ankara; Türkiye
[4] LAPP, Université Savoie Mont Blanc, CNRS/IN2P3, Annecy; France
[5] APC, Université Paris Cité, CNRS/IN2P3, Paris; France
[6] High Energy Physics Division, Argonne National Laboratory, Argonne IL; United States of America
[7] Department of Physics, University of Arizona, Tucson AZ; United States of America
[8] Department of Physics, University of Texas at Arlington, Arlington TX; United States of America
[9] Physics Department, National and Kapodistrian University of Athens, Athens; Greece
[10] Physics Department, National Technical University of Athens, Zografou; Greece
[11] Department of Physics, University of Texas at Austin, Austin TX; United States of America
[12] Institute of Physics, Azerbaijan Academy of Sciences, Baku; Azerbaijan
[13] Institut de Física d'Altes Energies (IFAE), Barcelona Institute of Science and Technology, Barcelona; Spain
[14] [(a)] Institute of High Energy Physics, Chinese Academy of Sciences, Beijing;[(b)] Physics Department, Tsinghua University, Beijing;[(c)] Department of Physics, Nanjing University, Nanjing;[(d)] School of Science, Shenzhen Campus of Sun Yat-sen University;[(e)] University of Chinese Academy of Science (UCAS), Beijing; China
[15] Institute of Physics, University of Belgrade, Belgrade; Serbia
[16] Department for Physics and Technology, University of Bergen, Bergen; Norway
[17] [(a)] Physics Division, Lawrence Berkeley National Laboratory, Berkeley CA;[(b)] University of California, Berkeley CA; United States of America
[18] Institut für Physik, Humboldt Universität zu Berlin, Berlin; Germany
[19] Albert Einstein Center for Fundamental Physics and Laboratory for High Energy Physics, University of Bern, Bern; Switzerland
[20] School of Physics and Astronomy, University of Birmingham, Birmingham; United Kingdom
[21] [(a)] Department of Physics, Bogazici University, Istanbul;[(b)] Department of Physics Engineering, Gaziantep University, Gaziantep;[(c)] Department of Physics, Istanbul University, Istanbul; Türkiye
[22] [(a)] Facultad de Ciencias y Centro de Investigaciónes, Universidad Antonio Nariño, Bogotá;[(b)] Departamento de Física, Universidad Nacional de Colombia, Bogotá; Colombia
[23] [(a)] Dipartimento di Fisica e Astronomia A. Righi, Università di Bologna, Bologna;[(b)] INFN Sezione di Bologna; Italy
[24] Physikalisches Institut, Universität Bonn, Bonn; Germany
[25] Department of Physics, Boston University, Boston MA; United States of America
[26] Department of Physics, Brandeis University, Waltham MA; United States of America
[27] [(a)] Transilvania University of Brasov, Brasov;[(b)] Horia Hulubei National Institute of Physics and Nuclear Engineering, Bucharest;[(c)] Department of Physics, Alexandru Ioan Cuza University of Iasi, Iasi;[(d)] National Institute for Research and Development of Isotopic and Molecular Technologies, Physics Department, Cluj-Napoca;[(e)] National University of Science and Technology Politechnica, Bucharest;[(f)] West University in Timisoara, Timisoara;[(g)] Faculty of Physics, University of Bucharest, Bucharest; Romania
[28] [(a)] Faculty of Mathematics, Physics and Informatics, Comenius University, Bratislava;[(b)] Department of Subnuclear Physics, Institute of Experimental Physics of the Slovak Academy of Sciences, Kosice; Slovak Republic
[29] Physics Department, Brookhaven National Laboratory, Upton NY; United States of America
[30] Universidad de Buenos Aires, Facultad de Ciencias Exactas y Naturales, Departamento de Física, y CONICET, Instituto de Física de Buenos Aires (IFIBA), Buenos Aires; Argentina
[31] California State University, CA; United States of America
[32] Cavendish Laboratory, University of Cambridge, Cambridge; United Kingdom
[33] [(a)] Department of Physics, University of Cape Town, Cape Town;[(b)] iThemba Labs, Western Cape;[(c)] Department of Mechanical Engineering Science, University of Johannesburg, Johannesburg;[(d)] National Institute of Physics, University of the Philippines Diliman (Philippines);[(e)] University of South Africa, Department of Physics, Pretoria;[(f)] University of Zululand, KwaDlangezwa;[(g)] School of Physics, University of the Witwatersrand, Johannesburg; South Africa
[34] Department of Physics, Carleton University, Ottawa ON; Canada

JHEP10(2024)130

[35] [(a)] Faculté des Sciences Ain Chock, Université Hassan II de Casablanca;[(b)] Faculté des Sciences, Université Ibn-Tofail, Kénitra;[(c)] Faculté des Sciences Semlalia, Université Cadi Ayyad, LPHEA-Marrakech;[(d)] LPMR, Faculté des Sciences, Université Mohamed Premier, Oujda;[(e)] Faculté des sciences, Université Mohammed V, Rabat;[(f)] Institute of Applied Physics, Mohammed VI Polytechnic University, Ben Guerir; Morocco
[36] CERN, Geneva; Switzerland
[37] Affiliated with an institute covered by a cooperation agreement with CERN
[38] Affiliated with an international laboratory covered by a cooperation agreement with CERN
[39] Enrico Fermi Institute, University of Chicago, Chicago IL; United States of America
[40] LPC, Université Clermont Auvergne, CNRS/IN2P3, Clermont-Ferrand; France
[41] Nevis Laboratory, Columbia University, Irvington NY; United States of America
[42] Niels Bohr Institute, University of Copenhagen, Copenhagen; Denmark
[43] [(a)] Dipartimento di Fisica, Università della Calabria, Rende;[(b)] INFN Gruppo Collegato di Cosenza, Laboratori Nazionali di Frascati; Italy
[44] Physics Department, Southern Methodist University, Dallas TX; United States of America
[45] Physics Department, University of Texas at Dallas, Richardson TX; United States of America
[46] National Centre for Scientific Research "Demokritos", Agia Paraskevi; Greece
[47] [(a)] Department of Physics, Stockholm University;[(b)] Oskar Klein Centre, Stockholm; Sweden
[48] Deutsches Elektronen-Synchrotron DESY, Hamburg and Zeuthen; Germany
[49] Fakultät Physik , Technische Universität Dortmund, Dortmund; Germany
[50] Institut für Kern- und Teilchenphysik, Technische Universität Dresden, Dresden; Germany
[51] Department of Physics, Duke University, Durham NC; United States of America
[52] SUPA — School of Physics and Astronomy, University of Edinburgh, Edinburgh; United Kingdom
[53] INFN e Laboratori Nazionali di Frascati, Frascati; Italy
[54] Physikalisches Institut, Albert-Ludwigs-Universität Freiburg, Freiburg; Germany
[55] II. Physikalisches Institut, Georg-August-Universität Göttingen, Göttingen; Germany
[56] Département de Physique Nucléaire et Corpusculaire, Université de Genève, Genève; Switzerland
[57] [(a)] Dipartimento di Fisica, Università di Genova, Genova;[(b)] INFN Sezione di Genova; Italy
[58] II. Physikalisches Institut, Justus-Liebig-Universität Giessen, Giessen; Germany
[59] SUPA — School of Physics and Astronomy, University of Glasgow, Glasgow; United Kingdom
[60] LPSC, Université Grenoble Alpes, CNRS/IN2P3, Grenoble INP, Grenoble; France
[61] Laboratory for Particle Physics and Cosmology, Harvard University, Cambridge MA; United States of America
[62] [(a)] Department of Modern Physics and State Key Laboratory of Particle Detection and Electronics, University of Science and Technology of China, Hefei;[(b)] Institute of Frontier and Interdisciplinary Science and Key Laboratory of Particle Physics and Particle Irradiation (MOE), Shandong University, Qingdao;[(c)] School of Physics and Astronomy, Shanghai Jiao Tong University, Key Laboratory for Particle Astrophysics and Cosmology (MOE), SKLPPC, Shanghai;[(d)] Tsung-Dao Lee Institute, Shanghai;[(e)] School of Physics and Microelectronics, Zhengzhou University; China
[63] [(a)] Kirchhoff-Institut für Physik, Ruprecht-Karls-Universität Heidelberg, Heidelberg;[(b)] Physikalisches Institut, Ruprecht-Karls-Universität Heidelberg, Heidelberg; Germany
[64] [(a)] Department of Physics, Chinese University of Hong Kong, Shatin, N.T., Hong Kong;[(b)] Department of Physics, University of Hong Kong, Hong Kong;[(c)] Department of Physics and Institute for Advanced Study, Hong Kong University of Science and Technology, Clear Water Bay, Kowloon, Hong Kong; China
[65] Department of Physics, National Tsing Hua University, Hsinchu; Taiwan
[66] IJCLab, Université Paris-Saclay, CNRS/IN2P3, 91405, Orsay; France
[67] Centro Nacional de Microelectrónica (IMB-CNM-CSIC), Barcelona; Spain
[68] Department of Physics, Indiana University, Bloomington IN; United States of America
[69] [(a)] INFN Gruppo Collegato di Udine, Sezione di Trieste, Udine;[(b)] ICTP, Trieste;[(c)] Dipartimento Politecnico di Ingegneria e Architettura, Università di Udine, Udine; Italy
[70] [(a)] INFN Sezione di Lecce;[(b)] Dipartimento di Matematica e Fisica, Università del Salento, Lecce; Italy
[71] [(a)] INFN Sezione di Milano;[(b)] Dipartimento di Fisica, Università di Milano, Milano; Italy
[72] [(a)] INFN Sezione di Napoli;[(b)] Dipartimento di Fisica, Università di Napoli, Napoli; Italy
[73] [(a)] INFN Sezione di Pavia;[(b)] Dipartimento di Fisica, Università di Pavia, Pavia; Italy

JHEP10(2024)130

[74] [(a)] INFN Sezione di Pisa; [(b)] Dipartimento di Fisica E. Fermi, Università di Pisa, Pisa; Italy
[75] [(a)] INFN Sezione di Roma; [(b)] Dipartimento di Fisica, Sapienza Università di Roma, Roma; Italy
[76] [(a)] INFN Sezione di Roma Tor Vergata; [(b)] Dipartimento di Fisica, Università di Roma Tor Vergata, Roma; Italy
[77] [(a)] INFN Sezione di Roma Tre; [(b)] Dipartimento di Matematica e Fisica, Università Roma Tre, Roma; Italy
[78] [(a)] INFN-TIFPA; [(b)] Università degli Studi di Trento, Trento; Italy
[79] Universität Innsbruck, Department of Astro and Particle Physics, Innsbruck; Austria
[80] University of Iowa, Iowa City IA; United States of America
[81] Department of Physics and Astronomy, Iowa State University, Ames IA; United States of America
[82] Istinye University, Sariyer, Istanbul; Türkiye
[83] [(a)] Departamento de Engenharia Elétrica, Universidade Federal de Juiz de Fora (UFJF), Juiz de Fora; [(b)] Universidade Federal do Rio De Janeiro COPPE/EE/IF, Rio de Janeiro; [(c)] Instituto de Física, Universidade de São Paulo, São Paulo; [(d)] Rio de Janeiro State University, Rio de Janeiro; Brazil
[84] KEK, High Energy Accelerator Research Organization, Tsukuba; Japan
[85] Graduate School of Science, Kobe University, Kobe; Japan
[86] [(a)] AGH University of Krakow, Faculty of Physics and Applied Computer Science, Krakow; [(b)] Marian Smoluchowski Institute of Physics, Jagiellonian University, Krakow; Poland
[87] Institute of Nuclear Physics Polish Academy of Sciences, Krakow; Poland
[88] Faculty of Science, Kyoto University, Kyoto; Japan
[89] Research Center for Advanced Particle Physics and Department of Physics, Kyushu University, Fukuoka; Japan
[90] Instituto de Física La Plata, Universidad Nacional de La Plata and CONICET, La Plata; Argentina
[91] Physics Department, Lancaster University, Lancaster; United Kingdom
[92] Oliver Lodge Laboratory, University of Liverpool, Liverpool; United Kingdom
[93] Department of Experimental Particle Physics, Jožef Stefan Institute and Department of Physics, University of Ljubljana, Ljubljana; Slovenia
[94] School of Physics and Astronomy, Queen Mary University of London, London; United Kingdom
[95] Department of Physics, Royal Holloway University of London, Egham; United Kingdom
[96] Department of Physics and Astronomy, University College London, London; United Kingdom
[97] Louisiana Tech University, Ruston LA; United States of America
[98] Fysiska institutionen, Lunds universitet, Lund; Sweden
[99] Departamento de Física Teorica C-15 and CIAFF, Universidad Autónoma de Madrid, Madrid; Spain
[100] Institut für Physik, Universität Mainz, Mainz; Germany
[101] School of Physics and Astronomy, University of Manchester, Manchester; United Kingdom
[102] CPPM, Aix-Marseille Université, CNRS/IN2P3, Marseille; France
[103] Department of Physics, University of Massachusetts, Amherst MA; United States of America
[104] Department of Physics, McGill University, Montreal QC; Canada
[105] School of Physics, University of Melbourne, Victoria; Australia
[106] Department of Physics, University of Michigan, Ann Arbor MI; United States of America
[107] Department of Physics and Astronomy, Michigan State University, East Lansing MI; United States of America
[108] Group of Particle Physics, University of Montreal, Montreal QC; Canada
[109] Fakultät für Physik, Ludwig-Maximilians-Universität München, München; Germany
[110] Max-Planck-Institut für Physik (Werner-Heisenberg-Institut), München; Germany
[111] Graduate School of Science and Kobayashi-Maskawa Institute, Nagoya University, Nagoya; Japan
[112] Department of Physics and Astronomy, University of New Mexico, Albuquerque NM; United States of America
[113] Institute for Mathematics, Astrophysics and Particle Physics, Radboud University/Nikhef, Nijmegen; Netherlands
[114] Nikhef National Institute for Subatomic Physics and University of Amsterdam, Amsterdam; Netherlands
[115] Department of Physics, Northern Illinois University, DeKalb IL; United States of America
[116] [(a)] New York University Abu Dhabi, Abu Dhabi; [(b)] United Arab Emirates University, Al Ain; United Arab Emirates

JHEP10(2024)130

[117] Department of Physics, New York University, New York NY; United States of America
[118] Ochanomizu University, Otsuka, Bunkyo-ku, Tokyo; Japan
[119] Ohio State University, Columbus OH; United States of America
[120] Homer L. Dodge Department of Physics and Astronomy, University of Oklahoma, Norman OK; United States of America
[121] Department of Physics, Oklahoma State University, Stillwater OK; United States of America
[122] Palacký University, Joint Laboratory of Optics, Olomouc; Czech Republic
[123] Institute for Fundamental Science, University of Oregon, Eugene, OR; United States of America
[124] Graduate School of Science, Osaka University, Osaka; Japan
[125] Department of Physics, University of Oslo, Oslo; Norway
[126] Department of Physics, Oxford University, Oxford; United Kingdom
[127] LPNHE, Sorbonne Université, Université Paris Cité, CNRS/IN2P3, Paris; France
[128] Department of Physics, University of Pennsylvania, Philadelphia PA; United States of America
[129] Department of Physics and Astronomy, University of Pittsburgh, Pittsburgh PA; United States of America
[130] [(a)] Laboratório de Instrumentação e Física Experimental de Partículas — LIP, Lisboa;[(b)] Departamento de Física, Faculdade de Ciências, Universidade de Lisboa, Lisboa;[(c)] Departamento de Física, Universidade de Coimbra, Coimbra;[(d)] Centro de Física Nuclear da Universidade de Lisboa, Lisboa;[(e)] Departamento de Física, Universidade do Minho, Braga;[(f)] Departamento de Física Teórica y del Cosmos, Universidad de Granada, Granada (Spain);[(g)] Departamento de Física, Instituto Superior Técnico, Universidade de Lisboa, Lisboa; Portugal
[131] Institute of Physics of the Czech Academy of Sciences, Prague; Czech Republic
[132] Czech Technical University in Prague, Prague; Czech Republic
[133] Charles University, Faculty of Mathematics and Physics, Prague; Czech Republic
[134] Particle Physics Department, Rutherford Appleton Laboratory, Didcot; United Kingdom
[135] IRFU, CEA, Université Paris-Saclay, Gif-sur-Yvette; France
[136] Santa Cruz Institute for Particle Physics, University of California Santa Cruz, Santa Cruz CA; United States of America
[137] [(a)] Departamento de Física, Pontificia Universidad Católica de Chile, Santiago;[(b)] Millennium Institute for Subatomic physics at high energy frontier (SAPHIR), Santiago;[(c)] Instituto de Investigación Multidisciplinario en Ciencia y Tecnología, y Departamento de Física, Universidad de La Serena;[(d)] Universidad Andres Bello, Department of Physics, Santiago;[(e)] Instituto de Alta Investigación, Universidad de Tarapacá, Arica;[(f)] Departamento de Física, Universidad Técnica Federico Santa María, Valparaíso; Chile
[138] Department of Physics, University of Washington, Seattle WA; United States of America
[139] Department of Physics and Astronomy, University of Sheffield, Sheffield; United Kingdom
[140] Department of Physics, Shinshu University, Nagano; Japan
[141] Department Physik, Universität Siegen, Siegen; Germany
[142] Department of Physics, Simon Fraser University, Burnaby BC; Canada
[143] SLAC National Accelerator Laboratory, Stanford CA; United States of America
[144] Department of Physics, Royal Institute of Technology, Stockholm; Sweden
[145] Departments of Physics and Astronomy, Stony Brook University, Stony Brook NY; United States of America
[146] Department of Physics and Astronomy, University of Sussex, Brighton; United Kingdom
[147] School of Physics, University of Sydney, Sydney; Australia
[148] Institute of Physics, Academia Sinica, Taipei; Taiwan
[149] [(a)] E. Andronikashvili Institute of Physics, Iv. Javakhishvili Tbilisi State University, Tbilisi;[(b)] High Energy Physics Institute, Tbilisi State University, Tbilisi;[(c)] University of Georgia, Tbilisi; Georgia
[150] Department of Physics, Technion, Israel Institute of Technology, Haifa; Israel
[151] Raymond and Beverly Sackler School of Physics and Astronomy, Tel Aviv University, Tel Aviv; Israel
[152] Department of Physics, Aristotle University of Thessaloniki, Thessaloniki; Greece
[153] International Center for Elementary Particle Physics and Department of Physics, University of Tokyo, Tokyo; Japan
[154] Department of Physics, Tokyo Institute of Technology, Tokyo; Japan

JHEP10(2024)130

[155] Department of Physics, University of Toronto, Toronto ON; Canada
[156] [(a)] TRIUMF, Vancouver BC; [(b)] Department of Physics and Astronomy, York University, Toronto ON; Canada
[157] Division of Physics and Tomonaga Center for the History of the Universe, Faculty of Pure and Applied Sciences, University of Tsukuba, Tsukuba; Japan
[158] Department of Physics and Astronomy, Tufts University, Medford MA; United States of America
[159] Department of Physics and Astronomy, University of California Irvine, Irvine CA; United States of America
[160] University of Sharjah, Sharjah; United Arab Emirates
[161] Department of Physics and Astronomy, University of Uppsala, Uppsala; Sweden
[162] Department of Physics, University of Illinois, Urbana IL; United States of America
[163] Instituto de Física Corpuscular (IFIC), Centro Mixto Universidad de Valencia — CSIC, Valencia; Spain
[164] Department of Physics, University of British Columbia, Vancouver BC; Canada
[165] Department of Physics and Astronomy, University of Victoria, Victoria BC; Canada
[166] Fakultät für Physik und Astronomie, Julius-Maximilians-Universität Würzburg, Würzburg; Germany
[167] Department of Physics, University of Warwick, Coventry; United Kingdom
[168] Waseda University, Tokyo; Japan
[169] Department of Particle Physics and Astrophysics, Weizmann Institute of Science, Rehovot; Israel
[170] Department of Physics, University of Wisconsin, Madison WI; United States of America
[171] Fakultät für Mathematik und Naturwissenschaften, Fachgruppe Physik, Bergische Universität Wuppertal, Wuppertal; Germany
[172] Department of Physics, Yale University, New Haven CT; United States of America

[a] Also Affiliated with an institute covered by a cooperation agreement with CERN
[b] Also at An-Najah National University, Nablus; Palestine
[c] Also at Borough of Manhattan Community College, City University of New York, New York NY; United States of America
[d] Also at Center for High Energy Physics, Peking University; China
[e] Also at Center for Interdisciplinary Research and Innovation (CIRI-AUTH), Thessaloniki; Greece
[f] Also at Centro Studi e Ricerche Enrico Fermi; Italy
[g] Also at CERN, Geneva; Switzerland
[h] Also at Département de Physique Nucléaire et Corpusculaire, Université de Genève, Genève; Switzerland
[i] Also at Departament de Fisica de la Universitat Autonoma de Barcelona, Barcelona; Spain
[j] Also at Department of Financial and Management Engineering, University of the Aegean, Chios; Greece
[k] Also at Department of Physics, Ben Gurion University of the Negev, Beer Sheva; Israel
[l] Also at Department of Physics, California State University, Sacramento; United States of America
[m] Also at Department of Physics, King's College London, London; United Kingdom
[n] Also at Department of Physics, Stanford University, Stanford CA; United States of America
[o] Also at Department of Physics, Stellenbosch University; South Africa
[p] Also at Department of Physics, University of Fribourg, Fribourg; Switzerland
[q] Also at Department of Physics, University of Thessaly; Greece
[r] Also at Department of Physics, Westmont College, Santa Barbara; United States of America
[s] Also at Faculty of Physics, Sofia University, 'St. Kliment Ohridski', Sofia; Bulgaria
[t] Also at Hellenic Open University, Patras; Greece
[u] Also at Institucio Catalana de Recerca i Estudis Avancats, ICREA, Barcelona; Spain
[v] Also at Institut für Experimentalphysik, Universität Hamburg, Hamburg; Germany
[w] Also at Institute for Nuclear Research and Nuclear Energy (INRNE) of the Bulgarian Academy of Sciences, Sofia; Bulgaria
[x] Also at Institute of Applied Physics, Mohammed VI Polytechnic University, Ben Guerir; Morocco
[y] Also at Institute of Particle Physics (IPP); Canada
[z] Also at Institute of Physics and Technology, Mongolian Academy of Sciences, Ulaanbaatar; Mongolia
[aa] Also at Institute of Physics, Azerbaijan Academy of Sciences, Baku; Azerbaijan
[ab] Also at Institute of Theoretical Physics, Ilia State University, Tbilisi; Georgia
[ac] Also at L2IT, Université de Toulouse, CNRS/IN2P3, UPS, Toulouse; France

JHEP10(2024)130

[ad] Also at Lawrence Livermore National Laboratory, Livermore; United States of America
[ae] Also at National Institute of Physics, University of the Philippines Diliman (Philippines); Philippines
[af] Also at Technical University of Munich, Munich; Germany
[ag] Also at The Collaborative Innovation Center of Quantum Matter (CICQM), Beijing; China
[ah] Also at TRIUMF, Vancouver BC; Canada
[ai] Also at Università di Napoli Parthenope, Napoli; Italy
[aj] Also at University of Colorado Boulder, Department of Physics, Colorado; United States of America
[ak] Also at Washington College, Chestertown, MD; United States of America
[al] Also at Yeditepe University, Physics Department, Istanbul; Türkiye
[*] Deceased

JHEP10(2024)130